

Gabor Analysis for a Class of Signals called Music

Dissertation
zur Erlangung des akademischen Grades einer Doktorin
an der
Formal- und naturwissenschaftlichen Fakultät
der
Universität Wien

Eingereicht von
Mag. Monika Dörfler

Begutachtet von
Prof. Dr. Hans G. Feichtinger
Prof. Dr. Karlheinz Gröchenig

Ausgeführt am
Institut für Mathematik der Universität Wien

Wien, 26.7.2002

Meinen Eltern.

Contents

German Summary	ix
Prologue	xi
1 Basics and Notation	1
2 Time-frequency Analysis for Music Signals	5
2.1 Introduction	5
2.2 Time can be Frequency	6
2.2.1 Bases and frames	7
2.2.2 Frame bounds	9
2.3 The Bridge to Applications	10
2.3.1 Mastering the frame operator - the Walnut representation . . .	13
2.4 A Lattice that reads the Music	18
2.4.1 Adapting window and lattice	18
2.4.2 A new approach: Multiple Gabor systems	19
2.5 Outline	21
3 Multiple Gabor Frames	23
3.1 Main Idea	23
3.1.1 Multi-window Gabor expansions	24
3.1.2 Reducing the size of a multi-window Gabor dictionary	26
3.2 Multiple Gabor Frames	26
3.2.1 Preliminaries	26
3.2.2 Existence of reduced multiple Gabor frames	28
3.3 Application: Gabor Regression	30
3.3.1 Gabor regression using a general linear model	30
3.3.2 Performance of the proposed scheme	31
3.4 Dual Frame and Reconstruction	32
3.4.1 Existence of dual frame	33
3.4.2 Approximation of the dual frame	33
3.4.3 Numerical simulations	34
3.5 Generalisations	37

4	Compactness Criteria in Modulation Spaces	41
4.1	Introduction	41
4.2	Modulation Spaces	44
4.2.1	Preliminaries and definition	44
4.2.2	Compactness in modulation spaces	47
4.3	Compactness of STFT Multipliers	49
5	Theory and Application of Gabor Multipliers	51
5.1	Introduction	51
5.2	The Kohn-Nirenberg Symbol	55
5.3	The Spreading Function	56
5.4	The Lower and Upper Symbol of a Gabor Multiplier	56
5.4.1	$(P_\lambda)_{\lambda \in \Lambda}$ as Riesz basis	59
5.5	Best-Approximation of General Linear Operators	63
5.5.1	Numerical realization and examples	64
5.6	Changing the Parameters	66
5.6.1	Changing the window	66
5.6.2	The relation between upper and lower signal	69
5.6.3	Varying the lattice	70
5.7	Characterizing the Operator by its Eigenvectors	73
5.7.1	Simulation examples	77
5.8	Summary and Conclusions	86
6	Time-Frequency BUPUs in Modulation Spaces	95
6.1	Partitioning Operators over the TF-Plane	95
6.2	The S_0 Norm and Partitions in the TF-Domain	98
6.3	Frames of Finite-Rank Operators	102
7	Multiple Gabor Systems with Windows in S_0	105
7.1	Varying the System in one Domain	105
7.1.1	Reconstruction	109
7.1.2	Lower frame bound	111
7.1.3	Upper frame bound	112
7.2	Outlook: Time-Frequency Adaptive Systems	114
A	MATLAB files	117
A.1	stftl.m	117
A.2	windows.m	118
A.3	opeig.m	119
A.4	ogabgrw.m	120
A.5	upp2low.m	121
A.6	gmult.m	122
A.7	imp2mh.m	123
A.8	fupro.m	123

List of Figures

2.1	<i>Time-frequency shifted versions of a Gaussian window</i>	8
2.2	<i>Dual windows and stability.</i>	10
2.3	<i>Gaussian window and dual window (Redundancy 4)</i>	15
2.4	<i>Hanning window and dual window (Redundancy 2)</i>	16
2.5	<i>Gaussian window and tight window (Redundancy 4)</i>	17
2.6	<i>Hanning window and tight window (Redundancy 2)</i>	17
2.7	<i>Two windows and resulting STFT of music signal.</i>	20
3.1	<i>Members of a BAPU (dotted) summing up to 1.</i>	24
3.2	<i>Constructing multiple Gabor frames</i>	27
3.3	<i>A member of the BAPU and translates of the corresponding window family.</i>	28
3.4	<i>Reconstruction of sample signal</i>	31
3.5	<i>Spectrograms of the noisy and clean speech signal</i>	32
3.6	<i>Comparison of speech signal reconstruction using a full and reduced dictionary</i>	32
3.7	<i>Sampling Lattice for full Gabor family and subset.</i>	35
3.8	<i>Exact and approximate local dual window</i>	36
3.9	<i>The three local systems. The dual windows are dotted.</i>	37
3.10	<i>Reconstruction by means of approximate dual family.</i>	38
3.11	<i>Example 1 for behavior of dual frame</i>	38
3.12	<i>Example 2 for behavior of dual frame</i>	39
3.13	<i>Example 3 for behavior of dual frame</i>	39
3.14	<i>Example 4 for behavior of dual frame</i>	40
5.1	<i>Gabor multiplier applied to synthesized signal</i>	53
5.2	<i>Gabor multiplier applied to real signal</i>	53
5.3	<i>Eigenvalues of \mathcal{A} for different Gabor systems</i>	65
5.4	<i>Upper symbols</i>	68
5.5	<i>Upper symbols with different smoothness</i>	68
5.6	<i>Changing the lattice</i>	71
5.7	<i>Effect of lattice change on TF-concentration</i>	72
5.8	<i>Eigenvectors and eigenvalues of a 0/1 Gabor multiplier</i>	78
5.9	<i>Projection onto eigenspaces</i>	80

5.10	<i>Projection onto eigenspaces</i>	81
5.11	<i>Typical action of the operators P_N</i>	84
5.12	<i>Number of eigenvectors inside a mask</i>	85
5.13	<i>Dependence on the shape of the multiplier</i>	87
5.14	<i>Approximation of an underspread operator</i>	89
5.15	<i>TF-concentration of regular and iterated Gabor multiplier</i>	90
5.16	<i>Eigenvalues of common and iterated Gabor multiplier</i>	91
5.17	<i>TF-concentration of common and iterated Gabor multiplier</i>	92

Deutschsprachige Zusammenfassung

Diese Arbeit befasst sich mit der Adaptierung von Gabor Frames für akustische Signale, insbesondere für Musiksingale. Zunächst werden konkrete Beispiele aus den Anwendungen vorgestellt und die Nützlichkeit von Methoden aus der Gabor Analysis in diesem Kontext beschrieben. Für Musiksingale ergibt sich die Notwendigkeit, in verschiedenen Frequenzbereichen unterschiedliche Frequenzauflösung anzustreben. Kapitel 3 führt die *multiple Gabor Frames* ein, die eine derartige, flexible, Frequenzauflösung ermöglichen. Ein Anwendungsbeispiel wird mit konkreten Daten ausgeführt. Um eine Verallgemeinerung der Idee von multiple Gabor Frames zu ermöglichen, wird im nächsten Kapitel ein neues Kompaktheitskriterium für Modulation Spaces bewiesen. Es wird gezeigt, dass Kompaktheit in Modulation Spaces äquivalent ist zur Straffheit der Short-time Fourier Transformation in den entsprechenden $\mathbf{L}_m^{p,q}$ -Räumen. Gabor-Multiplier, die Modifikation der Gaborkoeffizienten mit nachfolgender Synthese, sind ein Werkzeug zum zeitvarianten Filtern, das als Verallgemeinerung der Short-time Fourier Transformation-Multiplier verstanden werden kann. In Kapitel 5 werden die Eigenschaften von Gabor-Multipliern in Abhängigkeit von den freien Parametern untersucht. Die Analyse von Eigenvektoren und Eigenwerten der Operatoren wird die Zeit-Frequenz Konzentration, die durch zeitvariantes Filtern mit Gabor-Multipliern erreicht werden kann, untersucht.

Short-time Fourier Transformation-Multiplier und Gabor-Multiplier mit bestimmten, in der Zeit-Frequenz Ebene konzentrierten Multipliern, können als Zeit-Frequenz Konzentrationsoperatoren interpretiert werden. In Kapitel 6 wird die naheliegende Frage studiert, unter welchen Bedingungen das Aufsplitten von Funktionen in der Zeit-Frequenz Ebene äquivalente Normen in verschiedenen Funktionenräumen liefern kann. Die Beantwortung dieser Frage ist schliesslich entscheidend für die Möglichkeit der Konstruktion von allgemeinen zeit-frequenzadaptiven Systemen, die im letzten Kapitel eingeführt werden. Für den Fall der Adaptivität bezüglich Zeit oder Frequenz wird gezeigt, dass \mathbf{L}^2 -Funktionen aus lokalisierten Koeffizienten rekonstruierbar sind. Weiters wird gezeigt, dass die Vereinigung von speziell gewählten Teilmengen von gegebenen Gabor Frames jedenfalls eine Besselfolge liefern. Die untere Frameschranke wird diskutiert. Die Arbeit schliesst mit einem Ausblick auf das Konzept von *quilted Gabor frames*. Diese sollen unter bestimmten Voraussetzungen an Fenster und Gitter die Konstruktion von beliebig zeit-frequenzadaptiven Frames erlauben.

Prologue - Mathematics and Music.

An intimate Dialogue

It seems to be almost common knowledge, that there are strong connections between mathematics and music. Can the relations between both, however, be reduced to the frequently heard statement that numbers and counting play an important role in both mathematics and music, such that mathematicians are readily expected to be practising musicians or passionate music lovers?

In this brief exposition I will try to give a slightly deeper account of the links between mathematics and music, beyond those arising from the possibility to numerically describe, seize and process music or rather signals related to music. The latter will be the motivation for some of the topics treated in the main part of this thesis. Here, some more subtle parallels will be disclosed, parallels between two disciplines which were not even considered separately until a few centuries ago.¹

Common History

J.Ph.Rameau, the greatest French musicologist of the eighteenth century, wrote in his *Traité de l'harmonie réduite à ses principes naturels* ([56]):

Music is a science which must have determined rules. These rules must be drawn from a principle which should be evident, and this principle cannot be known without the help of mathematics. I must confess that in spite of all the experience which I have acquired in music by practising it for a fairly long period, it is nevertheless only with the help of mathematics that my ideas became disentangled and that light has succeeded to a certain darkness of which I was not aware before.

A Greek mathematical treatise from the beginning of our era would usually contain four sections: Number Theory, Geometry, Music and Astronomy. It is well known that Pythagoras, Plato or Aristotle considered music as part of mathematics. Later on, it was not until the Renaissance, that (theoretical) music became an independent field, with strong links to mathematics being maintained, such that several important mathematicians of the seventeenth and eighteenth centuries, such as Descartes, Euler

¹In December 1999 a Diderot Mathematical Forum on Mathematics and Music was organized simultaneously in Lisbon, Vienna and Paris. A book with a number of contributions to these conferences, illustrating the rich and deep interactions between Mathematics and Music, is now available, [1].

or d'Alembert, were also music theorists.² The mutual influences are manifold. Mathematical diagrams such as the cartesian coordinates developed under the influence of models from music notation, where staves with the x-coordinate representing time and the y-coordinate representing frequency started to be used in the eleventh century – long before they were introduced in geometry. Diagrams resulting from time-frequency analysis, the topic of the major part of this thesis, can even be interpreted as a generalized music notation.

Another example for the importance of influences from music theory in mathematics is the logarithm, which was used by music theorists in an intuitive way long before the introduction of its abstract notion in mathematics.

Apparently, the human mind tends to apply similar models for mapping both musical and mathematical findings to a descriptive medium.

Structures

Both mathematics and music appear as highly structured disciplines. Transparency, lucidity and a certain kind of simplicity are desired in both mathematical theory and in music, be it music in the sense of composition and improvisation or music theory. Musical phrases obeying strict structures, though often not consciously understood as such by the listener, are perceived as particularly pleasing. The rather rigorous rules of counterpoint, as, e.g., in the compositions of J. S. Bach and his contemporaries, are a typical example, more recent ones are given by the harmonic regularities in jazz harmony.³ On the other hand, Bach as well as all famous improvisers in jazz don't recoil from a controlled breach of the rules – leading to the advent of new perspectives and connections. The same principles hold analogously for mathematics: first, the given rules of a mathematical theory have to be thoroughly studied and practised in order to be able to finally make a step beyond their limits.

Both mathematical theories and compositions build on micro-structures on the one hand and more fundamental ideas of the over-all work on the other hand. It is only by mastery of the tools responsible for linking the fragments that a composition or mathematical theory, respectively, become convincing and consistent. At the same time, a fundamental idea guarantees unity and conclusiveness.

Abstractions and generalizations are important and necessary tools to accomplish the above-mentioned issues. In fact, a lot of the micro-structures are generalized from actual instances to abstract concepts. Basic notions in harmony, such as scales or intervals are idealizations of specific sound-events, just as the notion of, e.g., a Hilbert space is an idealized concept derived from more specific mathematical objects like the Euclidean spaces. It appears to be a characteristic of both music and mathematics to use abstractions of a particular phenomenon in order to build generalizable models. In the process of achieving the necessary ease in handling the tools of abstraction, prac-

²[52] gives more details about the history of music theory in mathematics.

³Mark Levine, the author of several important textbooks on jazz harmony and theory, gives a detailed account of harmonic structures in improvisation in [48].

tise is a decisive ingredient, more obvious in music, but as important in mathematics. Mathematics and music require active and repeated examination of the subject. Without spending time focussing on music, no deeper understanding and, consequently, no full appreciation can be achieved. The same holds true for mathematics: it is only by repeated and continual practise, that a mathematical theory can be truly mastered – in a sense going beyond repeating trained patterns in order to solve certain, well-specified problems.

Thus, repetition enables humans to internalize major parts of what is needed to find the paths in the maze of operator theory, of a composition by Schoenberg. What is often called mathematical intuition as well as what goes by the term musicality, are acquired abilities in most cases. The knowledge resulting from *experiencing* the subject, its tools, its particularities, gradually disappears from consciousness and contributes to the building of a new, unique universe, step by step, inside the human mind.

An inventive universe

Improvising a piece on an instrument one is familiar with, writing a composition, extending a mathematical theory by inventing new notions, theorems and proofs – all these activities resemble a mental excursion in a well-known region. For either of the two disciplines, mathematics and music, it does not suffice to read and reproduce knowledge. The active pursuit and the creative extension of the subject are in fact the essential concern of mathematicians and musicians alike. And, miraculously, the realm which is being discovered, grows with the size of the ground already investigated: the more we know, the bigger is the universe we are facing. The process leading to a step-wise conquest of "new land", is a strictly non-linear one, including the often frustrating necessity to return to the seemingly same point.

Hence, description of a non-linear process, such as the development of parts of a mathematical theory, as it is undertaken in a mathematical thesis, by means of a linear medium, is bound to be an approximation. Just as written music is only a faint image of the sound in the composer's head. Written music needs musicians to be filled with sound, listeners to be filled with relevance, written mathematics need a human mind giving meaning to the symbols, a scientific community providing a suitable context.

In this thesis I give an account of some new findings on *Gabor analysis*, [35], applied to music signals. One intention of the organization of this thesis is to mirror to a certain extent the gradual development of the ideas. Hence, I give examples and illustrative figures whenever possible. At the same time, this approach is intended to point out that some statements first existed as a numerical evidence⁴, which was then given a more precise mathematical counterpart. Several preliminary results are stated as "conjectures", as they seem evident from intuition and numerical experiments, but could not yet be proved in a sound mathematical manner.

The next section briefly describes the problems which may arise in a mathematical

⁴MATLAB code corresponding to the respective experiments is presented in the appendix.

analysis of music and point out to which parts of the complex accomplishment of solving these problems the mathematics of time-frequency analysis can contribute.

Problems

A comprehensive discussion of the applications of mathematics in signal processing of music signals was given in [17]. Here, we are going to focus on two specific tasks, namely automatic transcription and time-varying filtering, and explain their connections to the results given in this thesis.

• Transcription

By transcription we mean the extraction of an acceptable notation from performed music, i.e., from a sound signal, which has been digitalized and can thus be numerically processed. Transcription is a task which is well accomplished by trained humans. However, the automatic transcription problem is still unsolved for any class of fairly complex music signals. In fact, tackling the task of transcription requires the consideration of several levels of processing. First of all, an appropriate signal representation must be achieved, often by time-frequency methods from signal analysis. Pattern recognition methods or methods from artificial intelligence then yield information on onset timing, [16, 10], and fundamental frequencies, [64, 7, 36], resulting in data in a format similar to MIDI ⁵. Finally, it seems to be a highly non-trivial issue in artificial intelligence to obtain written music from MIDI data, see, e.g., [16, 8].

In fact, mathematics can mainly contribute to the low-level part of processing concerning the quality of the time-frequency methods used. A major part of this thesis deals with the development of a time-frequency representation particularly suited for music signals, a representation which we call *multiple Gabor systems*.

• Time-varying filtering

As opposed to linear time-invariant filtering, in which the spectrum is multiplied by a transfer function, in time-varying filtering, the transfer function explicitly depends on time. Time-varying filtering appears in applications such as noise-reduction or signal separation. By the latter we mean the extraction of signal components from a multi-component signal, for example the part of a musical piece which is performed by a certain instrument or group of instruments. We discuss a specific tool for time-varying filtering called *Gabor multipliers*. An overview of existing methods for time-varying filtering based on joint time-frequency distributions was given in [45]. Gabor multipliers are a generalization

⁵MIDI (short for Musical Instrument Digital Interface) is a music industry standard communications protocol that lets MIDI instruments and sequencers (or computers running sequencer software) talk to each other to play and record music. More and more of the music heard every day is written with and played by MIDI sequencers, see [59].

of short-time Fourier transform multipliers, which are discussed in the above-mentioned article. The freedom in the choice of parameters in Gabor multipliers introduces certain ambiguities which are investigated in Chapter 5.

Naturally, this thesis can only scratch the surface of possible applications of mathematics, and in particular of time-frequency analysis, in music. Mathematics is a universe which is discovered and invented simultaneously: This thesis gives a summary of some years of my experiences in a small part of this universe. I hope that I provided the necessary signposts for anyone who is interested in following me on a part of my expedition.

At this point I want to mention, that without quite a few important companions, I would have abandoned my mathematical adventures a long time ago. Above all I want to thank my advisors and tutors Hans Feichtinger and Charly Gröchenig for their inspiration, assistance and encouragement as well as for their own enthusiasm for the subject. Working at NuHAG (The Numerical Harmonic Analysis Group at the Department of Mathematics, University of Vienna) would seem almost impossible without my colleagues Norbert Kaiblinger, Harald Schwab, Tobias Werther, Josef Mattes, Mario Hampejs and our wonderful visitors in the past few years, among them Patrick Wolfe, Elena Cordero, Massimo Fournasier, Bernard Keville, Ole Christensen and Kasso Okoudjou, to all of whom I owe valuable mathematical and other discussions.

Without music, many things in my life wouldn't make sense. Thank you to all who have shared this invaluable gift over the years.

This thesis leaves some questions open and has produced many more, so I am looking forward to continuing my explorations in the near future.

Chapter 1

Basics and Notation

This chapter collects the most important facts on basic theory used in this work, along with some references to books and articles for further reading.

1. We define the **Fourier transform** on $\mathbf{L}^2(\mathbb{R}^d)$ as

$$\hat{f}(\omega) = \int_{\mathbb{R}^d} f(t) e^{-2\pi i \omega t} dt$$

2. The **convolution** of two functions $f, g \in \mathbf{L}^1(\mathbb{R}^d)$ is the function $f * g$ defined by

$$(f * g)(x) = \int_{\mathbb{R}^d} f(y) g(x - y) dy.$$

It satisfies

$$\|f * g\|_1 \leq \|f\|_1 \|g\|_1,$$

and more generally, for $g \in \mathbf{L}^p(\mathbb{R}^d)$:

$$\|f * g\|_p \leq \|f\|_1 \|g\|_p.$$

Under Fourier transform, the convolution turns in a pointwise multiplication:

$$\widehat{(f * g)} = \hat{f} \cdot \hat{g}.$$

3. **Time-frequency shifts**

Time-frequency shift operators are crucial elements in Gabor analysis.

- (a) M_ω and T_x denote frequency-shift by ω and time-shift by x , respectively, of a function g , i.e., $M_\omega T_x g(t) = e^{2\pi i t \omega} g(t - x)$ for $(x, \omega) \in \mathbb{R}^{2d}$. $M_\omega T_x$ is a **time-frequency shift** operator.

Writing $\lambda = (x, w)$, $M_\omega T_x$ is often denoted by $\pi(\lambda)$ in the sequel.

- (b) A tensor product $(\pi \otimes \pi^*)(\lambda)$ of time-frequency shift operators can be defined by its action on operators \mathbf{K} :

$$(\pi \otimes \pi^*)(\lambda)\mathbf{K} = \pi(\lambda)\mathbf{K}\pi^*(\lambda). \quad (1.1)$$

Sometimes it will be convenient to denote $(\pi \otimes \pi^*)(\lambda)$ by $\pi_2(\lambda)$.

$(\pi \otimes \pi^*)(\lambda)$ corresponds to a **time-frequency shift of the operator \mathbf{K}** , see Section 5 and [29] for further details.

4. Short-time Fourier transform

The short-time Fourier transform (STFT) of a function $f \in \mathbf{L}^2(\mathbb{R}^d)$ with respect to a window function $g \in \mathbf{L}^2(\mathbb{R}^d)$ is defined as

$$\mathcal{V}_g f(x, \omega) = \int_{\mathbb{R}^d} f(t) \bar{g}(t - x) e^{-2\pi i \omega \cdot t} dt = \langle f, M_\omega T_x g \rangle. \quad (1.2)$$

5. A *lattice* $\Lambda \subset \mathbb{R}^d$ is a discrete subgroup of \mathbb{R}^d of the form $\Lambda = A\mathbb{Z}^d$, where A is an invertible $d \times d$ -matrix over \mathbb{R} . The special case

$$\Lambda = \alpha\mathbb{Z}^d \times \beta\mathbb{Z}^d, \quad (1.3)$$

where $\alpha, \beta > 0$ are the lattice parameters, is called a separable or product lattice. Unless otherwise stated, we always assume that the lattice Λ in use is a product lattice. The *adjoint* lattice Λ° of a product lattice is given by

$$\Lambda^\circ = \frac{1}{\beta}\mathbb{Z}^d \times \frac{1}{\alpha}\mathbb{Z}^d \quad (1.4)$$

6. Frames, Gabor frames, the frame operator and the dual frame

- A set of functions f_k in $L^2(\mathbb{R}^d)$ is called a frame, if there exist constants $A, B > 0$, so that

$$A\|f\|^2 \leq \sum_{k \in \mathbb{Z}} |\langle f, f_k \rangle|^2 \leq B\|f\|^2 \text{ for all } f \in \mathbf{L}^2(\mathbb{R}^d) \quad (1.5)$$

Assumption (1.5) can be understood as an “approximate Plancherel formula”. It guarantees *completeness* of the set of building blocks in the given function space; i.e., any signal $f \in \mathcal{H}$ can be represented as infinite series with square integrable coefficients, or, in the finite case, linear combination of the f_k .

- For any frame dual frames \tilde{h}_k exist, allowing an expansion of f as:

$$f = \sum_k \langle f, f_k \rangle \tilde{h}_k = \sum_k \langle f, \tilde{h}_k \rangle f_k \quad (1.6)$$

- The frame bounds A and B are the infimum and supremum, respectively, of the eigenvalues of the *frame operator* S , defined as

$$Sf = \sum_k \langle f, f_k \rangle f_k.$$

- The *canonical dual frame* (\tilde{f}_k) , which guarantees minimal-norm coefficients in the expansion (1.6), is given by $S^{-1}(f_k)$.
- The special case $f_k = g_{m,n} := M_{mb}T_{na}g$ is called Gabor or Weyl-Heisenberg frame. In this case we write $S = S_g$, where g is the window generating the frame. The *analysis mapping* T_g mapping the function $f \in \mathbf{L}^2$ to its coefficients $c(f)(\lambda) = T_g f(\lambda)$, $T_g f \in \ell^2(\mathbb{Z})$ is given by

$$T_g : f \mapsto [\langle f, g_{m,n} \rangle]_{m,n}$$

and its adjoint, the *synthesis mapping* $T_g^* : \ell^2(\mathbb{Z}) \mapsto \mathbf{L}^2$, is given by

$$[c_{m,n}] \mapsto \sum_{m,n \in \mathbb{Z}} c_{m,n} g_{m,n}.$$

Then, the frame operator is the concatenation of these two linear and, in the frame case, bounded operators: $S_g = T_g^* T_g$.

- Note that the coefficients of a Gabor frame, given by $[\langle f, g_{m,n} \rangle]_{m,n}$ correspond to the samples of the STFT on the product lattice $\Lambda = a\mathbb{Z}^d \times b\mathbb{Z}^d$

7. Spaces of bandlimited functions

$$\mathbf{L}_\Omega^2(\mathbb{R}) := \{f \in \mathbf{L}^2(\mathbb{R}) : \text{supp}(\hat{f}) \subseteq \Omega\}$$

$$\ell^2(\mathbb{Z}) := \{f : \mathbb{Z} \rightarrow \mathbb{C} : \sum_{n=-\infty}^{\infty} |f(n)|^2 < \infty\}$$

8. **Wiener amalgam spaces** were introduced by H. Feichtinger, see [23], for example. By means of their definition, Wiener amalgam spaces decouple the connection between local and global properties of functions inherit in the definition of most common function spaces.

Definition 1 (Wiener amalgam spaces).

The Wiener amalgam space $W(\mathbf{L}^p, \ell^q)$ is defined as follows:

$$W(\mathbf{L}^p, \ell^q) = \left\{ f \in \mathbf{L}^p(\mathbb{R}^d) : \|f\|_{W(\mathbf{L}^p, \ell^q)} = \left(\sum_k \|f \cdot \mathbf{1}_{[k, k+1]} \|_p^q \right)^{\frac{1}{q}} < \infty \right\}.$$

A comprehensive review of Wiener amalgam spaces, which can be defined in a much more general setting, can be found in [42]. Here we state without proof some important properties which will be needed in this work.

- $\mathbf{L}^2 \cup \mathbf{L}^\infty \subseteq W(\mathbf{L}^\infty, \ell^2)$.
- If $B_1 * B_2 \subset B_3$ and $C_1 * C_2 \subset C_3$, then $W(B_1, C_1) * W(B_2, C_2) \subset W(B_3, C_3)$.
- If $B_1 \subset B_2$ and $C_1 \subset C_2$, then $W(B_1, C_1) \subset W(B_2, C_2)$.

Chapter 2

Time-frequency Analysis for Music Signals

In this introductory chapter we establish a link between Gabor analysis and certain problems that arise in digital audio signals processing. Going back to the work of D. Gabor in 1946, [37], Gabor analysis is based on the idea of representing arbitrary signals of finite energy in terms of building blocks which have a well-defined “center of gravity” in a time-frequency sense. Indeed, various widely used spectral domain methods correspond to the use of particular Gabor frames. The interpretation of this situation from the point of view of Gabor analysis makes the calculation of the so called dual window computationally efficient and post-processing by a weighting function unnecessary.

We thus intend to point out the difficulties which can arise when theory is turned to practice, on the other hand, the usefulness of theoretical consideration for practical situations is emphasized.

Furthermore, the idea of locally adaptive sets of building blocks, which will yield a generalisation of spectral domain methods especially helpful in the investigation of music signals, is introduced.

Most of the material presented in this chapter has been published as a journal paper, [18].

2.1 Introduction

Time-frequency analysis¹ is omnipresent in the processing of music. It might often not be called by this name, but in fact any method cutting a signal into pieces and doing Fourier analysis or filtering on the single pieces is time-frequency analysis. In this chapter we aim to introduce the main features of Gabor analysis, see [35], which align in many ways with “practical” time-frequency analysis in a numerical setting. Gabor analysis yields a mathematically well-defined and precise framework helping to understand important issues in the processing of audio signals. Since the basic prob-

¹Material on time-frequency analysis can be found e.g. in [55] or [62], among many others.

lems of Gabor analysis (arising from the fact that the collection of building blocks is non-orthogonal and even redundant) have been analysed in great detail by mathematicians and engineers over the last 20 years, we believe that it makes sense to exhibit the potential of Gabor analysis to applied scientists, in particular to electronic musicians who certainly are familiar with very similar ideas. Ambiguities arising from the rather arbitrary choice of window, sampling constants in time and frequency and the consequences of these choices are better understood within this framework. The merits of a mathematical approach discussed in this work in more detail are twofold.

On the one hand, it facilitates certain steps in implementation by incorporating knowledge gained from knowing about the theoretical background. In this chapter and throughout this work, we will discuss some of the topics in a numerical setting. Realisations of some of these calculations can be found in the appendix as MATLAB m-files.

On the other hand, a mathematical approach offers a framework for desirable generalisation and adaption to a given class of signals.

The first point will be discussed in this chapter, recalling the most basic facts from the theory about Gabor frames and pointing out the merits of applying these results to a practical situation. The subsequent chapters will be devoted to introducing and exploring the concept of time-frequency localisation and time-frequency adaptive systems.

2.2 Time can be Frequency

One fundamental idea in a mathematical approach to time-frequency analysis is looking at time and frequency in a symmetric way, which makes the theory more unified and flexible. Instead of thinking of cutting a signal into pieces, Fourier analysing it and putting it back together after some processing, with the Gabor approach in mind we think of a signal as being composed of basic functions concentrated in certain regions of the time-frequency plane.

Excursus: Three kinds of looking at signals

An essential part of this thesis deals with different function spaces. One of the reasons is the fact that different spaces often allow taking different points of view. When thinking about natural signals such as music, the first idea is to think of them as continuous signals. Of course they can't have infinite energy, so it is appropriate to assume that they are members of $\mathbf{L}^2(\mathbb{R})$, the space of square-integrable functions $\mathbb{R} \rightarrow \mathbb{C}$. This is a space with many nice properties, e.g. an inner product can be defined and it is in fact a Hilbert space. A lot of theory, e.g. on uncertainty, continuous dependencies or approximation is done in the Hilbert space \mathbf{L}^2 , more generally Banach spaces of Lebesgue integrable functions \mathbf{L}^p , with $p \in \mathbb{N}$, or more general spaces of continuous functions, such as modulation spaces, which will be introduced in Chapter 4.

On the other hand, signal processing is mostly done on digital computers, using discrete signals, so that $l^2(\mathbb{Z})$ would be the more appropriate choice of Hilbert space. However, in real life, we can only process signals of finite length, say L , i.e. they are most easily understood as members in \mathbb{C}^L , a complex vector space of finite dimension L . This choice simplifies some questions and complicates others. To give an example for the kind of problems that can arise, think of how to define convolution, an operation with an important role in signal processing. On l^2 it is defined as

$$(f * g)(n) = \sum_m f(m)g(n - m)$$

so the computation of $f * g$ may ask for values such as $f(-1)$, which are not defined in \mathbb{C}^L . A trick to solve this kind of problem is to think of periodic sequences as members of the group $\mathbb{Z}_L = \mathbb{Z} \bmod L$, corresponding to a *circular extension* of the signal.

In this chapter, we'll mostly be talking about functions $f \in \mathbb{C}^L$. Subsequently, we will sometimes refer to one of the introduced spaces depending on the context.

2.2.1 Bases and frames

The Gauss function $g(t) = e^{-\pi t^2} \in \mathbf{L}^2$ is invariant under Fourier transform and has minimal “extension in the time-frequency plane” in the sense that it achieves equality in Heisenberg’s uncertainty principle inequality.² If the energy in a signal is now thought of as being distributed over the time-frequency plane, indicating the amount of energy a certain frequency contributes at a specific time, then the Gabor approach can be described as “cutting” out pieces of at least the size of the Gauss function’s time-frequency spread from this distribution. The energy thus captured can be thought of as the *inner product* of the given signal f with the Gaussian or any other window function.

Definition 2. Let f and $g \in \mathbb{C}^L$. Their inner product is defined as

$$\langle f, g \rangle = \sum_{n=0}^{L-1} f(n) \overline{g(n)}$$

g will from now on be called window function.³ Let us now consider how a function g , centered around zero, can be moved to other points in the time-frequency plane, or, as we may prefer to call it in the discrete case, time-frequency lattice $\mathbb{C}^L \times \mathbb{C}^L$.

²Heisenberg’s inequality states that for all functions $f \in \mathbf{L}^2(\mathbb{R})$ and for all points (t_0, w_0) in the time-frequency plane

$$\|f\|_2^2 \leq 4\pi \|(t - t_0)f(t)\|_2 \|(w - w_0)\hat{f}(w)\|_2$$

where equality is achieved only by functions of the form

$$g(t) = C e^{2\pi i t w_0} e^{-s(t - t_0)^2}, \quad C \in \mathbb{C}, s > 0$$

which are modulated and translated (i.e. time-frequency shifted) Gaussians. A more detailed discussion of uncertainty principles in time-frequency analysis can be found in [40, Chapter 2]

³The Gaussian function is optimal in a certain, especially theoretical sense. In engineering Hanning or Hamming windows are most frequently used.

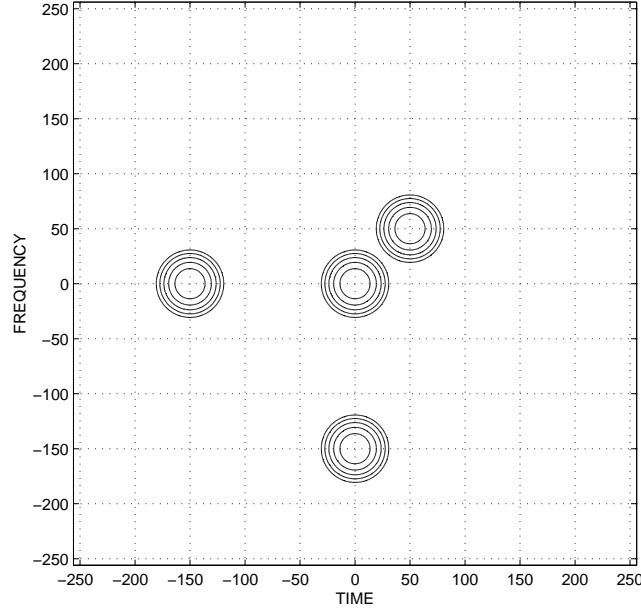


Figure 2.1: Time-frequency shifted versions of a Gaussian window

Definition 3 (Time-frequency shifts of discrete signals). $T_k f(t) := f(t + k)$ is called translation operator or time shift.

$M_l f(t) := e^{\frac{-2\pi i l t}{L}}$, $l \in \mathbb{Z}$ is called modulation operator or frequency shift.

The composition of these operators, $M_l T_k$, is a time-frequency shift operator.

Generally, we are not interested in calculating the inner product in every point of the time-frequency lattice. Calculating the inner product in every point of the time-frequency lattice would yield the *full short-time Fourier transform* (STFT).⁴ This would yield a representation with redundancy L , where L is the length of the given signal. Instead, we downsample the STFT in time by a and in frequency by b , so that the redundancy reduces to $\frac{L}{ab}$. a and b are referred to as time-frequency lattice constants or time and frequency shift parameters. The family

$$g_{m,n} := M_{mb} T_{na} g$$

for $m = 0, \dots, M-1$ and $n = 0, \dots, N-1$, where $Na = Mb = L$, is called the set of *Gabor analysis functions*.

Let us assume the $g_{m,n}$ were an orthogonal basis for a moment. In this case, the inner products $\langle f, g_{m,n} \rangle$ uniquely determine f , each representing a single and unique coefficient in the expansion

$$f = \sum_m \sum_n \langle f, g_{m,n} \rangle g_{m,n}$$

⁴The term “short-time Fourier transform” is often used for sampled short-time Fourier transforms as well. The spectrogram, its modulus squared, is one of the most popular time-frequency representations.

Together with Plancherel's formula $\|f\|_2^2 = \sum_m \sum_n |\langle f, g_{m,n} \rangle|^2$ this gives a beautiful split of f in pieces, preserving the signal's energy in the coefficients.

Of course there is a problem. Theory⁵ tells us, that the members of a basis of the above form can never be well-localised in both time and frequency.⁶ Therefore we have to balance between nice properties of the representation on the one hand and satisfactory mathematical properties, similar to those of a basis, on the other hand.

The theory of *frames* gives the appropriate framework. Recall that a set of functions f_k in $L^2(\mathbb{R})$ is called a frame, if there exist constants $A, B > 0$, so that

$$A\|f\|^2 \leq \sum_{k \in \mathbb{Z}} |\langle f, f_k \rangle|^2 \leq B\|f\|^2 \text{ for all } f \in \mathbf{L}^2(\mathbb{R})$$

Note that above inequality can be understood as an “approximate Plancherel formula”. For any frame a dual frame \tilde{f}_k exists, allowing an expansion of f as:

$$f = \sum_k \langle f, f_k \rangle \tilde{f}_k = \sum_k \langle f, \tilde{f}_k \rangle f_k \quad (2.1)$$

If the frame is not a basis, as will be the case in most applications, then the coefficients $c_k = \langle f, f_k \rangle$ are not unique, still optimal in the sense of minimising $\sum_k |c_k|^2$.

Remark 1. The special case $f_k = g_{m,n}$ is called Gabor or Weyl-Heisenberg frame.

2.2.2 Frame bounds

The frame bounds A and B are the infimum and supremum, respectively, of the eigenvalues of the *frame operator* S . In the finite discrete case, i.e., for signals $f \in \mathbb{C}^L$, a collection $\{g_{m,n}\} \in \mathbb{C}^L$ with $k = NM$ can only be a frame, if $L \leq k$ and if the matrix G , defined as the $k \times L$ matrix having $\overline{g_{m,n}}$ as its $(m + nM)$ -th row, such that $T_g f = G \cdot f$, has full rank. In this case the frame bounds are the maximum and minimum eigenvalues, respectively, of S . They yield information about numerical stability. If the A and B differ too much, the condition number of the matrix increases and the inversion of the frame operator is numerically unstable. Why are we interested in the inversion of the frame operator?

The canonical *dual frame* $\tilde{g}_{m,n}$, which yields reconstruction as in (2.1), is given by

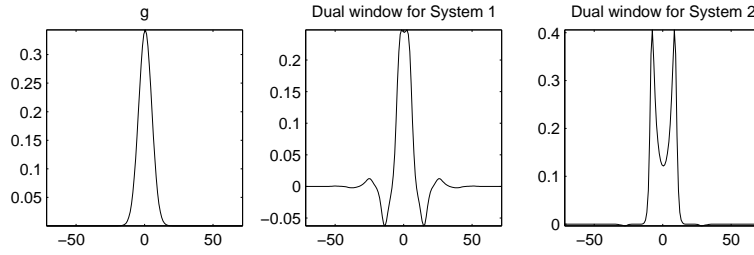
$$\tilde{g}_{m,n} = S^{-1} g_{m,n}$$

⁵The *Balian-Low theorem* is a key result in time-frequency analysis. It states that if a Gabor system in $\mathbf{L}^2(\mathbb{R})$ forms an orthogonal basis for $\mathbf{L}^2(\mathbb{R})$, then

$$\left(\int_{-\infty}^{\infty} |tg(t)|^2 dt \right) \left(\int_{-\infty}^{\infty} |\omega g(\omega)|^2 d\omega \right) = +\infty.$$

There exist several extensions, first of all to the case of *exact* frames, which are frames that cease to be complete when any element is deleted. See [3] for more details.

⁶Pure sinusoid form an orthogonal basis and are a nice example for functions having unbounded support in time.

Figure 2.2: *Dual windows and stability.*

as

$$f = S^{-1}Sf = \sum \langle f, g_{m,n} \rangle S^{-1}g_{m,n} = \sum \langle f, g_{m,n} \rangle \tilde{g}_{m,n}$$

Example 1. We give an example for the dual windows resulting from a badly conditioned frame operator. We consider a Gaussian window g and two different lattices $\Lambda_1 = 9\mathbb{Z} \times 12\mathbb{Z}$ and $\Lambda_2 = 18\mathbb{Z} \times 6\mathbb{Z}$, with redundancy 1.333 in both cases. The frame bounds of the first system are $A = 0.7603$ and $B = 1.9040$, hence the condition number is 2.5043, whereas for the second system $A = 0.1650$ and $B = 2.8284$, such that the condition number is 17.1420. The dual windows for the two systems are shown in Figure 2.2. It is apparent that the shape of the second dual window is due to the high time-shift constant a for the second system.

For the case $A = B$ the frame is called tight. In this case $S = A \cdot \text{Id}$. (Id denotes the identity operator) and therefore $S^{-1} = \frac{1}{A} \text{Id}$. Tight frames will be further discussed in section 2.3.1.

In the next section the special case arising from applications in audio signal processing is discussed. By observing that in this case the frame operator takes a simple form, we will be able to suggest a fast way to calculate dual and tight windows.

2.3 The Bridge to Applications

Let us from now on assume that we are given a signal $f \in \mathbb{C}^L$. This signal represents a piece of music or a spoken sentence etc., which we want to investigate and/or modify. Modifications might aim to achieve noise reduction in old or degraded recordings, see e.g. [38]. Another issue might be the extraction of certain features of the signal, for example single instrument components. Let us further assume that an engineer approaches the problem by using a Fourier transform of length l in a first step. This implies that the window used for cutting out the part of interest must have this length. Looking at the definition of the Gabor coefficients:

$$c_{m,n} = \langle f, g_{m,n} \rangle = \sum_{j=0}^{L-1} f(j) \overline{g_{m,n}(j)}$$

as an inner product, which can be interpreted as correlation between the window and the respective part of the signal, we can see that the signals f and $g_{m,n}$ must have

the same length, at least theoretically. Practically, of course, as $l \ll L$, most of the “theoretical” g would be zero. As we don’t tend to waste computation time on multiplying with 0, only the *effective* length of g , here l , is multiplied with the part of interest of f . This procedure implicitly introduces a frequency lattice constant $b = \frac{L}{l}$. The time constant a is related to what is often called *overlap*. If $a = \frac{1}{2}$ or $a = \frac{1}{4}$, the overlap is $\frac{1}{2}$ and $\frac{3}{4}$, respectively. The redundancy of the representation is thus given by $red = \frac{l}{a}$, e.g., if the overlap is half the windowlength, we get twice as many datapoints as in the original signal. This is in accordance with the general case where

$$red = \frac{\frac{L}{a} \frac{L}{b}}{L} = \frac{L}{ab} = \frac{L}{a \frac{L}{l}} = \frac{l}{a}$$

Remark 2. The reduction of redundancy from L in the case of the full short-time Fourier transform to a reasonable amount of redundancy in the Gabor setting ensures a balance between computability on the one hand and sufficient localisation on the other hand. The choice of a reasonable window-length and overlap common in applications corresponds roughly to such a rather balanced situation in the Gabor setting. Gabor theory, though, allows for more general choices of lattices, concerning the redundancy as well as the distribution of the lattice-points. It also provides detailed knowledge about the dependance of results on the choice of analysis parameters. This is especially decisive in the case of modification of the synthesis coefficients, which are non-unique due to the redundant nature of the expansion. Modification on the coefficient level corresponds to applying *Gabor multipliers*, which will be discussed in Chapter 5 in detail.

Let us now look at the calculation of the inner products $c_{m,n} = \langle f, g_{m,n} \rangle$ more closely. We set

$$\mathbf{c}(j) := c_{m,n},$$

with $j = (n-1)a + m$ for $j = 1, \dots, k$, $m = 1, \dots, M$ and $n = 1, \dots, N$. Then the inner products can also be written as

$$\mathbf{c} = G \cdot f$$

where G is the operator (matrix) introduced in Section 2.2.2. G consists of blocks

$$G_n, \quad n = 0, \dots, N-1$$

each corresponding to one time-position of the window g . Defining g^l as the restriction of $g \in \mathbb{C}^L$ to its non-zero part of length l , we obtain the following. Up to a phase factor, the block G_n acts on the samples $f(na+1), \dots, f(na+l) =: f_{na}(t)$ by taking inner products of this slice f_{na} of the signal with each of the l modulated windows:

$$\begin{aligned} M_{mb} g^l(t) &= e^{\frac{-2\pi i m b t}{L}} g^l(t) \\ &= e^{\frac{-2\pi i m \frac{L}{l} t}{L}} g^l(t) = e^{\frac{-2\pi i m t}{l}} g^l(t) \end{aligned}$$

$m = 0, \dots, M-1 \quad \text{and} \quad t = 0, \dots, l-1$

The coefficients $e^{\frac{-2\pi imt}{l}}$ are exactly the entries of the Fourier matrix \mathcal{F}_l of the FFT of length l with $\hat{f} = \mathcal{F}_l f$. Therefore, up to a phase factor, which will be described in Theorem 1, we have

$$\begin{aligned} G_n f_{na} &= \mathcal{F}_l(f_{na} \cdot g^l) \\ n &= 0, \dots, N-1 \end{aligned}$$

and the action of G_n on f_{na} corresponds to multiplying f with g , skipping zero entries and taking the Fourier transform of the non-zero part. This allows for a fast implementation even for very long signals via the FFT.

Remark 3. Although for implementation in real-life situations, the FFT-approach is always preferred, it is useful to look at the expansion from an operator point of view. Many important theoretical issues, yielding better understanding also for the applications, can be investigated more easily. For example the dependance of the coefficients on the choice of window g , see [32], or the sensitivity of an expansion to perturbations of the signal or sampling lattice, see [13], are questions also of practical relevance. Additionally, as mentioned before, this approach is more flexible in allowing adaption to cases requiring other than the regular product lattice, see [25] or [47].

As mentioned before, all operators in Gabor theory generally act on the whole signal length L . In the definition of the building blocks $g_{m,n}$, the modulation operator is therefore defined as

$$M_{mb}g(t) = e^{\frac{-2\pi imbt}{L}}g(t) \text{ for } m = 0, \dots, N-1 \text{ and } t = 0, \dots, L-1$$

The blocks G_n , as opposed to the situation arising from implementation as discussed above, will not have identical entries, as the zero entries are in different positions.

Example 2. Let $g \in \mathbb{C}^{32}$ with

$$g(t) \begin{cases} \neq 0 & \text{for } t = 0, \dots, 7 \\ = 0 & \text{else} \end{cases}$$

Then (by assumption $b = \frac{L}{l}$, so that $e^{\frac{-2\pi imbt}{L}} = e^{\frac{-2\pi imt}{l}}$)

$$M_{mb}g(t) = (g(0), e^{\frac{-2\pi im}{l}}g(1), e^{\frac{-2\pi i2m}{l}}g(2), \dots, e^{\frac{-2\pi i7m}{l}}g(7), 0, \dots, 0)$$

whereas

$$M_{mb}T_ag(t) = (0, \dots, 0, e^{\frac{-2\pi ima}{l}}g(a), e^{\frac{-2\pi im(a+1)}{l}}g(a+1), \dots, e^{\frac{-2\pi im(a+7)}{l}}g(a+7), 0, \dots, 0)$$

$e^{\frac{-2\pi ima}{l}}$ is not necessarily 1, so that the blocks will differ by a phase factor.

The following statement makes the above considerations precise.

Theorem 1. *Let $g \in \mathbb{C}^L$ be a window function with*

$$g(t) \begin{cases} \neq 0 & \text{for } t = 0, \dots, l-1 \\ = 0 & \text{else} \end{cases}$$

where $\frac{L}{l} \in \mathbb{N}$. g^l is the restriction of g to its non-zero entries. Let furthermore $b = \frac{L}{l}$ and a be a divisor of l .

Then the blocks in the Gabor analysis matrix G differ from the identical blocks G_n in the matrix G^l arising from FFT _{l} -implementation only by a phase factor

$$w_0^{(d-1)ak}$$

where d is the block index, k is the row index in the respective block G_m of G and $w_0 = e^{\frac{-2\pi i}{l}}$.

Proof. The proof consists of a lengthy but trivial calculation. □

Corollary 1. *In the situation of Theorem 1, the Gabor coefficients $\mathbf{c} = G \cdot f$ are obtained from $\tilde{\mathbf{c}} = G^l \dot{f}$ by multiplication of a phase factor as follows:*

$$\mathbf{c}((n-1)a + m) = e^{\frac{-2\pi i(n-1)am}{l}} \tilde{\mathbf{c}}((n-1)a + m),$$

for $m = 1, \dots, M$ and $n = 1, \dots, N$.

Remark 4. The restriction that a be a divisor of l is also due to the usual choice of parameters in applications. Two common cases would be $a = \frac{l}{2}$ and $a = \frac{l}{4}$, in which cases the number of *different* kinds of blocks reduce to 2 and 4, respectively.

The difference only concerns the phase spectrum, which is usually not considered in further processing, except for reconstruction. The dual window does not depend on the phase factor in the case discussed in the theorem as will be seen below.

Implementation

An implementation of the STFT for long signals as well as its reconstruction in MATLAB can be found in the Appendix A.1.

Reconstruction of a signal from its STFT requires either the knowledge of the dual window or the usage of a tight frame. The next section shows how we can easily obtain tight and dual frames in the situation described above.

2.3.1 Mastering the frame operator - the Walnut representation

Let us now come back to the central question of how to find a set of windows $\tilde{g}_{m,n}$ for reconstruction as in (2.1). If it is possible to find a window \tilde{g} which is smooth and similar to the original window g especially in decaying to zero and if the rest

of the dual family can be deduced in analogy to the Gabor analysis function set by time-frequency shifts, this will make reconstruction in a kind of overlap-add process easier. In fact, all the above conditions can be fulfilled. Generally, the elements of the dual frame $(\tilde{g}_{m,n})$ are generated from a single function (the dual window \tilde{g}), just as the original family. This follows from the fact that S and S^{-1} (the frame operator and its inverse) commute with the modulation and translation operators M_{nb} and T_{ma} , for $m = 1, \dots, M$ and $n = 1, \dots, N$, see e.g. [15].

The higher redundancy, the closer the shape of the dual window gets to the original window's shape. As in applications redundancy of 2, 4 or even higher are common, well localised dual windows can be found. Even more is true. The special situation in which the effective length of the window g is equal to or shorter⁷ than the FFT-length, the frame operator takes a surprisingly simple form.

From the definition of the frame operator

$$Sf = \sum_{m,n} \langle f, g_{m,n} \rangle g_{m,n}$$

we deduce that the single entries of S are given by

$$S_{j,k} = \sum_{n=0}^{N-1} \sum_{m=0}^{M-1} M_{mb} T_{na} g(j) \overline{M_{mb} T_{na} g(k)}$$

Looking at the inner sum, note that $\sum_{m=0}^{M-1} e^{\frac{2\pi i m b(j-k)}{L}} = 0$ if $(j-k)$ is not equal to 0 or a multiple of M . In these cases

$$\sum_{m=0}^{M-1} e^{\frac{2\pi i m b(j-k)}{L}} = \sum_{m=0}^{M-1} e^{\frac{2\pi i m b M}{L}} \quad bM \equiv L \quad M$$

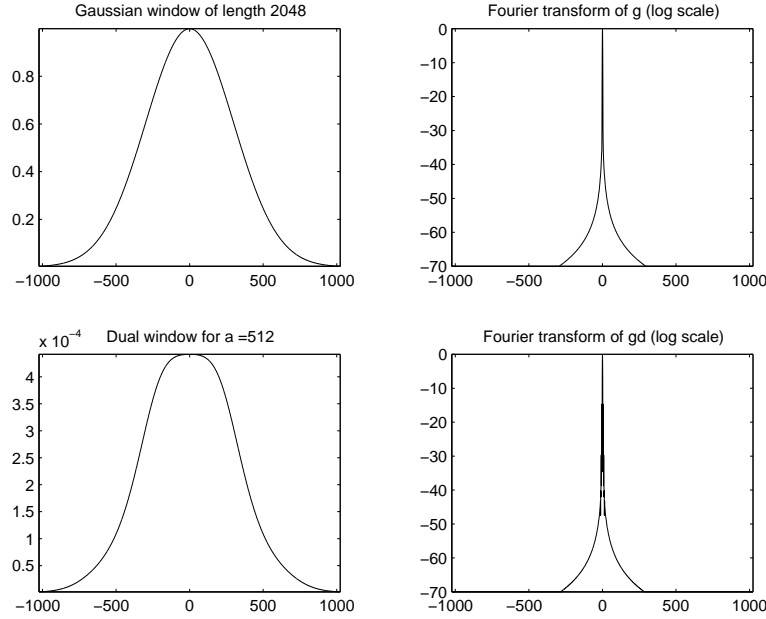
This leads to the *Walnut representation* [43] of the frame operator for the discrete case:

$$S_{jk} = \begin{cases} M \sum_{n=0}^{N-1} T_{na} g(j) \overline{T_{na} g(k)} & \text{if } |j-k| \bmod M = 0 \\ 0 & \text{else} \end{cases} \quad (2.2)$$

There will obviously be non-zero entries in the diagonal, $j = k$, but as $M = l$, i.e. the window-length, $j = k$ is in fact the only case for which $|j-k| \bmod M = 0$ holds and $g(j)$ and $g(k)$ both have non-zeros values. Therefore, the frame operator is diagonal and the dual window \tilde{g} is calculated as

$$\tilde{g}(t) = g / (M \sum_{n=0}^{N-1} T_{na} |g(t)|^2) \quad (2.3)$$

⁷E.g. in the case of zero padding.

Figure 2.3: *Gaussian window and dual window (Redundancy 4)*

Some dual windows

Figures 2.3 and 2.4 show a Gaussian window of length 2048 and a Hanning window of length 512, respectively, their duals and their Fourier transform. The Fourier transforms of the windows are shown in logarithmic scale in order to make the differences in frequency concentration more visible. The whole frequency range is shown. Note that the frequency concentration is very good for the Gaussian window and its dual (to 40db down). The weaker frequency concentration of the Hanning window's dual is due less overlap which leads to some more smearing in frequency. Note that this detail is one of the reasons why it has proved advisable to use a redundancy of 4 in overlap-add procedures.

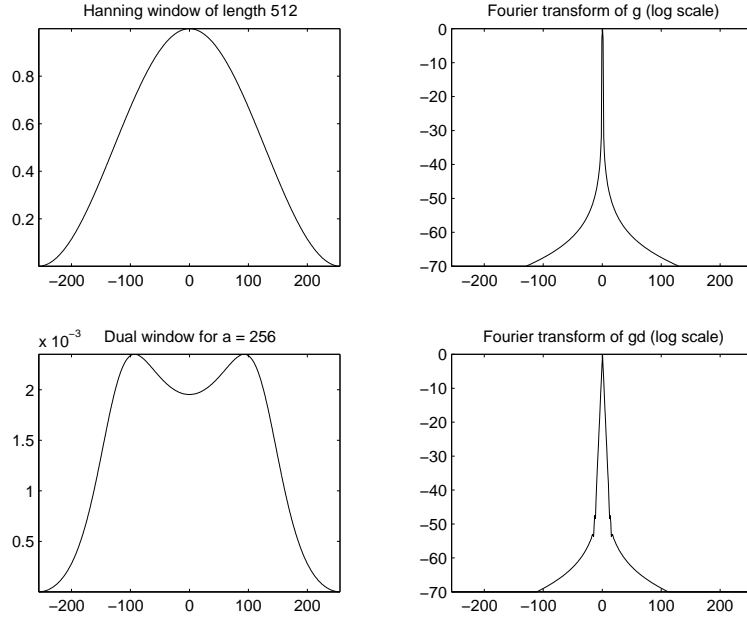
Tight frames: synthesising with the analysis window

The definition of a *tight frame* was given in section 2.2.2. As a matter of fact for any given Gabor frame a corresponding tight frame can be found for which $\tilde{g} = g$.

Note that the frame operator S is a positive and symmetric and therefore selfadjoint operator. Consequently S^{-1} and $S^{-\frac{1}{2}}$ are selfadjoint as well, moreover, they commute with each other and with S .

These properties allow the following manipulations of the expansion (2.1):

$$\begin{aligned} \sum_{m,n} \langle f, g_{m,n} \rangle \tilde{g}_{m,n} &= S^{-1} S f \\ &= S^{-\frac{1}{2}} S S^{-\frac{1}{2}} f = \sum_{m,n} \langle f, S^{-\frac{1}{2}} g_{m,n} \rangle S^{-\frac{1}{2}} g_{m,n} \end{aligned}$$

Figure 2.4: *Hanning window and dual window (Redundancy 2)*

Remark 5. Note that the tight window given by $g_t = S^{-\frac{1}{2}}g$ is closest to the original window in the following sense:

Let g be a window generating a frame for lattice constants a and b and let g_t be the tight window given as $g_t = S^{-\frac{1}{2}}g$. Then for any function h generating a tight frame for lattice constants a and b , the following holds [44]:

$$\|g - g_t\|_2 \leq \|g - h\|_2$$

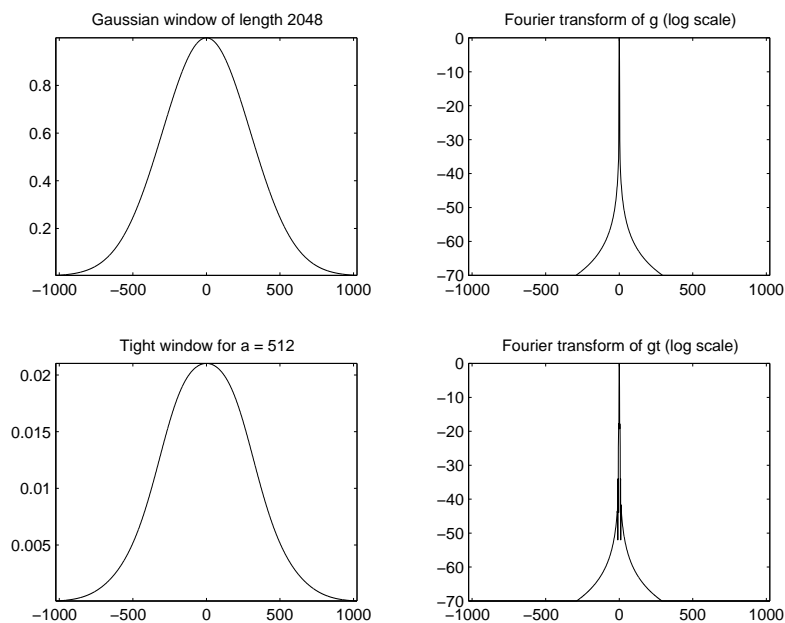
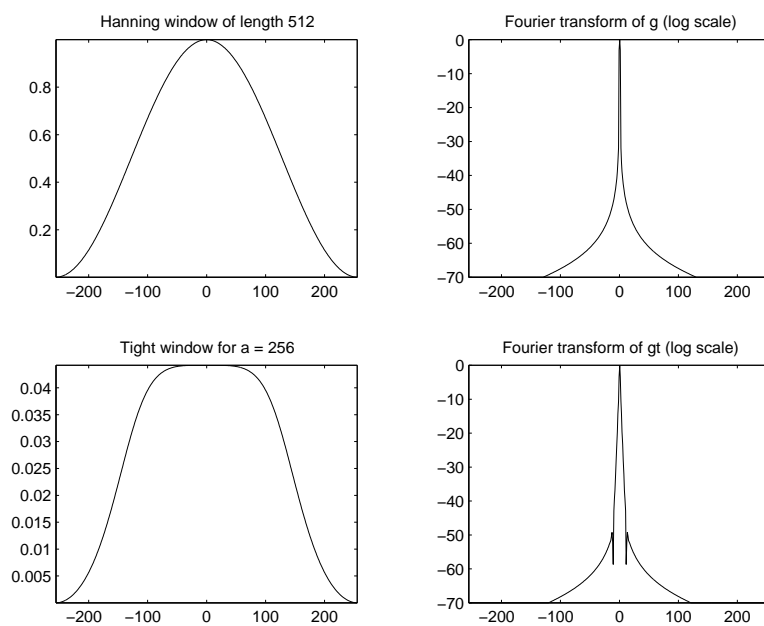
This result shows that the tight window calculated as $g_t = S^{-\frac{1}{2}}g$ combines the advantage of using the same window for analysis and synthesis with optimal similarity to a given analysis window. At the same time no “correction” by multiplication with a gain function is necessary after processing, which makes processing more efficient and the results less ambiguous in the case of modification of the synthesis coefficients.

The tight window g_t corresponding to a given window g and the time constant a can therefore be calculated as:

$$g_t = S^{-\frac{1}{2}}g = g / \sqrt{(M \sum_{n=0}^{N-1} T_{na} |g(t)|^2)}. \quad (2.4)$$

Some tight windows

Figures 2.5 and 2.6 show the same windows as before, the corresponding tight windows and their Fourier transform.

Figure 2.5: *Gaussian window and tight window (Redundancy 4)*Figure 2.6: *Hanning window and tight window (Redundancy 2)*

Implementation

The MATLAB code for calculating dual and tight windows for a given Gabor frame according to (2.3) and (2.4), respectively, can be found in the Appendix A.2.

2.4 A Lattice that reads the Music

When analysing any class of signals, one is naturally interested in features specific to that particular class. In the case of music signals, for example, transients are important for several reasons. They give important cues for onset timing, and they carry information about instrument timbre (often instrument perception hinges on the perception of transients.) As another example, in low-frequency regions, very fine frequency resolution is required, because notes in this region lay the harmonic basis, musically speaking. This is especially true in music such as Jazz, where the function of the bass determines the harmonic structure and function of the whole piece.

Although at first glance the above description suggests the usage of wavelets for the given problem, they have not yet been shown to be well-adapted for most applications in processing of music signals [20]. This is probably due to the fact that wavelet bases do not appropriately represent sinusoidal signal components, which constitute important parts of music signals. Several other approaches to deal with this problem are well-known; e.g. the use of wavelet packets, or certain classes of smoothed Wigner distributions [54].⁸

In this work we develop an approach using the background and tools of Gabor analysis in order to incorporate knowledge about the class of signals in question, by constructing a flexible, signal-adaptive partition of the time-frequency plane. We can thus overcome the drawbacks of uncertainty principle by tuning the time-frequency properties of the Gabor frame to the signal characteristics, while maintaining the appealing advantages, both practical and theoretical, of Gabor analysis.

The next section outlines this idea in more detail.

2.4.1 Adapting window and lattice

Time-frequency analysis is ubiquitous in audio signal processing. Dictionaries of time-frequency atoms play an important role in signal analysis, synthesis [9] and modification, in algorithms such as matching pursuit [50] and basis pursuit [11], as well as for compression and coding of digital signals [63]. Of course, the choice of a particular dictionary D is dependent upon the application at hand. In the design of dictionaries for signal processing, two factors are to be considered. On the one hand, any dictionary should be complete for the class of signals under inspection, on the other hand a priori knowledge can be used to keep the size of the dictionary and therefore the

⁸In fact, the modulus squared of the short-time Fourier transform itself (the spectrogram) may be shown to be a smoothed Wigner distribution, in which the smoothing kernel is the Wigner transform of the window function used in the analysis, see [17].

amount of computational cost to a minimum. It is trivial to construct complete or over-complete dictionaries for $\mathbf{L}^2(\mathbb{R})$; however, the difficulty lies in constructing the dictionary to bring up a salient representation for the class of signals most likely to be encountered. A natural first step, then, is to choose the atoms of the dictionary to best model the structures in the class of signals under consideration. Of course, despite strong a priori believe in such structures, the dictionary must be capable of representing arbitrary signals which may be encountered. It is obviously impractical to have overall unnecessarily high redundancy. Thus, in a certain sense, an optimal dictionary results from smart design, allowing a salient representation at a minimum computational cost.

In order to achieve a setting adapted to music as discussed above, it will be necessary to use wider windows with good frequency concentration in low-frequency regions, whereas in the high-pass regions, where mainly transients and broadband signals components occur, rather short windows, which don't have to be very localised in frequency, will be of use.

Figure 2.7 illustrates the effect of the usage of windows of different widths. The plots show the Gabor transform of a short segment from a piece performed by a piano, a double-bass and a drummer. The signal was analysed with two Gaussian windows of different widths. From the resulting spectrograms it becomes obvious that especially in low frequency regions, the wider window yields a far better representation of the signal components. Signal components which are close in frequency become blurred if the analysing window is too narrow hence yielding a bad frequency resolution. Note that the two Gabor systems generating the results have the *same* redundancy. On the other hand, in high frequency regions, we are interested in precise time resolution, hence, windows with a small essential support in the time-domain should be used.

2.4.2 A new approach: Multiple Gabor systems

Classical time-frequency analysis with redundant systems is restricted by using systems with the *same* time-frequency resolution for the whole time-frequency plane. Intuitively, what we are looking for is a generalisation of a tiling of the time-frequency plane by means of wavelet packages or local Fourier bases, see [50]. However, we want to give up the restriction that the system in use has to be an (orthogonal) basis. We develop a new approach that allows us to locally use Gabor systems which are well suited to the characteristics of a given signal or class of signals. We can construct frames corresponding to this idea, by using sets of building blocks corresponding to the frequency region they cover. These new frames will be called *multiple Gabor frames*, emphasising that various different Gabor frames are used to generate the new system. The reconstruction of a signal in the context of Gabor analysis is accomplished by first finding a dual family of building blocks and then effecting an expansion similar to a basis expansion, as given in (1.6). In order to keep reconstruction feasible, the frequency regions corresponding to the different sets of building blocks must be overlapping. An approximate reconstruction can then be accomplished by means of *local*

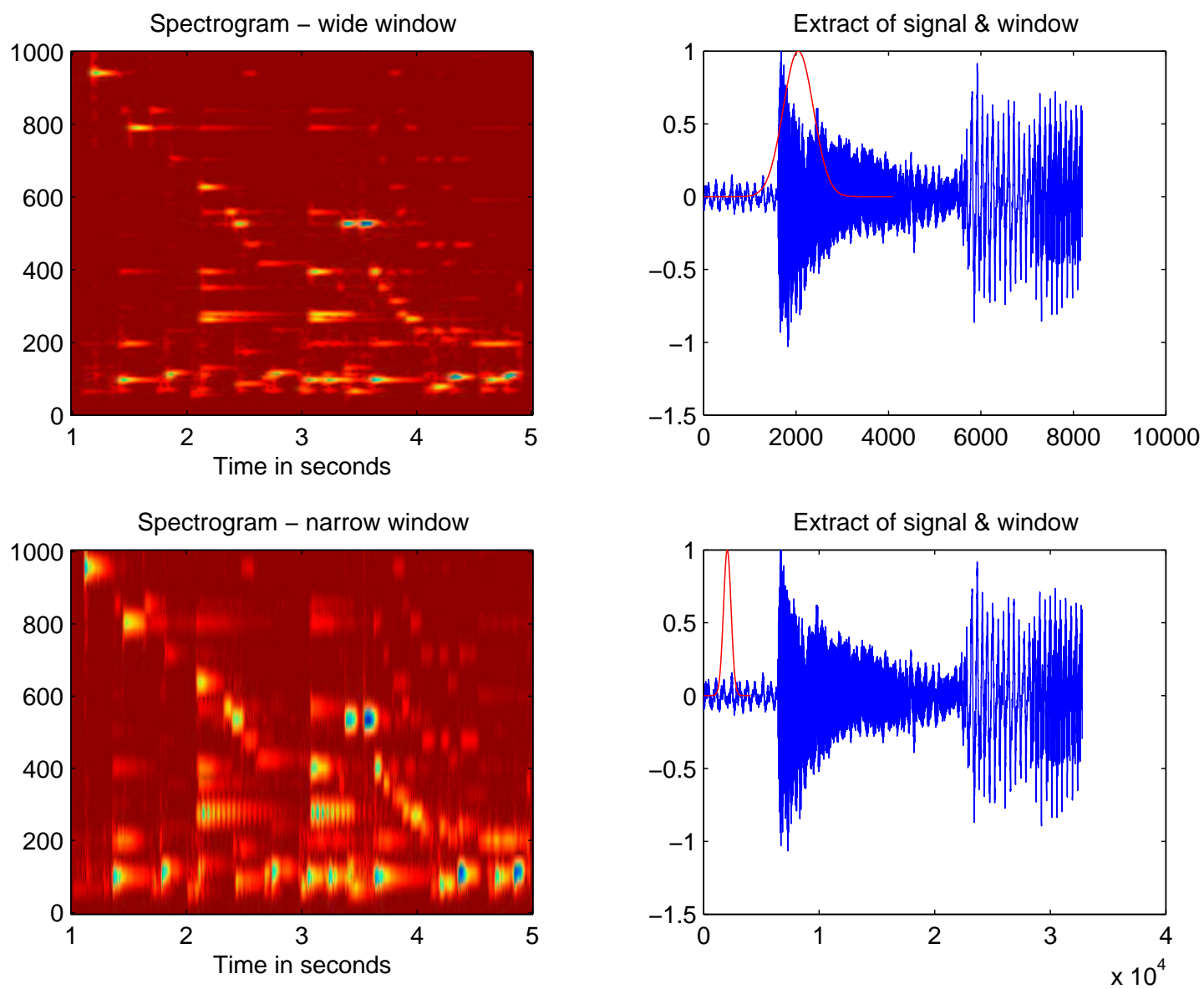


Figure 2.7: *Two windows and resulting STFT of music signal.*

dual families, resembling the dual families of the original systems.

2.5 Outline

Now we give a brief outline of the rest of this work. In Chapter 3 the idea of multiple Gabor frames will be studied in detail for the special case of strictly band-limited or compactly supported windows. This special case is interesting for applications, such as noise reduction. An example application is briefly described and some results on real signals are given. The main theoretical result consists of showing that the system constructed from different given Gabor frames is indeed a frame. In order to be able to state a similar result for more general windows with good time-frequency concentration, we introduce a result on compactness in modulation spaces in Chapter 4.

The theory of Gabor multipliers is not only closely related to the issue of localised Gabor systems, it also establishes a theory of time-variant filtering in the Gabor context, a topic of particular interest for the processing of music signals. Gabor-multipliers are discussed in detail in Chapter 5.

Chapter 6 develops some theory on partitioning of functions in the time-frequency plane. A norm-equivalence result is shown to hold for functions in S_0 .

Finally, with all these ingredients at hand, in Chapter 7 we can prove a general result for multiple Gabor frames with windows in S_0 .

Chapter 3

Multiple Gabor Frames

This chapter gives an introduction to the theory and applications of the new concept of multiple Gabor systems. We consider the construction of variable resolution Gabor dictionaries appropriate for audio signal analysis. Motivated by a desire for parsimony and efficiency, we propose and formalise the idea of reduced multi-Gabor systems, showing that they constitute a frame for $L^2(\mathbb{R})$ and other Hilbert spaces of interest. In order to demonstrate the practical usefulness of such a scheme, we apply it to the atomic decomposition of music and speech signals observed in noise. Qualitative results indicate the potential of this method to yield a salient representation of typical audio signals while at the same time reducing computational costs as compared to a full multi window decomposition.

3.1 Main Idea

It is the aim of this chapter to construct a partition of the time-frequency plane which is adapted to audio signals of practical interest, such as speech and music. We propose to start from principles of Gabor analysis [35], which is particularly suited to the processing of audio signals. It employs sinusoidal building blocks, which are a natural choice for (Western) music and furthermore assure (through the existence of the FFT) a fast implementation. Having particular potential for music signals, it can at the same time be developed in a rigorous, general framework which will allow extensions to other applications and signal types. The theoretical rigor, however, precludes neither the intuitive nature nor the applicability of the final outcome, furthermore yields the existence of reconstruction methods. Beyond the necessity of reconstruction for applications such as signal modification and enhancement, by methods from Gabor analysis we ensure that the given representation is related to the signal in a well-defined manner, and that no potentially important parts of information are lost. Roughly speaking, the idea is the following:

Assume that a BAPU $(\psi_r)_{r \in I}$ (bounded admissible partition of unity, see Definition 4 in Section 3.2.1) of \mathbb{R} (time-domain) or $(\phi_r)_{r \in I}$ of $\hat{\mathbb{R}}$ (frequency-domain) is given, so

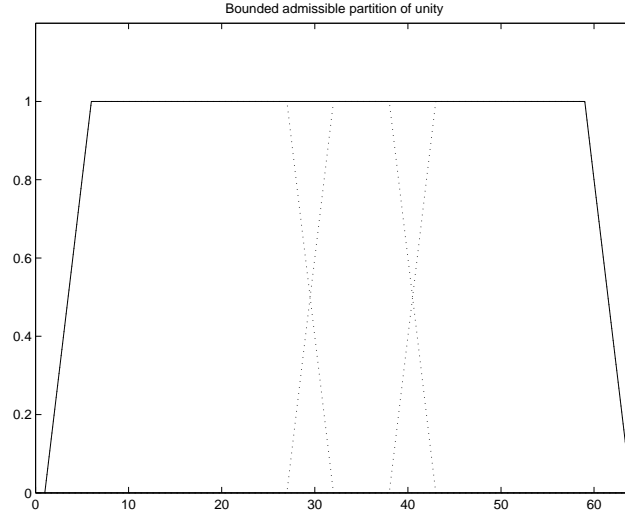


Figure 3.1: *Members of a BAPU (dotted) summing up to 1.*

that

$$f = \sum_{r \in I} \psi_r \cdot f \quad \text{for all } f \in \mathbf{L}^2(\mathbb{R}),$$

and $\text{supp}(\psi_r) \subseteq \Omega_r$ or

$$\hat{f} = \sum_{r \in I} \phi_r \cdot \hat{f} \quad \text{for all } f \in \mathbf{L}^2(\mathbb{R}),$$

and $\text{supp}(\phi_r) \subseteq \hat{\Omega}_r$, respectively. We assume that the $(\psi_r)_{r \in I}$ are derived from a ψ_0 by a coordinate transform $\Upsilon_{\alpha,r}$. Ω_0 , the support of ψ_0 must be a compact neighborhood of 0, i.e., in \mathbb{R} , a closed interval containing 0. $\Upsilon_{\alpha,r}$ might just be a translation by $r \cdot \alpha$, in which case the BAPU is a BUPU (bounded uniform partition of unity) and with $\Omega_0 = [-t_0, t_0]$, $\Omega_r = r\alpha + [-t_0, t_0]$. As another example, $\Upsilon_{\alpha,r}$ might be composed of a dilation followed by a translation, such that different Gabor systems are used for bandwidths of varying size. Figure 3.1 shows an example for a typical BAPU in \mathbb{R} .

Assuming, now, that different given Gabor frames have been assigned to the localised regions determined by the support of ψ_r for all $r \in \mathcal{I}$, we show that with a certain overlap between the different localised families, the new system will constitute a frame again. The resulting frame will be called a multiple Gabor frame.

As an application, this approach has been successfully applied to the task of denoising corrupted audio signals via a reconstruction within a multiple Gabor scheme, see also [66].

3.1.1 Multi-window Gabor expansions

Driven by the desire to better model natural signals, the notion of *multi-window* Gabor expansions [69] has become increasingly popular. As opposed to the original Gabor analysis, a finite number of windows of different shape are being used in order to obtain

a richer dictionary with the ability to better represent certain characteristics in a given signal class. Let \mathcal{H} be the Hilbert space of functions of interest.¹ The representation of a signal $f \in \mathcal{H}$ can then be written as:

$$f = \sum_{r=0}^{R-1} \sum_{m,n \in \mathbb{Z}} c_{m,n}^r g_{m,n}^r,$$

where $c_{m,n}^r$ are the expansion coefficients, and the Gabor atoms $g_{m,n}^r$ are given by time-frequency shifts of distinct window functions g_r :

$$g_{m,n}^r(t) = g_r(t - na_r) e^{j2\pi mb_r t}, \quad m, n \in \mathbb{Z},$$

where $a_r, b_r > 0$ are the time-frequency shift parameters corresponding to the R different windows.

In general, it is not necessary for the R distinct windows to have the same shape or effective support. A wavelet-type scheme can be constructed by exploiting this degree of freedom [67]: given a window function g , let $g_r(t) = \alpha^{-\frac{r}{2}} g(\alpha^{-r} t)$ where α and β are positive real numbers such that for all $r \in \{0, 1, \dots, R-1\}$, $a_r = \beta \alpha^r$ and $a_r b_r = R/d$. We then have

$$g_{m,n}^r(t) = \alpha^{-\frac{r}{2}} g_r(\alpha^{-r} t - n\beta) e^{j2\pi m t / M_r}. \quad (3.1)$$

Defined in this manner, the width of the window is proportional to a_r and the atoms exhibit scaling similar to that of wavelets.

Note that the different systems, which arise from the definitions given above, can be transformed into each other by metaplectic transforms and will therefore, as Gabor frames, have the same quality, cf. [40], and the following example.

Example 3 (Different lattices). If a Gabor system (g, Λ) is a (tight) frame with frame bounds A and B for $L^2(\mathbb{R})$, where Λ is a product lattice of the form $a\mathbb{Z} \times b\mathbb{Z}$, then the system

$$(D_{2^l} g, D_{2^l} \Lambda),$$

where

$$D_{2^l} g(t) := g(2^l x) \text{ (Dilation)}$$

and

$$D_{2^l} \Lambda = \frac{a}{2^l} \mathbb{Z} \times 2^l b \mathbb{Z},$$

is a (tight) frame with frame bounds $\frac{A}{2^l}$ and $\frac{B}{2^l}$.

This follows easily from the fact that

$$\sum_k \sum_n |\langle f, M_{2bk} T_{\frac{a}{2}n} D_{2^l} g \rangle|^2 = \frac{1}{4} \sum_k \sum_n |\langle D_{\frac{1}{2}} f, M_{bk} T_{an} g \rangle|^2,$$

and, as $D_2 = 2D_{\frac{1}{2}}^*$,

$$\|D_{\frac{1}{2}} f\|_2^2 = 2 \langle D_2 D_{\frac{1}{2}} f, f \rangle = 2 \|f\|_2^2.$$

¹According to the application at hand, this might be $\mathbf{L}^2(\mathbb{R})$, $l^2(\mathbb{Z})$ or just \mathbb{C}^L .

According to the multi-window approach, the dictionary will have high redundancy as it is basically the combination of R complete Gabor dictionaries.² Due to the structure of audio signals as discussed above, it is an appealing idea to reduce this highly redundant dictionary to fit to the special characteristics of these signals.

3.1.2 Reducing the size of a multi-window Gabor dictionary

The main motivation for using distinct Gabor schemes in different regions of the time-frequency plane in the analysis of audio signals is given by the observation that harmonic, sustained signal components mainly occur in low frequency regions, in which therefore long windows can and should be used, whereas in high frequency regions transient signal components are encountered, which are better described using short windows with higher bandwidth. The next section is going to show that this concept is realisable and leads to a valid model.

3.2 Multiple Gabor Frames

Figure 3.2 schematically illustrates the construction of a multiple Gabor frame from various distinct Gabor frames. The following sections will make the concept precise.

3.2.1 Preliminaries

We start by formalizing the notion of a *bounded admissible partition of unity*, see Figure 3.1, which will serve as a tool for assigning appropriate Gabor systems to different regions in the time-frequency plane.

Definition 4. A family $\Omega = (\Omega_r)_{r \in \mathcal{I}}$ of intervals of \mathbb{R} is called an **admissible covering** of \mathbb{R} if

- $\bigcup_{r \in \mathcal{I}} \Omega_r = \mathbb{R}$
- There exists $n_0 \in \mathbb{N}$ such that $|r^*| \leq n_0$ for all $r \in \mathcal{I}$, where

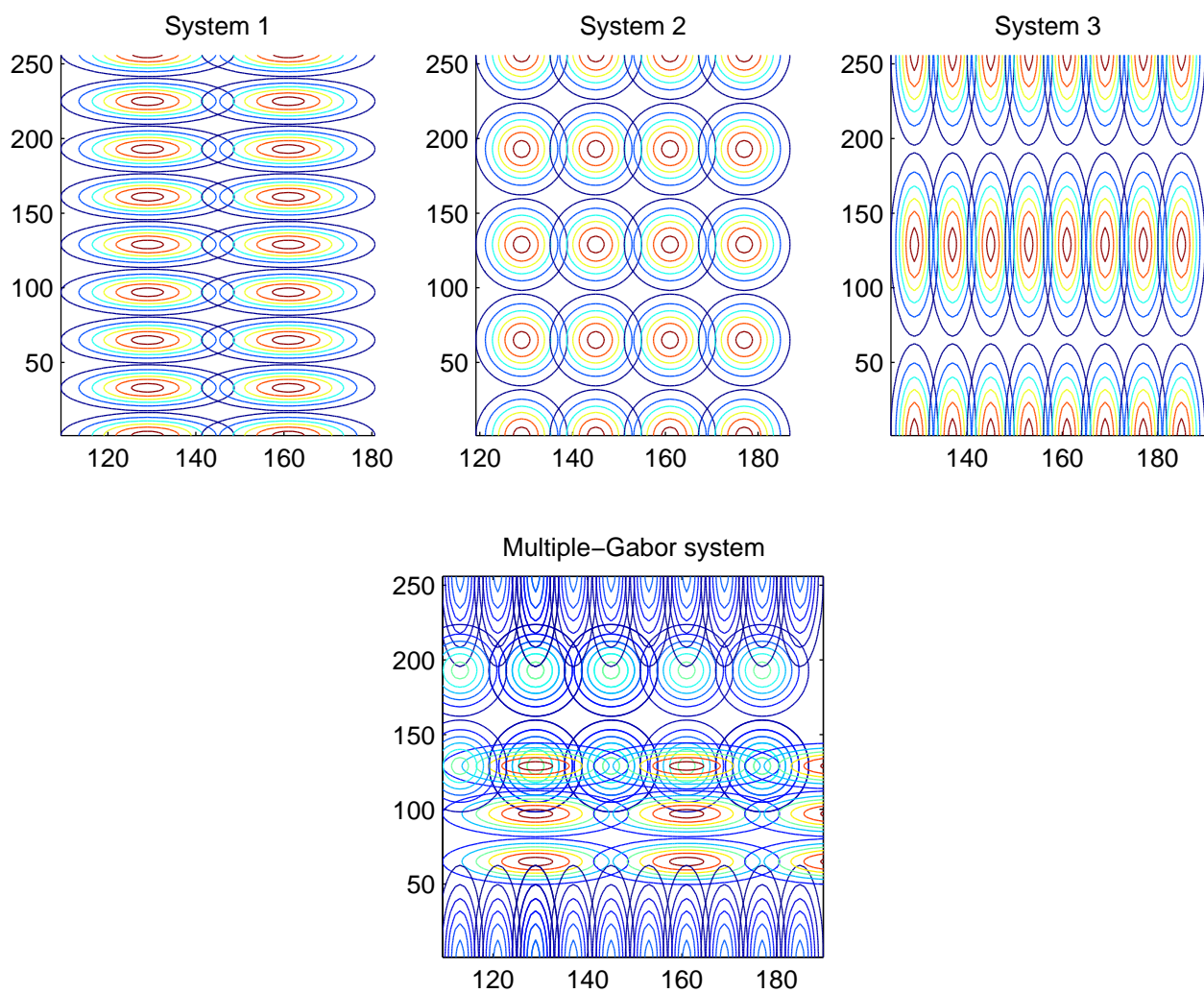
$$r^* \stackrel{\text{def}}{=} \{s : s \in \mathcal{I}, \Omega_s \cap \Omega_r \neq \emptyset\}.$$

(Admissibility condition)

Given an admissible covering $\Omega = (\Omega_r)_{r \in \mathcal{I}}$ of \mathbb{R} , a family $(\psi_r)_{r \in \mathcal{I}}$ is called a **bounded admissible partition of unity (BAPU)** subordinate to $\Omega = (\Omega_r)_{r \in \mathcal{I}}$ in $L^2(\mathbb{R})$ if the following is satisfied:

- $0 \leq |\psi_r(x)| \leq 1$

²In Section 6.3 $\Omega = (\Omega_r)_{r \in \mathcal{I}}$ a criterion to determine completeness of multi-window systems will be presented.

Figure 3.2: *Constructing multiple Gabor frames*

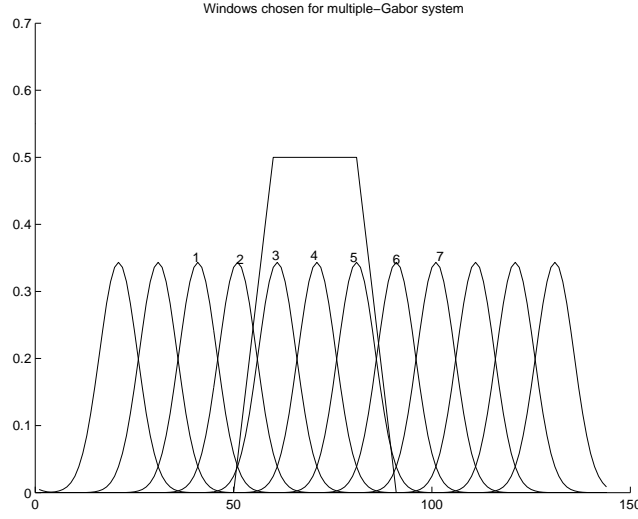


Figure 3.3: A member of the BAPU and translates of the corresponding window family.

- $\psi_r(x) = 0$ for all $x \in \mathbb{R} \setminus \Omega_r$
- $\sum_{r \in \mathcal{I}} \psi_r(x) = 1$ for all $x \in \mathbb{R}$.

For further notational convenience we define

$$\psi_{r^*} \stackrel{\text{def}}{=} \sum_{r \in r^*} \psi_r$$

and $\text{supp } f$, the support of a function $f \in L^2(\Omega)$, as the closure of the set where $f \neq 0$.

3.2.2 Existence of reduced multiple Gabor frames

We now show that *reduced* multiple Gabor frames can be constructed. The situation described in [69] is a special case of Theorem 2 obtained by setting $\mathcal{I}^r = \mathbb{Z} \times \mathbb{Z}$ for all r .

In practical situations, the windows in the given Gabor systems $(g_{m,n}^r)$ will necessarily have compact support in either the time or frequency domain. We first assume that the (g^r) and hence all $(g_{m,n}^r)$ are compactly supported. As $(\psi_r)_{r \in \mathcal{I}}$, the members of the BAPU, have compact support by definition, the number of $n \in \mathbb{Z}$ such that $\text{supp } \psi_r \cap \text{supp } T_{an} g^r \neq \emptyset$ is finite for all $r \in \mathcal{I}$. Using this simple fact, we can construct index sets $\mathcal{I}^r \subseteq \mathbb{Z} \times \mathbb{Z}$, such that $\text{supp } \psi_r \cap \text{supp } g_{m,n}^r = \emptyset$ for all $m, n \notin \mathcal{I}^r$, such that the windows with index $m, n \notin \mathcal{I}^r$ can be omitted from the system without loss of information. In this case, the index sets $\mathcal{I}^r \subseteq \mathbb{Z} \times \mathbb{Z}$ will have the form $[n_1^r, \dots, n_2^r] \times \mathbb{Z}$. The construction of these index sets is illustrated in Figure 3.3. The figure shows a member of the BAPU, ψ_r , and the family of translates of the window g^r . In this schematic example, 7 time-indexes lead to non-empty overlap with ψ_r . If we choose the basic atoms such that the g_r are bandlimited, i.e. \hat{g}_r , $r \in \{1, 2, \dots, R\}$, where

\hat{g} denotes the Fourier transform of a function g , have compact support, we obtain a completely analogous situation in the frequency domain. By invariance of $L^2(\mathbb{R})$ under Fourier transform, the following theorem shows that a *reduced* multiple Gabor frame can be constructed in the time-or the frequency-domain.

Theorem 2. *Given Gabor frames $(g_{m,n}^r)_{r \in \mathcal{I}}$ for $L^2(\mathbb{R})$ and a BAPU $(\psi_r)_{r \in \mathcal{I}}$ of \mathbb{R} with the additional property that index sets $\mathcal{I}^r \subseteq \mathbb{Z} \times \mathbb{Z}$ can be chosen such that*

$$\text{supp } \psi_r \cap \text{supp } g_{m,n}^r = \emptyset \text{ for all } m, n \notin \mathcal{I}^r, \quad (3.2)$$

then

$$(g_{m,n}^r)_{r \in \mathcal{I}; m, n \in \mathcal{I}^r} \quad (3.3)$$

is a frame for $L^2(\mathbb{R})$.

Proof. Note that by assumption there exist frame bounds A_r and B_r for the given frames $(g_{m,n}^r)_{r \in \mathcal{I}}$. To find an upper frame bound B for the combined multi-Gabor system (3.3), note that for all $f \in L^2(\mathbb{R})$

$$\begin{aligned} \sum_r \sum_{m, n \in \mathcal{I}^r} |\langle f, g_{m,n}^r \rangle|^2 &= \sum_r \sum_{m, n \in \mathcal{I}^r} \left| \left\langle \sum_{r'} \psi_{r'} f, g_{m,n}^r \right\rangle \right|^2 \\ &= \sum_r \sum_{m, n \in \mathbb{Z}} |\langle f \psi_{r^*}, g_{m,n}^r \rangle|^2, \end{aligned}$$

due to condition (3.2). For $B = \max_r B_r$, this yields

$$\sum_r \sum_{m, n \in \mathcal{I}^r} |\langle f, g_{m,n}^r \rangle|^2 \leq B \sum_r \|f \psi_{r^*}\|^2$$

Due to the admissibility condition for (ψ_r) , we have

$$\sum_r \|f \psi_{r^*}\|^2 \leq n_0 \|f\|^2$$

and thus find the upper frame bound of the combined family (3.3) to be bounded above by $\max_r (B_r) n_0$.

A lower bound is given by $A = \min_r (A_r)$, as, by $f = \sum_{r'} f \psi_{r'}$, we have for all $r \in \mathcal{I}$:

$$\begin{aligned} A \|f\|_2^2 &\leq \sum_r \sum_{m, n \in \mathbb{Z}} \left| \left\langle \sum_{r'} \psi_{r'} f, g_{m,n}^r \right\rangle \right|^2 \\ &= \sum_r \sum_{m, n \in \mathcal{I}^r} |\langle f \psi_{r^*}, g_{m,n}^r \rangle|^2 \end{aligned}$$

because of condition (3.2). Therefore

$$A \|f\|_2^2 \leq \sum_r \sum_{m, n \in \mathcal{I}^r} |\langle f, g_{m,n}^r \rangle|^2,$$

as $0 \leq |\psi_{r^*}(x)| \leq 1$. This completes the proof. \square

3.3 Application: Gabor Regression

Recall that a Gabor frame admits a representation of any $f \in \mathcal{H}$, and that such a frame may be constructed as we have detailed in Section 3.2.2. In such a multi-window Gabor scheme it is not necessary for the R distinct windows to have the same shape or effective support. By exploiting this degree of freedom it is possible to construct a multi-window expansion in which the atoms exhibit scaling similar to that of wavelets [67].³ Following [51], we make use of such a dictionary for the purpose of demonstrating our proposed reduced multi-Gabor scheme.

We consider the task of noise-reduction, a prominent issue in the processing of audio signals, see [38, 5].

3.3.1 Gabor regression using a general linear model

For the purpose of demonstrating the application of a reduced multi-Gabor dictionary to regression via atomic decomposition, we assume an additive observation model

$$\mathbf{y} = \mathbf{x} + \mathbf{e},$$

where $\mathbf{y} = [y_0 \ y_1 \ \dots \ y_{N-1}]^T$ is the vector of the observed waveform, \mathbf{x} is that of the underlying (audio) signal we wish to estimate, and \mathbf{e} is an independent, identically distributed, continuous Gaussian noise process with variance σ^2 .

Let the atomic decomposition of $\mathbf{x} \in \mathbb{R}^N$ be given by a reduced multi-Gabor system represented by the $N \times K$ matrix \mathcal{G} , with the individual synthesis atoms forming its K columns. Our goal is to select elements of \mathcal{G} to efficiently represent the underlying audio signal \mathbf{x} based on the observed waveform \mathbf{y} . This may be accomplished with the help of a diagonal matrix of (unobservable) binary indicator variables $\mathbf{\Gamma}$ such that $\mathbf{G}_k = \mathcal{G}\mathbf{\Gamma}_k$ for any one of 2^K particular configurations $\mathbf{\Gamma}_k$. Thus we wish to select the most parsimonious linear model k such that

$$\mathbf{y} = \mathbf{G}_k \mathbf{c}_k + \mathbf{e},$$

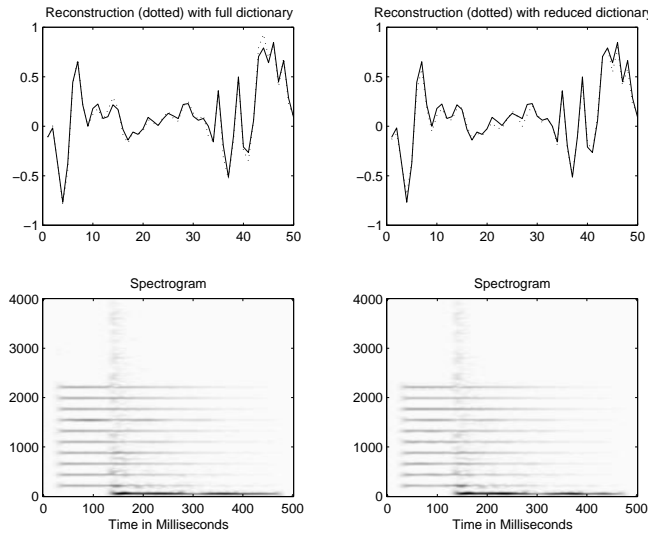
and hence the resultant likelihood over all possible choices of model may be formulated as

$$p(\mathbf{y}|\mathbf{\Gamma}, \mathbf{c}, \sigma^2) = \frac{1}{(2\pi\sigma^2)^{\frac{N}{2}}} \exp\left(-\frac{1}{2\sigma^2}\|\mathbf{y} - \mathcal{G}\mathbf{\Gamma}\mathbf{c}\|^2\right).$$

By posing this variable selection problem in a Bayesian framework we may assign prior distributions to the unknown parameters $(\mathbf{\Gamma}, \mathbf{c}, \sigma^2)$ and formulate the optimal posterior estimate of \mathbf{x} given \mathbf{y} .⁴ As the resultant posterior distribution cannot in general be evaluated analytically, we sample from it using Markov chain Monte Carlo methods [60].

³Note that the different systems arising from the definitions given above may be transformed into one other by metaplectic transforms, and will therefore, as Gabor frames, have the same quality [40].

⁴For example, by computing it as a function of the posterior mean taken over all possible models.

Figure 3.4: *Reconstruction of sample signal*

3.3.2 Performance of the proposed scheme

We now demonstrate two examples illustrating the performance of this scheme. In the first case a signal comprising sustained sinusoidal components, as well as a transient component generated from a MIDI sample of a drum sound, has been synthesised to test the performance of the reduced dictionary as compared to its counterpart with full frequency coverage at each of four resolution levels. To this end a reduced multi-Gabor wavelet-type dictionary has been employed, along with its corresponding full version. Figure 3.4 shows a section of the original signal and its time-domain estimate, as well as spectrograms of the respective reconstructions. In this case the reconstruction performance is similar, and the application of a reduced dictionary has lowered the computational cost by a factor of 4.5 with respect to the full version thereof.

The second example is a short segment of speech, sampled at 16 kHz and artificially degraded by additive white Gaussian noise to yield a signal-to-noise ratio (SNR) of 20 dB. Figure 3.5 shows a comparison of the original and degraded versions of this signal. A reduced Gabor dictionary comprising four equi-spaced, overlapping resolutions levels, each of an approximate bandwidth of 3 kHz, was applied in order to estimate the underlying signal as described in Section 3.3.1. Figure 3.6 shows a comparison of the minimum mean-square error reconstruction of this signal, with the noise variance set to its true value, taken after the Markov chain of the employed Gibbs sampler appeared to have reached a stationary regime.

In this case again the reduced dictionary performs on a par with the full dictionary. For this particular example, the resultant SNR for the reduced dictionary is only 1.5 dB lower than for the full one, and the required number of flops was reduced by a factor of 2.5. Additionally, the reduced dictionary yields a more parsimonious representation of the signal, employing approximately 7 000 atoms (out of a total of over 13 000) as

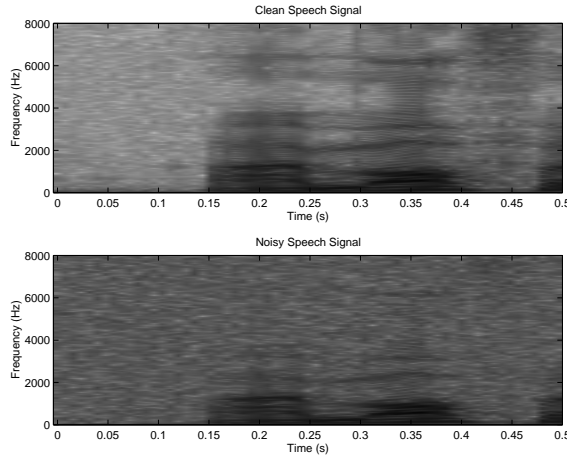


Figure 3.5: *Spectrograms of the noisy and clean speech signal*

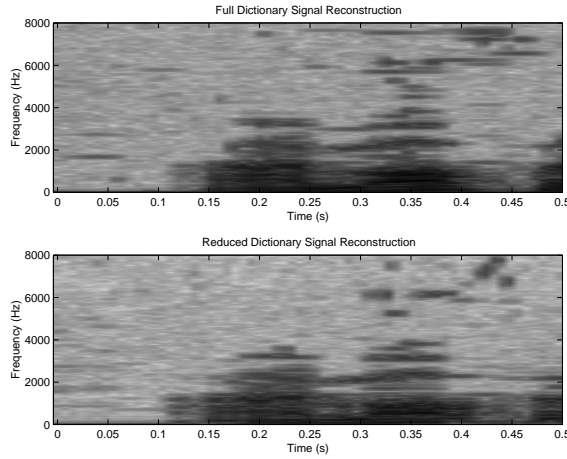


Figure 3.6: *Comparison of speech signal reconstruction using a full and reduced dictionary*

compared to over 17 000 (out of a total of over 32 000) in the case of the full dictionary.

3.4 Dual Frame and Reconstruction

Once coefficients are obtained by means of a multiple Gabor frame, one is naturally interested in finding a way of reconstruction of the original or modified signal. On the other hand, as is the case in the application described in Section 3.3.1, if the given frame is used for synthesis, one might be interested in obtaining a robust initialization. In both cases, we need to find a dual frame or a reliable approximation thereof.

3.4.1 Existence of dual frame

As stated in Chapter 1, it follows immediately from the frame condition (1.5) that a dual frame exists for any valid frame. Hence, once a dual frame is found, reconstruction of f according to (1.6) is possible. The canonical dual frame (*the* dual frame) is, by definition, the inverse of the frame operator applied to the original frame. For single Gabor systems as well as the multi-window scheme introduced in Section 3.1.1, the dual frame has the same coherent structure as the original frame, i.e. it can be obtained by applying the same time-frequency shifts to the basic building block g of the r different windows g^r .

In the case of a reduced multi-Gabor frame, interferences occur in the transition regions between the different (overlapping) Gabor schemes, thus complicating the calculation of the dual frame. However, numerical experiments indicate that *inside* the individual frequency regions, the members of the global dual frame can be well approximated by the corresponding members of the dual frames of the original single global systems. *Approximate* dual frames can thus be obtained by applying the same time-frequency shifts to a basic dual window over the respective points in the time-frequency plane. The next section explains the idea of approximate dual frames in more detail and in Section 3.4.3 some numerical experiments are presented.

3.4.2 Approximation of the dual frame

For the given Gabor frames $(g_{m,n}^r)_{r \in \mathcal{I}}$ let $(\tilde{g}_{m,n}^r)_{r \in \mathcal{I}}$ denote the canonical dual frames, hence, for all f we have a reconstruction by means of these dual frames. In particular, for all $r \in \mathcal{I}$ we can write $\psi_r f = \sum_{m,n \in \mathbb{Z}} \langle \psi_r f, \tilde{g}_{m,n}^r \rangle g_{m,n}^r$. Assuming, now, that the $(\tilde{g}_{m,n}^r)_{r \in \mathcal{I}}$ have the same or similar compact support in time- or frequency-domain, we may conclude that $(\psi_r \cdot \tilde{g}_{m,n}^r)_{m,n \in \mathbb{Z}, r \in \mathcal{I}}$ is a dual frame for the frame given in (3.3). In a more general situation, however, this argument fails. For example, it cannot be generally assumed, that the dual frames have the same, compact support as the original frames, see [6]. A natural question arising in this context is how the frames constructed from the original dual frames by the same time-frequency shifts and restriction to certain areas of the time-frequency plane relate to the canonical dual frames of system (3.3).

Remark 6. Corollary 4 in Section 5.7 will give a precise characterization of the local inversion of *partial* frame operators, i.e., operators corresponding to a certain local system.⁵ Intuitively the reasoning is as follows: Despite the fact that we are not dealing with linear independent elements, we expect that for elements g^r which are sufficiently time-frequency concentrated, we can assume almost independence for elements well-separated in the time-frequency plane. In particular, in the case of the multiple Gabor frames as constructed above, we assume that an approximate inversion can be performed locally. By the nature of our construction, elements originating from a certain system should not influence the inversion well inside the regions of the time-frequency

⁵These operators can be understood as time-frequency localization operators, see also Section 5.7.1.

plane assigned to a different system. Furthermore, any signal, and in particular the building blocks from one of the given systems, which is concentrated in the *interior* of one of the regions of interest in the time-frequency plane, will hardly be affected by any of the other systems. Corollary 4 will show by means of eigenanalysis of the partial frame operators, that these heuristic arguments can in fact be made precise. Following the statement in Corollary 4, the interior of a region corresponding to a local Gabor system can be described as the subspace generated by the eigenvectors belonging to the most salient eigenvalues of the partial frame operator.

The subsequently described simulations were carried out to answer the following questions:

- What does the dual system of the multiple Gabor frame look like?
- Can an (approximate) dual frame be generated by applying the same transformations to the given 'basic' dual windows, which generated the multi-Gabor frame?
- How well can a given signal f be reconstructed by means of these approximate dual frames?

3.4.3 Numerical simulations

Numerical simulations have been performed in MATLAB to observe the behavior of dual systems of multiple Gabor frames.

Experiment 1

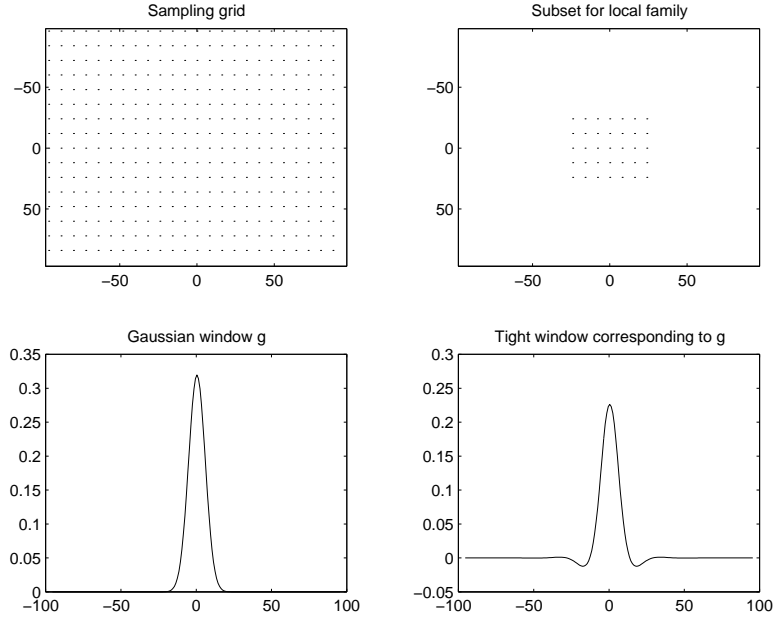
In a numerical setting the minimal-norm dual family for any family of building blocks can be found by calculating the *pseudo-inverse* of the matrix comprised of the original family's members.⁶ For any $k \times L$ -matrix M a *singular value decomposition* exists, by which M can be written as

$$M = V \cdot D \cdot U'.$$

Here, D is a $k \times L$ -matrix with non-zero values only for D_{jj} , $j \leq \text{rank}(M)$ and V and U are unitary matrices comprised of the eigenvectors of $M \cdot M'$ and $M' \cdot M$, respectively. Now in the case of a local set of building blocks, k , the number of blocks, will be a lot smaller than L , the length of the signal. Furthermore, due to the redundancy of the given Gabor frames only r_1 singular values for $r_1 < \text{rank}(M)$ will lie above a given threshold $\rho : 0 < \rho < 1$.

Remark 7. This threshold corresponds to the threshold defining the interior of time-frequency localization operators in Corollary 4. Note that the eigenvalues of these operators are exactly the singular values D_{jj} squared.

⁶See [12] for more details about frames and pseudo-inverses.

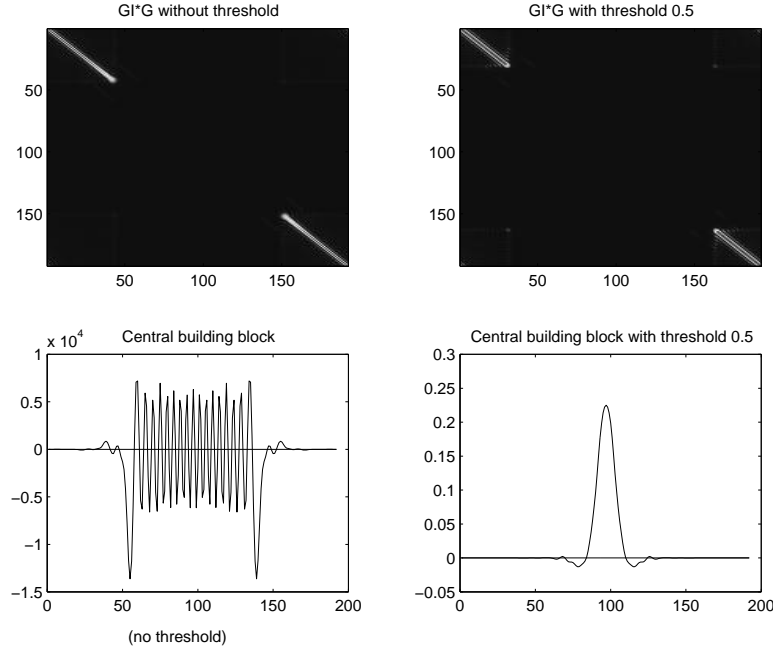
Figure 3.7: *Sampling Lattice for full Gabor family and subset.*

Considering that only singular values above the threshold ρ correspond to salient eigenvalues in the construction of the pseudo-inverse, all singular values below ρ may be set to zero in the inversion. The eigenvectors of $M' \cdot M$ corresponding to small singular values are concentrated at the boundary of the area of interest, whereas eigenvectors corresponding to 0 will be concentrated outside this region. The pseudo-inverse of M is given by

$$M^+ = U' \cdot (D')^{-1} \cdot V$$

where $(D')^{-1}$ is the matrix D with inverted non-zero entries. From this we can see that the eigenvectors corresponding to low singular values will blow up in the calculation of M^+ , so that all members of the true dual family would be concentrated at the boundary of the region of interest. This can be avoided by means of a thresholding routine as described above. The resulting family of atoms thus only represents an approximately dual to the original one. On the other hand the time-frequency concentration of the approximate dual family is similar to the original building blocks' behavior. In particular, we hope to be able to get an appropriate approximation by means of time-frequency shifted version of *one* basic (dual) window, i.e., that the locally coherent structure is maintained.

Figures 3.7 and 3.8 illustrate this situation for a subfamily of building blocks in a Gabor family. Figure 3.7 shows the full sampling lattice and the subset corresponding to the given local family, the analysis window and corresponding tight window. Figure 3.8 shows the operator corresponding to reconstruction with true and approximate dual families and a typical member of the respective families. Note that the approximate dual window is very similar to the original tight window. This means that inside the

Figure 3.8: *Exact and approximate local dual window*

regions covered by one adaptive sub-family, the overall dual frame will have members similar to those of the dual frame of a regular Gabor analysis family, whereas at the boundaries modifications will be necessary.

Experiment 2

We next address the question whether a collection of overlapping patches according to requested local resolution can be constructed in the manner described in Experiment 2. The second experiment investigates a system comprising three different local families as depicted in Figure 3.9. The windows and their dual windows (normalized) corresponding to the complete lattice are shown in the lower plots in Figure 3.9. The lattice constants were $a_1 = 8$, $b_1 = 9$; $a_2 = 4$, $b_2 = 12$ and $a_3 = 12$, $b_3 = 3$, respectively. Now the pseudo-inverse G_{mul}^+ of the analysis matrix G_{mul} , composed of the three local systems as shown in Figure 3.9, was calculated. The members of the system thus obtained were then compared to the approximate dual family, yielding the matrix \tilde{G}_{mul}^+ . \tilde{G}_{mul}^+ was constructed in analogy to the construction of the original multiple Gabor frame, using the dual windows of the original families. The results are shown in Figure 3.10 and Figures 3.11 to 3.14. Figure 3.10 shows the product $\tilde{G}_{mul}^+ \cdot G_{mul}$, which represents the analysis/synthesis operator. It is apparent that the operator is close to the identity, close to 0 off the diagonal. The deviation from constant 1 in the diagonal is mainly due to the overlap of the different regions in the time-frequency plane, which has to be made up for by scaling of the windows in \tilde{G}_{mul}^+ . Figures 3.11 to 3.13 show the behavior of the windows in G_{mul}^+ and \tilde{G}_{mul}^+ , respectively,

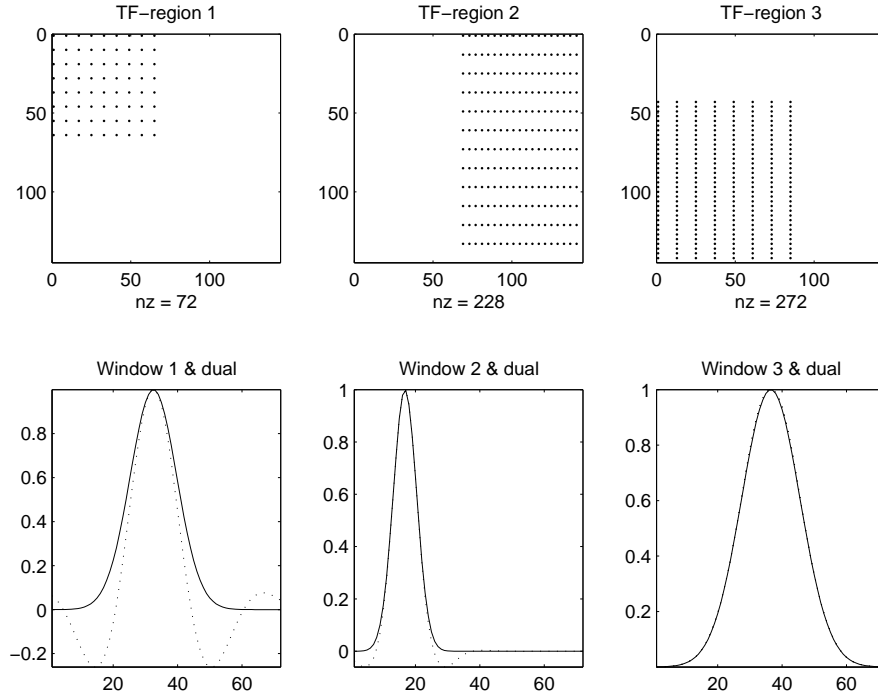


Figure 3.9: *The three local systems. The dual windows are dotted.*

in more detail.

Example 1 and Example 4 are typical for the behavior for members of the system situated well inside one of the time-frequency regions, whereas the two other examples clearly show the bias in the transient regions between different systems.

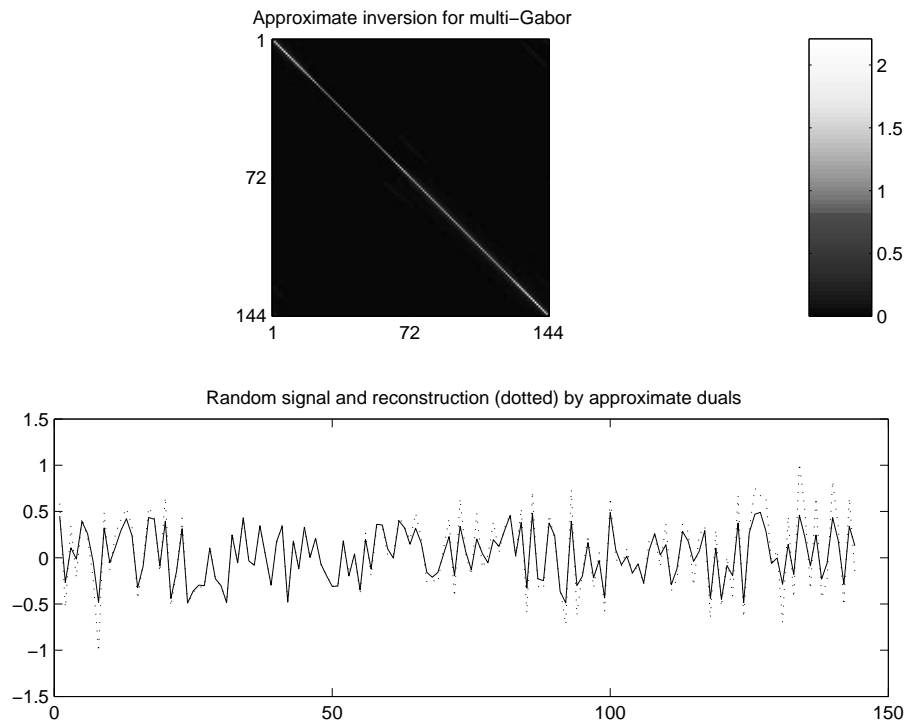
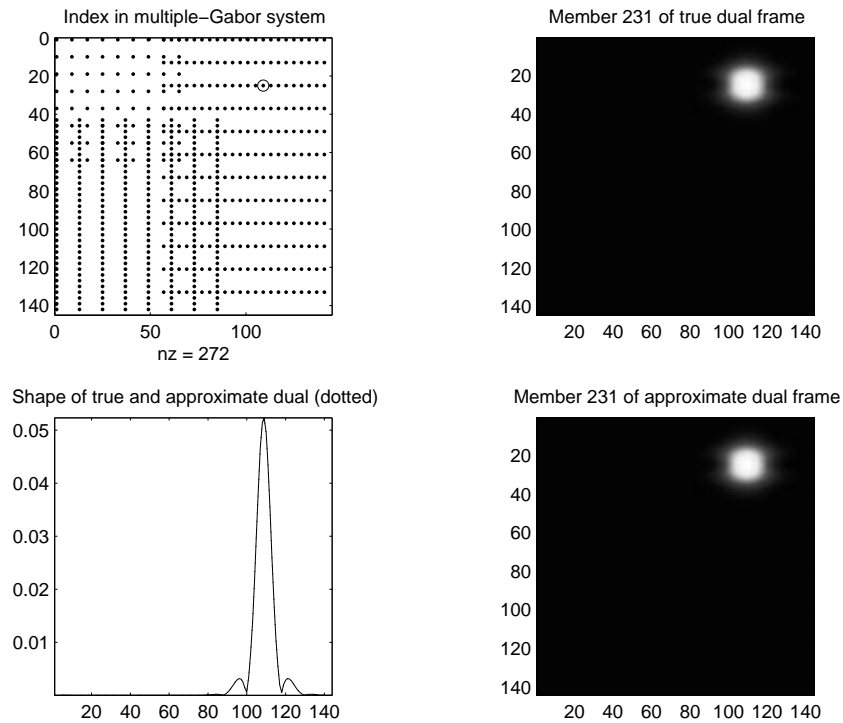
Discussion

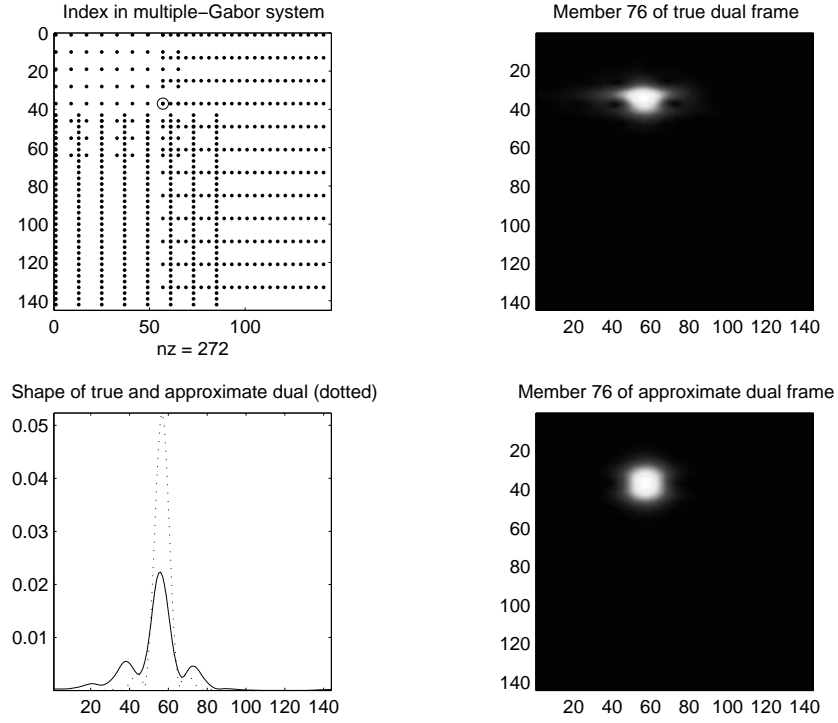
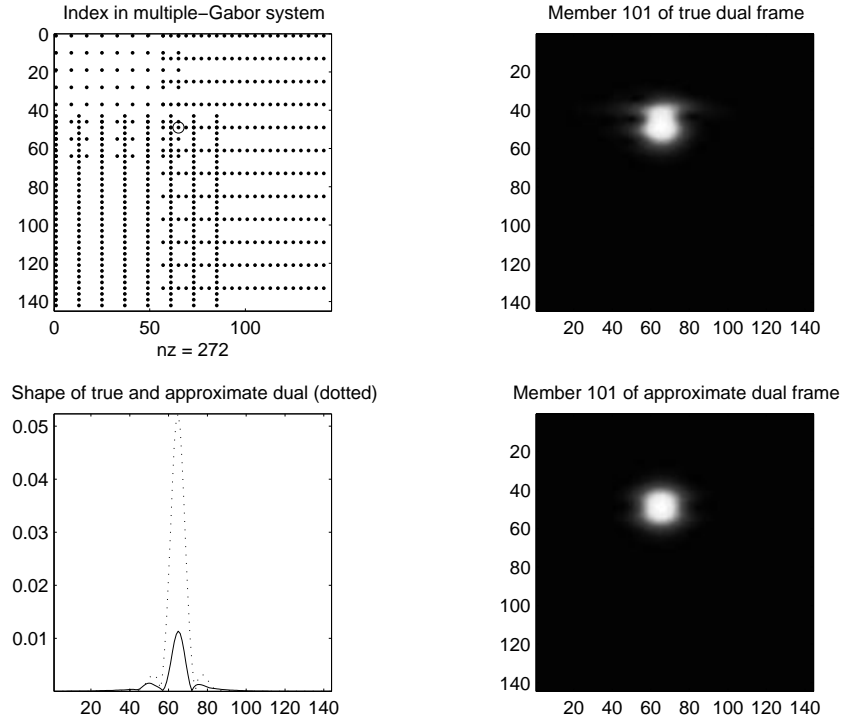
Typically, the true dual windows are only weakly biased inside the distinct regions localized in time-frequency. In the transient regions between the local systems the bias is considerable, as expected. On the one hand the bias is due to the overlap between the systems. The overlap is necessary for completeness of the multiple Gabor frame and can be made up for by appropriate scaling according to the partition of unity in use.

The remaining bias is mainly reflected in the non-zero off-diagonal entries of the matrix $\tilde{G}_{mul}^+ \cdot G_{mul}$, as shown in Figure 3.10. We expect this bias to be negligible after an appropriate rescaling of the approximate dual frame.

3.5 Generalisations

The condition that the windows are all compact or strictly band-limited is far too restrictive for a more general theory. In Chapter 7 we give a statement corresponding

Figure 3.10: *Reconstruction by means of approximate dual family.*Figure 3.11: *Example 1 for behavior of dual frame*

Figure 3.12: *Example 2 for behavior of dual frame*Figure 3.13: *Example 3 for behavior of dual frame*

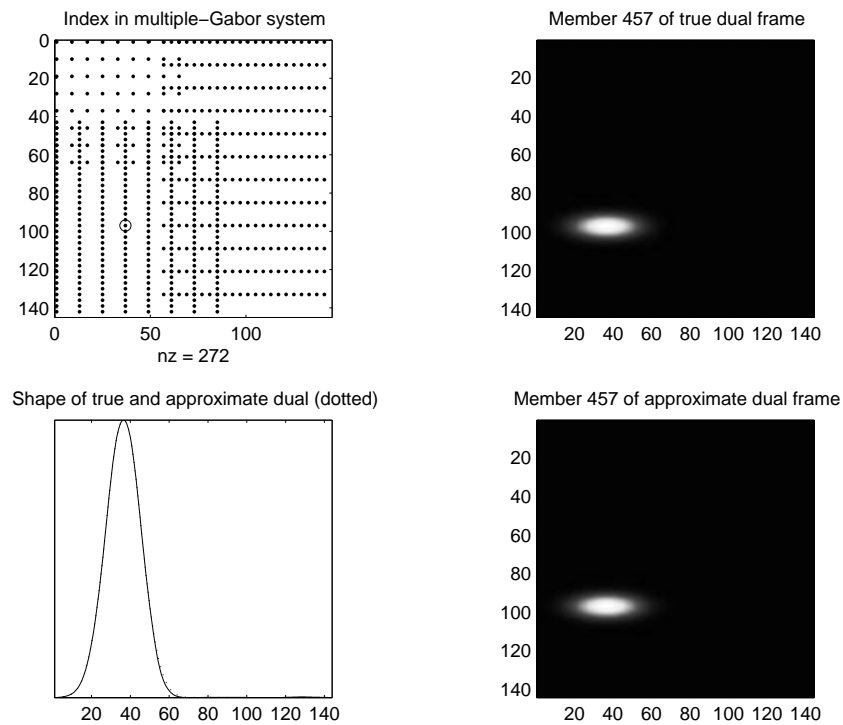


Figure 3.14: *Example 4 for behavior of dual frame*

to the main statement of this chapter in Theorem 4 for a more general class of windows. The next chapter provides a compactness result, which will be needed in the construction of multiple Gabor systems in more general situations.

Chapter 4

Compactness Criteria in Modulation Spaces

In this chapter we present a criterion for compactness based on the short-time Fourier transform. We show, that the classical criterion for compactness in Banach spaces of functions can be reformulated into a simple tightness condition in the time-frequency domain. This description preserves more explicitly the symmetry between time and frequency than the classical conditions. In particular, we show that the criterion can be applied in modulation spaces, which are defined by integrability conditions on the STFT. The result is first stated and proved for $\mathbf{L}^2(\mathbb{R}^d)$, and then generalized to modulation spaces. An important member of the class of modulation spaces is S_0 , also known as Feichtinger's algebra. The results of this chapter have been given in a more general context for the class of coorbit spaces, including classes of function spaces such as Besov-Triebel-Lizorkin spaces or Bargmann-Fock spaces, see [19].

4.1 Introduction

Compactness in function spaces is usually characterized by conditions of the Arzela-Ascoli type. Typically, what is necessary is an equicontinuity condition with respect to the norm of the space under consideration. If the underlying topological space is not compact, then in addition a tightness condition is required, i.e., all functions have the same “essential” support. The prototype of such a result is the characterization of compactness in L^p -spaces, which in its general form on locally compact abelian groups is due to A. Weil. In the sequel χ_U will denote the indicator function of a compact set U .

Theorem 3 ([65]). *A closed and bounded subset S of $\mathbf{L}^p(\mathbb{R}^d)$ for $1 \leq p < \infty$ is compact if and only if the following conditions are satisfied:*

(i) *Equicontinuity: for all $\epsilon > 0$ there exists $\delta > 0$ such that*

$$\sup_{f \in S} \sup_{|h| \leq \delta} \|f(\cdot - h) - f\|_p < \epsilon. \quad (4.1)$$

(ii) *Tightness: for all $\epsilon > 0$ there exists a compact set U in \mathbb{R}^d , such that*

$$\sup_{f \in S} \|f \chi_U - f\|_p < \epsilon. \quad (4.2)$$

Far-reaching generalizations of Theorem 3 for general translation invariant Banach spaces of distributions with a so-called double module structure were proved in [22].

Specializing to $\mathbf{L}^2(\mathbb{R}^d)$, it is well-known and not difficult to see that the equicontinuity condition (4.1) is equivalent to the tightness of the Fourier transforms $\hat{S} = \{\hat{f} : f \in S\}$ in $\mathbf{L}^2(\mathbb{R}^d)$. In particular, *a closed and bounded set $S \subseteq \mathbf{L}^2(\mathbb{R}^d)$ is compact if and only if S and \hat{S} are both tight in $\mathbf{L}^2(\mathbb{R}^d)$, see [22] and [53].*

The symmetry of this characterization under the Fourier transform motivated us to look at analytic tools which are designed expressly to deal with situations that treat a function and its Fourier transform *simultaneously* and to search for a characterization of compactness by means of these tools. In this regard the short-time Fourier transform is the tool that is used most frequently to describe both time and frequency simultaneously, i.e., a function and its Fourier transform. Recall that the short-time Fourier transform (STFT) of a function $f \in \mathbf{L}^2(\mathbb{R}^d)$ with respect to a window function $g \in \mathbf{L}^2(\mathbb{R}^d)$ is defined as

$$\mathcal{V}_g f(x, \omega) = \int_{\mathbb{R}^d} f(t) \bar{g}(t - x) e^{-2\pi i \omega \cdot t} dt = \langle f, M_\omega T_x g \rangle. \quad (4.3)$$

With slightly different normalization, the short-time Fourier transform also occurs under the names “(radar) ambiguity function” or “(cross-)Wigner distribution”, see [40]. For suitable windows g , e.g. g in the Schwartz class $\mathcal{V}(\mathbb{R}^d)$, the value $\mathcal{V}_g f(x, \omega)$ can be interpreted as a measure for the energy of f at $z = (x, \omega) \in \mathbb{R}^{2d}$. An important property in the study of compactness is the isometry property of the short-time Fourier transform which states that for any $f, g \in \mathbf{L}^2(\mathbb{R}^d)$:

$$\|\mathcal{V}_g f\|_2 = \|g\|_2 \|f\|_2. \quad (4.4)$$

It becomes intuitively obvious that a condition comprising the support conditions given in Theorem 3 for time and frequency separately can be formulated as a simultaneous tightness condition in time and frequency via the short-time Fourier transform.

Theorem 4 (Compactness in $\mathbf{L}^2(\mathbb{R}^d)$). *For a closed and bounded set $S \subseteq \mathbf{L}^2(\mathbb{R}^d)$ the following statements are equivalent:*

- (i) *S is compact in $\mathbf{L}^2(\mathbb{R}^d)$.*
- (ii) *The set $\{\mathcal{V}_g f : f \in S\}$ is tight in $\mathbf{L}^2(\mathbb{R}^{2d})$, this means that for all $\epsilon > 0$ exists a compact set $U \subseteq \mathbb{R}^{2d}$, such that*

$$\sup_{f \in S} \left(\int_{U^c} |\mathcal{V}_g f(x, \omega)|^2 dx d\omega \right)^{\frac{1}{2}} < \epsilon. \quad (4.5)$$

Proof. To get an understanding of the conditions necessary for the desired generalization, we give the pretty proof of this theorem right here. Without loss of generality we assume that $\|g\|_2 = 1$, so that \mathcal{V}_g is an isometry on $\mathbf{L}^2(\mathbb{R}^d)$.

(i) \Rightarrow (ii): By compactness of S we can find f_1, \dots, f_n such that

$$\min_{j=1, \dots, n} \|f - f_j\|_2 < \frac{\epsilon}{2} \quad \text{for all } f \in S.$$

Since $\mathcal{V}_g f_j \in \mathbf{L}^2(\mathbb{R}^{2d})$ by (4.4), we may choose a compact set $U \subseteq \mathbb{R}^{2d}$ such that $\int_{U^c} |\mathcal{V}_g f_j(x, \omega)|^2 dx d\omega < \epsilon^2/4$ for $j = 1, \dots, n$. By (4.4) we obtain for arbitrary $f \in S$ that

$$\begin{aligned} & \left(\int_{U^c} |\mathcal{V}_g f(x, \omega)|^2 dx d\omega \right)^{\frac{1}{2}} \\ & \leq \min_{j=1, \dots, n} \left\{ \left(\int_{U^c} |\mathcal{V}_g(f - f_j)(x, \omega)|^2 dx d\omega \right)^{\frac{1}{2}} + \left(\int_{U^c} |\mathcal{V}_g f_j(x, \omega)|^2 dx d\omega \right)^{\frac{1}{2}} \right\} \\ & \leq \min_j \|f - f_j\|_2 + \frac{\epsilon}{2} < \epsilon \end{aligned}$$

(ii) \Rightarrow (i): It suffices to show that every sequence (f_n) in S contains a convergent subsequence. By (ii) we can choose a compact set $U \subseteq \mathbb{R}^{2d}$ such that

$$\int_{U^c} |\mathcal{V}_g f(x, \omega)|^2 dx d\omega < \epsilon^2 \quad (4.6)$$

holds for all $f \in S$, in particular for the sequence (f_n) . Since by assumption S is bounded, it is weakly compact in $\mathbf{L}^2(\mathbb{R}^d)$ and thus (f_n) possesses a weakly convergent subsequence $f_j = f_{n_j}$ with limit f , i.e., $\langle f_j, h \rangle \rightarrow \langle f, h \rangle$ for all $h \in \mathbf{L}^2(\mathbb{R}^d)$. Choosing $h = M_\omega T_x g$ for $(x, \omega) \in \mathbb{R}^{2d}$, this implies the pointwise convergence of the short-time Fourier transforms

$$\mathcal{V}_g f_j(x, \omega) \rightarrow \mathcal{V}_g f(x, \omega) \quad \text{for } x, \omega \in \mathbb{R}^d. \quad (4.7)$$

Since by (4.3) and the Cauchy-Schwarz inequality we have for all (x, ω)

$$|\mathcal{V}_g(f - f_j)(x, \omega)| \leq \|f - f_j\|_2 \leq \sup_j \|f_j\|_2 + \|f\|_2 < C,$$

the restriction of $|\mathcal{V}_g(f - f_j)|^2$ to U is dominated by the constant function $C^2 \chi_U \in \mathbf{L}^1(\mathbb{R}^d)$. In view of (4.7) we may now apply the dominated convergence theorem and obtain:

$$\int_U |\mathcal{V}_g(f - f_j)(x, \omega)|^2 dx d\omega \rightarrow 0. \quad (4.8)$$

The combination of (4.8) and (4.6) now yields

$$\begin{aligned} \overline{\lim}_{j \rightarrow \infty} \|f - f_j\|_2 &= \overline{\lim}_{j \rightarrow \infty} \|\mathcal{V}_g(f - f_j)\|_2 \\ &\leq \overline{\lim}_{j \rightarrow \infty} \left(\int_U |\mathcal{V}_g(f - f_j)(x, \omega)|^2 dx d\omega \right)^{\frac{1}{2}} + \overline{\lim}_{j \rightarrow \infty} \left(\int_{U^c} |\mathcal{V}_g(f - f_j)(x, \omega)|^2 dx d\omega \right)^{\frac{1}{2}} \\ &\leq 0 + 2\epsilon \end{aligned}$$

Therefore $\lim_{j \rightarrow \infty} \|f - f_j\|_2 = 0$ and thus S is compact. \square

Theorem 4 and its proof suggest several extensions. On the one hand, we may replace the \mathbf{L}^2 -norm of the short-time Fourier transform by other norms and ask for which function spaces we can still characterize compactness as in Theorem 4. Pursuing this idea leads to the characterization of compactness in the so-called modulation spaces, which are of interest for this work and will be treated in detail in the sequel. On the other hand, if we are willing to give up the time-frequency interpretation of Theorems 3 and 4, we may replace the short-time Fourier transform by other transforms. Another example occurring in modern analysis is the wavelet transform, which shares the important isometry property with the STFT [15]. The same proof as for Theorem 4 with the wavelet transform in place of the STFT yields a similar criterion for compactness in $\mathbf{L}^2(\mathbb{R}^d)$, see [19].

The STFT and the wavelet transform do have other properties in common. Both are defined as the inner product of f with the action of a group of unitary operators on a fixed function g . More precisely, both the STFT and the wavelet transform are *representation coefficients* of a certain unitary continuous representations π of a group \mathcal{G} on a Hilbert space \mathcal{H} . This observation has been very fruitful for the evolution of a general wavelet theory associating a family of abstract function spaces, the so-called *coorbit spaces*, [33, 34, 39], to each irreducible unitary continuous representation π of a locally compact group on a Hilbert space \mathcal{H} . In our context, we are mainly interested in the class of spaces associated with the STFT, the so-called modulation spaces. The STFT can be interpreted as representation coefficients of the Heisenberg group with respect to the Schrödinger representation, see [19] and [40, Chapter 9] for details. We shall take the proof of Theorem 4 as an outline to obtain a compactness criterion for modulation spaces. However, the generalization of the proof to a non-Hilbert space context requires additional considerations on the properties of the Banach spaces under inspection. These concern the validity of dominated convergence and the theorem of Alaoglu-Bourbaki. We will show that the weighted mixed-norm spaces which are involved in the definition of modulation spaces, satisfy all necessary conditions for a straight-forward generalization of Theorem 4.

4.2 Modulation Spaces

4.2.1 Preliminaries and definition

We first recall the definition of the weighted mixed-norm spaces $\mathbf{L}_m^{p,q}(\mathbb{R}^{2d})$.

Definition 5 (Weight function). *A weight function m is a non-negative, integrable function on \mathbb{R}^{2d} . It is called submultiplicative, if m satisfies $m(z_1 + z_2) \leq m(z_1)m(z_2)$ and $m(z_1) \geq 1$ for all $z_1, z_2 \in \mathbb{R}^{2d}$. m is called s -moderate, if $m(z) \leq C\nu(z)$, with $\nu(z) = (1 + |z|)^s$ for some $s \geq 0$ and all $z \in \mathbb{R}^{2d}$.*

Remark 8. In practice weights of polynomial type are most commonly used, i.e. $\nu_s(z) = (1 + |z|)^s$, $z \in \mathbb{R}^{2d}$. To quantify faster decay, the subexponential weights $\nu(z) = e^{\alpha|z|^\beta}$ for $\alpha > 0$ and $0 \leq \beta < 1$ may be used.

Definition 6. Let m be a weight function on \mathbb{R}^{2d} and let $1 \leq p, q \leq \infty$. Then the weighted mixed norm space $\mathbf{L}_m^{p,q}(\mathbb{R}^{2d})$ consists of all measurable functions on \mathbb{R}^{2d} such that the norm

$$\|F\|_{\mathbf{L}_m^{p,q}} = \left(\int_{\mathbb{R}^d} \left(\int_{\mathbb{R}^d} |F(x, \omega)|^p m(x, \omega)^p dx \right)^{\frac{q}{p}} d\omega \right)^{\frac{1}{q}}$$

is finite, with the usual modifications when $p = \infty$ or $q = \infty$.

The following properties, which are crucial for the proof of our statement, are taken from [40, Prop. 11.1.3].

Proposition 1. If m is s -moderate, then

- (i) $\mathbf{L}_m^{p,q}(\mathbb{R}^{2d})$ is a solid Banach function space on \mathbb{R}^{2d} , i.e., if $F \in \mathbf{L}_m^{p,q}(\mathbb{R}^{2d})$ and G is measurable, satisfying $|G(z)| \leq |F(z)|$ for almost all $z \in \mathbb{R}^{2d}$, then $G \in \mathbf{L}_m^{p,q}(\mathbb{R}^{2d})$ and $\|G\|_{\mathbf{L}_m^{p,q}(\mathbb{R}^{2d})} \leq \|F\|_{\mathbf{L}_m^{p,q}(\mathbb{R}^{2d})}$.
- (ii) $\mathbf{L}_m^{p,q}(\mathbb{R}^{2d})$ is invariant under right and left translations and satisfies the convolution relation $\mathbf{L}_m^{p,q}(\mathbb{R}^{2d}) * \mathbf{L}_\nu^1(\mathbb{R}^{2d}) \subseteq \mathbf{L}_m^{p,q}(\mathbb{R}^{2d})$, with

$$\|F * G\|_{\mathbf{L}_m^{p,q}(\mathbb{R}^{2d})} \leq \|F\|_{\mathbf{L}_m^{p,q}(\mathbb{R}^{2d})} \|G\|_{\mathbf{L}_\nu^1(\mathbb{R}^{2d})}$$

for $F \in \mathbf{L}_m^{p,q}(\mathbb{R}^{2d})$, $G \in \mathbf{L}_\nu^1(\mathbb{R}^{2d})$.

Remark 9. It follows that $\mathbf{L}_0^\infty(\mathbb{R}^{2d})$, the space of bounded function with compact support on \mathbb{R}^{2d} is contained in Y , see [22]. This property will be crucial in the proof of our main statement.

Let \mathcal{S} be the Schwartz space of rapidly decreasing functions and \mathcal{S}' its dual, the space of tempered distributions.¹

Definition 7 (Modulation spaces). Fix a non-zero "window function" $g \in \mathcal{S}(\mathbb{R}^d)$ and consider s -moderate weight functions m for some constants $C, s \geq 0$. Then the modulation space $\mathbf{M}_m^{p,q}(\mathbb{R}^d)$ is defined as the space of all tempered distributions $f \in \mathcal{S}'(\mathbb{R}^d)$ with $\mathcal{V}_g f \in \mathbf{L}_m^{p,q}(\mathbb{R}^{2d})$, with norm

$$\|f\|_{\mathbf{M}_m^{p,q}(\mathbb{R}^d)} = \|\mathcal{V}_g f\|_{\mathbf{L}_m^{p,q}(\mathbb{R}^{2d})}.$$

Remark 10. For the detailed theory of the modulation spaces we refer to [40, Ch. 11–13] where several generalizations are discussed. In particular, \mathbb{R}^{2d} may be replaced by any locally compact group \mathcal{G} with Haar measure dz . On the other hand, other Banach spaces $(Y, \|\cdot\|_Y)$ of functions on \mathcal{G} may be considered, as long as some natural conditions, such as solidity and the convolution relation in Proposition 1, are satisfied.

¹[61] is one among many references for details on distribution theory.

As particularly important modulation space we mention $M_m^{1,1}$ with constant weight $m \equiv 1$. It is denoted by S_0 in harmonic analysis and is known as Feichtinger's algebra. Feichtinger and Zimmermann gave a slightly more straight-forward definition in [32] which we reproduce here for completeness.

Definition 8 (S_0). *Let g_0 be the Gauss-function $g_0 = e^{-\pi\|x\|^2}$. The space $S_0(\mathbb{R}^d)$ is given by*

$$S_0(\mathbb{R}^d) = \{f \in \mathbf{L}^2(\mathbb{R}^d) : \|f\|_{S_0} = \|\mathcal{V}_{g_0} f\|_{\mathbf{L}^1(\mathbb{R}^{2d})} < \infty\}.$$

An in-depth investigation of S_0 can be found in [32].

Note that S_0 is densely embedded in \mathbf{L}^2 , with $\|f\|_2 \leq \|g_0\|_2^{-1} \|f\|_{S_0}$. Its dual space S'_0 , the space of all linear, continuous functionals on S_0 , contains \mathbf{L}^2 and plays the role of a space of distributions.

Moreover, modulation spaces posses the following properties, see [40] or [33] for details:

- (i) $\mathbf{M}_m^{p,q}(\mathbb{R}^d)$ is a Banach space and invariant under the action of π . Specifically,

$$\|\pi(z)f\|_{\mathbf{M}_m^{p,q}(\mathbb{R}^d)} \leq C\nu(z)\|f\|_{\mathbf{M}_m^{p,q}(\mathbb{R}^d)} \quad \text{for } f \in \mathcal{C}o_\pi Y. \quad (4.9)$$

- (ii) In the definition of $\mathbf{M}_m^{p,q}(\mathbb{R}^d)$, $g \in \mathcal{S}$ can be replaced by any $g \in \mathbf{M}_\nu^1$, see [40, Theorem 11.3.7]. Furthermore, the definition of $\mathbf{M}_m^{p,q}(\mathbb{R}^d)$ is independent of the choice of $g \in \mathbf{M}_\nu^1$.

- (iii) Different functions $g \in \mathbf{M}_\nu^1 \setminus \{0\}$ define equivalent norms on $\mathbf{M}_m^{p,q}(\mathbb{R}^d)$.

- (iv) $\mathbf{M}_m^{p,q}(\mathbb{R}^d)$ is a subspace of $\mathbf{M}_{\frac{1}{\nu}}^\infty$, which is the dual space of \mathbf{M}_ν^1 and we also have

$$\|f\|_{\mathbf{M}_{\frac{1}{\nu}}^\infty} \leq C\|f\|_{\mathbf{M}_m^{p,q}(\mathbb{R}^d)} \quad (4.10)$$

In order to obtain compactness criteria analogous to Theorem 4 for modulation spaces, we have to exhaust some additional properties of the mixed-norm spaces. As pointed out at the end of Section 4.1, we need to use a norm for which dominated convergence holds. In our treatment of dominated convergence we follow [4, Ch. 1.3].

Definition 9. *A Banach function space Y on \mathcal{G} is said to have absolutely continuous norm, if $\|f\chi_{E_n}\|_Y \rightarrow 0$ for all f and for every sequence $\{E_n\}_{n=1}^\infty$ of measurable subsets of \mathcal{G} satisfying $E_n \rightarrow \emptyset$ almost everywhere with respect to Haar measure.*

Proposition 2 ([4]). *For a Banach function space Y the following are equivalent.*

- (i) Y has absolutely continuous norm.
- (ii) Dominated convergence holds for all $f \in Y$: If $f_n \in Y$, $n = 1, 2, \dots$, and $g \in Y$ satisfy $|f_n| \leq |g|$ for all n and $f_n(z) \rightarrow f(z)$ a. e., then $\|f_n - f\|_Y \rightarrow 0$.
- (iii) The dual space Y' of Y coincides with its associate space Y^* defined as

$$Y^* = \{g \text{ measurable, } \sup_{f \in Y, \|f\|_Y \leq 1} \int_{\mathcal{G}} |f(z)g(z)| dz < \infty\} \quad (4.11)$$

Lemma 1. *If $p, q < \infty$, then $L_m^{p,q}$ has an absolutely continuous norm.*

Proof. For $p = q = 1$ this is just Lebesgue's theorem on dominated convergence. If $p, q < \infty$, then the dual space is $L_{1/m}^{p',q'}$, where $1/p + 1/p' = 1$ [2]. As a consequence of Hölder's inequality the dual space coincides with the associate space defined in (4.11). By Proposition 2 $L_m^{p,q}$ possesses an absolutely continuous norm. \square

4.2.2 Compactness in modulation spaces

We are now ready to state and prove our main theorem, a criterion for compactness in modulation spaces.

Theorem 5 (Compactness in $\mathbf{M}_m^{p,q}(\mathbb{R}^d)$). *Let $0 \neq g \in \mathbf{M}_\nu^1(\mathbb{R}^d)$, $1 \leq p, q < \infty$ and S be a closed and bounded subset of $\mathbf{M}_m^{p,q}(\mathbb{R}^d)$. Then S is compact in $\mathbf{M}_m^{p,q}(\mathbb{R}^d)$ if and only if for all $\epsilon > 0$ exists a compact set $U \subseteq \mathbb{R}^{2d}$, such that*

$$\sup_{f \in S} \|\chi_{U^c} \cdot \mathcal{V}_g f\|_{\mathbf{L}_m^{p,q}} < \epsilon. \quad (4.12)$$

Remark: Clearly such a characterization cannot hold when $p = \infty$ or $q = \infty$. In this case $\mathbf{M}_m^{p,q}(\mathbb{R}^d)$ is the dual of a non-reflexive Banach space, and compactness in norm takes on a different shape.

Proof. The argument follows the simpler proof of Theorem 4. First assume that S is compact in $\mathbf{M}_m^{p,q}(\mathbb{R}^d)$ and let $\epsilon > 0$. Then there exist $f_1, \dots, f_n \in S$ such that

$$\min_{j=1,\dots,n} \|f - f_j\|_{\mathbf{M}_m^{p,q}(\mathbb{R}^d)} < \frac{\epsilon}{2} \quad \text{for all } f \in S.$$

Since $\mathbf{L}_0^\infty(\mathbb{R}^{2d})$ is contained in $\mathbf{L}_m^{p,q}(\mathbb{R}^{2d})$ as a consequence of Proposition 1, and since $\mathbf{L}_m^{p,q}(\mathbb{R}^{2d})$ has absolutely continuous norm, $\mathbf{L}_0^\infty(\mathbb{R}^{2d})$ is even dense in $\mathbf{L}_m^{p,q}(\mathbb{R}^{2d})$, see [22, Prop.1.4]. Hence, there exist $H_j \in \mathbf{L}_0^\infty \subseteq \mathbf{L}_m^{p,q}(\mathbb{R}^{2d})$ with $\|H_j - \mathcal{V}_g f_j\|_{\mathbf{L}_m^{p,q}(\mathbb{R}^{2d})} < \frac{\epsilon}{2}$. By solidity of $\mathbf{L}_m^{p,q}(\mathbb{R}^{2d})$, H_j can be chosen as the restriction $\chi_U \cdot \mathcal{V}_g f_j$ for some compact set $U \subseteq \mathbb{R}^{2d}$, and thus we obtain that

$$\|\chi_{U^c} \mathcal{V}_g f_j\|_{\mathbf{L}_m^{p,q}(\mathbb{R}^{2d})} < \frac{\epsilon}{2} \quad \text{for } j = 1, \dots, n.$$

Then for general $f \in S$ we find that

$$\begin{aligned} \|\chi_{U^c} \mathcal{V}_g f\|_{\mathbf{L}_m^{p,q}(\mathbb{R}^{2d})} &\leq \min_{j=1,\dots,n} \left(\|\chi_{U^c} \mathcal{V}_g (f - f_j)\|_{\mathbf{L}_m^{p,q}(\mathbb{R}^{2d})} + \|\chi_{U^c} \mathcal{V}_g f_j\|_{\mathbf{L}_m^{p,q}(\mathbb{R}^{2d})} \right) \\ &\leq \min_{j=1,\dots,n} \|\mathcal{V}_g (f - f_j)\|_{\mathbf{L}_m^{p,q}(\mathbb{R}^{2d})} + \frac{\epsilon}{2} \\ &= \min_{j=1,\dots,n} \|f - f_j\|_{\mathbf{M}_m^{p,q}(\mathbb{R}^d)} + \frac{\epsilon}{2} < \epsilon \end{aligned}$$

In the second inequality we have applied solidity of $\mathbf{L}_m^{p,q}(\mathbb{R}^{2d})$ to the pointwise estimate

$$|\chi_{U^c} \mathcal{V}_g (f - f_j)(z)| \leq |\mathcal{V}_g (f - f_j)(z)|.$$

Now we assume that for all $\epsilon > 0$ exists a compact set $U \subseteq \mathbb{R}^{2d}$, such that (4.12) holds. Again it suffices to show that every sequence $(f_n) \subseteq S$ contains a convergent subsequence.

To extract a weak-star convergent subsequence of $(f_n) \subseteq S$, we modify the argument for L^2 follows: Since S is bounded and closed in $\mathbf{M}_m^{p,q}(\mathbb{R}^d)$, it is also bounded and closed in $(\mathbf{M}_\nu^1)' = \mathbf{M}_\nu^\infty$ by (4.10), and therefore S is weak-star compact in $(\mathbf{M}_\nu^1)'$ by Alaoglu's theorem. Consequently we can find a weak-star convergent subsequence f_{n_j} of (f_n) , which we again denote by f_j , with limit f_∞ in S , i.e. $\langle f_j, h \rangle \longrightarrow \langle f_\infty, h \rangle$ for all $h \in \mathbf{M}_\nu^1$. In particular, for $h = \pi(z)g$, we obtain *pointwise* convergence of the STFT on \mathbb{R}^{2d}

$$\mathcal{V}_g f_j(z) \longrightarrow \mathcal{V}_g f_\infty(z) \quad \text{for all } z \in \mathbb{R}^{2d}.$$

Next we show that the sequence $\{\mathcal{V}_g(f_\infty - f_j), j \in \mathbb{N}\}$ is uniformly bounded on any compact set $U \subseteq \mathbb{R}^{2d}$. We have

$$|\langle f_\infty - f_j, \pi(z)g \rangle| \leq \|f_\infty - f_j\|_{(\mathbf{M}_\nu^1)'} \|\pi(z)g\|_{\mathbf{M}_\nu^1},$$

by duality, and $\|\pi(z)g\|_{\mathbf{M}_\nu^1} \leq \nu(z)\|g\|_{\mathbf{M}_\nu^1}$ by (4.9). Therefore

$$\sup_{z \in U} |\mathcal{V}_g(f_\infty - f_j)(z)| \leq \|g\|_{\mathbf{M}_\nu^1} \sup_{z \in U} \nu(z) \sup_{j \in \mathbb{N}} \|f_\infty - f_j\|_{(\mathbf{M}_\nu^1)'} \leq C \chi_U(z)$$

Since $\chi_U \in \mathbf{L}_m^{p,q}(\mathbb{R}^{2d})$ and $\mathbf{L}_m^{p,q}(\mathbb{R}^{2d})$ has an absolutely continuous norm, we can apply dominated convergence (Proposition 2 ii) to obtain

$$\lim_{j \rightarrow \infty} \|\chi_U \cdot \mathcal{V}_g(f_\infty - f_j)\|_{\mathbf{L}_m^{p,q}(\mathbb{R}^{2d})} = 0. \quad (4.13)$$

To deal with the behavior of $\mathcal{V}_g(f_\infty - f_j)$ on the complement U^c , we use assumption (4.12). Given $\epsilon > 0$, we choose $U \subseteq \mathbb{R}^{2d}$ so that $\|\chi_{U^c} \mathcal{V}_g f\|_{\mathbf{L}_m^{p,q}(\mathbb{R}^{2d})} < \epsilon/2$ for all $f \in S \cup \{f_\infty\}$. The combination of these steps now yields

$$\begin{aligned} \lim_{j \rightarrow \infty} \|f_\infty - f_j\|_{C_0 \mathbf{L}_m^{p,q}(\mathbb{R}^{2d})} &= \lim_{j \rightarrow \infty} \|\mathcal{V}_g(f_\infty - f_j)\|_{\mathbf{L}_m^{p,q}(\mathbb{R}^{2d})} \\ &\leq \lim_{j \rightarrow \infty} \|\chi_U \cdot \mathcal{V}_g(f_\infty - f_j)\|_{\mathbf{L}_m^{p,q}(\mathbb{R}^{2d})} \\ &\quad + \overline{\lim}_{j \rightarrow \infty} \|\chi_{U^c} \cdot \mathcal{V}_g(f_\infty - f_j)\|_{\mathbf{L}_m^{p,q}(\mathbb{R}^{2d})} \\ &\leq 0 + 2 \sup_{f \in S \cup \{f_\infty\}} \|\chi_{U^c} \cdot \mathcal{V}_g f\|_{\mathbf{L}_m^{p,q}(\mathbb{R}^{2d})} < 2\epsilon. \end{aligned}$$

Therefore any sequence in S has a subsequence that converges in $\mathbf{M}_m^{p,q}(\mathbb{R}^d)$ and so S is compact. \square

Loosely speaking, Theorem 5 states that a set of functions in $\mathbf{M}_m^{p,q}(\mathbb{R}^d)$ is compact, if and only if the set of their short-time Fourier transforms is tight in $\mathbf{L}_m^{p,q}(\mathbb{R}^{2d})$.

4.3 Compactness of STFT Multipliers

Theorem 6. *Let the STFT-multiplier $\mathbf{H} : \mathbf{M}_m^{p,q}(\mathbb{R}^d) \mapsto \mathbf{M}_m^{p,q}(\mathbb{R}^d)$ be defined as*

$$\mathbf{H}f = \int_{\mathbb{R}^{2d}} \mathcal{V}_g f(z) b(z) \pi(z) g(t) dz,$$

with $0 \neq g \in \mathbf{M}_\nu^1(\mathbb{R}^d)$. If $\mathbf{b} = b(z)$ is in $C^0(\mathbb{R}^{2d})$, \mathbf{H} is a compact operator.

Proof. Recall that an operator is compact if and only if the image of the closed unit ball is relatively compact. Let $S = \{\mathbf{H}f, \|f\|_{\mathbf{M}_m^{p,q}} \leq 1\}$ be the image of the closed unit ball in $\mathbf{M}_m^{p,q}(\mathbb{R}^d)$ under \mathbf{H} . According to Theorem 5, S is compact if and only if for any given $\varepsilon > 0$ a compact set $U \in \mathbb{R}^{2d}$ can be found such that $\sup_{h \in S} \|\chi_{U^c} \mathcal{V}_{g_0} h\|_{\mathbf{L}_m^{p,q}(\mathbb{R}^{2d})} < \varepsilon$. Now we have

$$\begin{aligned} \sup_{h \in S} \|\chi_{U^c} \mathcal{V}_{g_0} h\|_{\mathbf{L}_m^{p,q}(\mathbb{R}^{2d})} &= \sup_{\|f\|_{\mathbf{M}_m^{p,q}} \leq 1} \|\chi_{U^c} \mathcal{V}_{g_0} (\mathcal{V}_g^* \mathbf{b} \mathcal{V}_g f)\|_{\mathbf{L}_m^{p,q}(\mathbb{R}^{2d})} \\ &= \sup_{\|f\|_{\mathbf{M}_m^{p,q}} \leq 1} \|\chi_{U^c} (|\mathcal{V}_{g_0} g| * \mathbf{b} |\mathcal{V}_g f|)\|_{\mathbf{L}_m^{p,q}(\mathbb{R}^{2d})}. \end{aligned}$$

As $G = \mathcal{V}_{g_0} g$ is in S_0 , for any $\varepsilon_1 > 0$, G can be written as $G = G_1 + G_2$, such that $\text{supp}(G_1) \subseteq U_1$, where U_1 is a compact set in \mathbb{R}^{2d} and $\|G_2\|_{\mathbf{L}_\nu^1} < \varepsilon_1$. On the other hand, according to $\mathbf{b} \in C^0(\mathbb{R}^{2d})$, \mathbf{b} can be written as $\mathbf{b} = \mathbf{b}_1 + \mathbf{b}_2$, such that $\text{supp}(\mathbf{b}_1) \subseteq U_2$, U_2 again being compact in \mathbb{R}^{2d} and $\|\mathbf{b}_2\| < \varepsilon_2$. For the given ε we choose $\varepsilon_1 = \min(\sqrt{\frac{\varepsilon}{3}}, \frac{\varepsilon}{3\|\mathbf{b}_1\|_\infty})$ and $\varepsilon_2 = \min(\sqrt{\frac{\varepsilon}{3}}, \frac{\varepsilon}{3\|G_1\|_{\mathbf{L}_\nu^1}})$ and set $U = U_1 + U_2$. Then

$$\begin{aligned} \sup_{h \in S} \|\chi_{U^c} \mathcal{V}_{g_0} h\|_{\mathbf{L}_m^{p,q}(\mathbb{R}^{2d})} &\leq \|\chi_{U^c} [G_1 * (\mathbf{b}_1 \mathcal{V}_g f)]\|_{\mathbf{L}_m^{p,q}(\mathbb{R}^{2d})} + \|\chi_{U^c} [G_2 * (\mathbf{b}_1 \mathcal{V}_g f)]\|_{\mathbf{L}_m^{p,q}(\mathbb{R}^{2d})} \\ &\quad + \|\chi_{U^c} [G_1 * (\mathbf{b}_2 \mathcal{V}_g f)]\|_{\mathbf{L}_m^{p,q}(\mathbb{R}^{2d})} + \|\chi_{U^c} [G_2 * (\mathbf{b}_2 \mathcal{V}_g f)]\|_{\mathbf{L}_m^{p,q}(\mathbb{R}^{2d})} \end{aligned}$$

The first term is 0 by the choice of U . For the second term we have the following estimate:

$$\|\chi_{U^c} [G_2 * (\mathbf{b}_1 \mathcal{V}_g f)]\|_{\mathbf{L}_m^{p,q}} \leq \|G_2\|_{\mathbf{L}_\nu^1} \|\mathbf{b}_1 \mathcal{V}_g f\|_{\mathbf{L}_m^{p,q}} \leq \varepsilon_1 \|\mathbf{b}_1\|_\infty \|f\|_{\mathbf{M}_m^{p,q}} \leq \frac{\varepsilon}{3}.$$

Similarly, the third term is bounded by $\|G_1\|_{\mathbf{L}_\nu^1} \|\mathbf{b}_2\|_\infty \leq \|G_1\|_{\mathbf{L}_\nu^1} \varepsilon_2 \leq \frac{\varepsilon}{3}$, and for the last term in the sum we have the estimate:

$$\|[G_2 * (\mathbf{b}_2 \mathcal{V}_g f)]\|_{\mathbf{L}_m^{p,q}} \leq \|\chi_{U^c} G_2\|_{\mathbf{L}_\nu^1} \|\mathbf{b}_2 \mathcal{V}_g f\|_{\mathbf{L}_m^{p,q}} \leq \varepsilon_1 \varepsilon_2 \leq \varepsilon,$$

hence

$$\sup_{h \in S} \|\chi_{U^c} \mathcal{V}_{g_0} h\|_{\mathbf{L}_m^{p,q}(\mathbb{R}^{2d})} \leq \varepsilon,$$

which proves that the image of the unit ball in $\mathbf{M}_m^{p,q}(\mathbb{R}^d)$ is compact in $\mathbf{M}_m^{p,q}(\mathbb{R}^d)$. \square

Chapter 5

Theory and Application of Gabor Multipliers

This chapter deals with the theory and applications of Gabor multipliers. These operators arise as a method of time-varying filtering. As stated in the Chapter 2, time-varying filtering has a myriad of applications in the processing of music signals. Here we investigate the influence of the choice of parameters, especially the window and the lattice. Some numerical experiments give insight in the influence of several free parameters in the design of Gabor multipliers on the action of the operator. We then study the behavior of eigenvectors and eigenvalues of a Gabor multiplier. Finally the quality of approximation by Gabor multipliers in different classes of operators is investigated.

5.1 Introduction

Consider the task of extracting signal components which possess certain properties, e.g., belonging to a given instrument, from a complex audio signal. This obviously is not only a non-trivial problem, but also a highly nonlinear one, if the dependence on the specific signal under consideration is observed. The process of extracting parts of a given signal can be described by an operator $\mathbf{G}(f)$:

$$f \longrightarrow \mathbf{G}(f)f,$$

where $\mathbf{G}(f)$ denotes the time-varying filtering system depending on the properties of the signal f under inspection. Ignoring the dependance on f , however, we can fix the amount of filtering in time and frequency and \mathbf{G} becomes a linear operator. Here, we want to study the properties of a specific class of time-varying filter operators, the so-called Gabor multipliers. A similar approach has been studied in [57].

Definition 10 (Gabor multiplier). Let g_1 and g_2 be two functions in $S_0(\mathbb{R}^d)$, $\Lambda \subset \mathbb{R}^d \times \widehat{\mathbb{R}^d}$ a TF-lattice and $\mathbf{m} = (m(\lambda))_{\lambda \in \Lambda}$ a bounded, complex-valued sequence in $\ell^\infty(\Lambda)$.

Then the **Gabor multiplier** associated to the triple (g_1, g_2, Λ) is given as

$$G_{\mathbf{m}}(f) = \mathbf{G}_{g_1, g_2, \Lambda, \mathbf{m}}(f) = \sum_{\lambda \in \Lambda} m(\lambda) \langle f, \pi(\lambda)g_1 \rangle \pi(\lambda)g_2. \quad (5.1)$$

Lemma 2. *Note that the restriction that the multiplier \mathbf{m} be a bounded sequence leads to boundedness of $\mathbf{G}_{g_1, g_2, \Lambda, \mathbf{m}}$ with the following estimate of the operator norm:*

$$\|\mathbf{G}_{g_1, g_2, \Lambda, \mathbf{m}}\| \leq C \cdot \|\mathbf{m}\|_{\infty}, \quad (5.2)$$

with $C \leq C_{\Lambda} \|g_1\|_{S_0} \|g_2\|_{S_0}$.

Proof.

$$\begin{aligned} \|\mathbf{G}_{g_1, g_2, \Lambda, \mathbf{m}}(f)\|_2^2 &\leq \sum_{\lambda \in \Lambda} |m(\lambda)|^2 |\langle f, \pi(\lambda)g_1 \rangle|^2 \|\pi(\lambda)g_2\|_2^2 \\ &\leq \|\mathbf{m}\|_{\infty}^2 \|g_2\|_2^2 \sum_{\lambda \in \Lambda} |\langle f, \pi(\lambda)g_1 \rangle|^2 \end{aligned}$$

In [32, Chapter 3.3] the continuity of the operator

$$\mathbf{T}_{g_1, \Lambda} : \mathbf{L}^2(\mathbb{R}^d) \mapsto \ell^2(\Lambda), \quad \mathbf{T}_{g_1, \Lambda}(\lambda) = \langle f, \pi(\lambda)g_1 \rangle$$

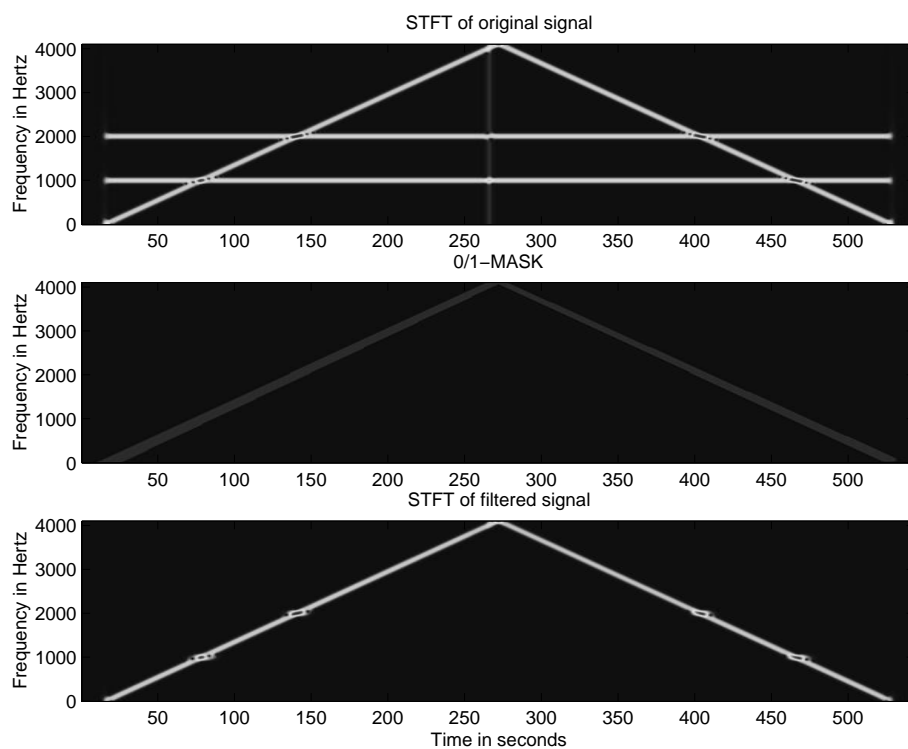
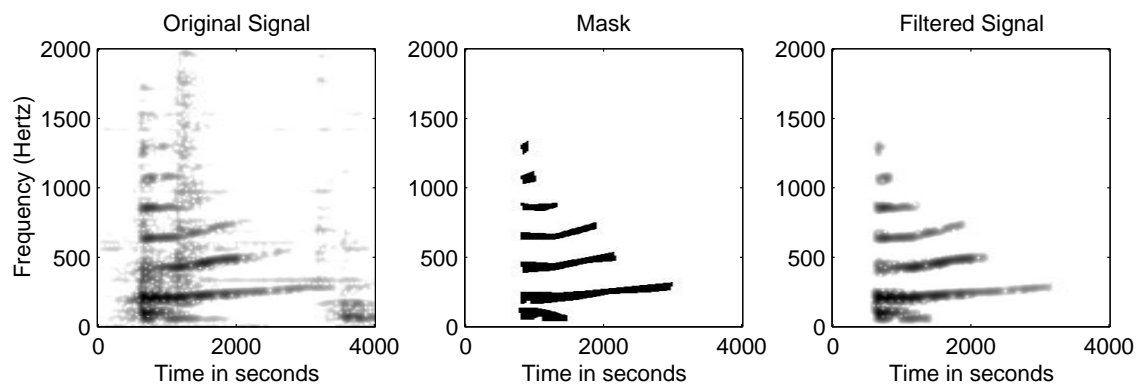
was shown, hence, for $\|f\|_2 = 1$, $\sum_{\lambda \in \Lambda} |\langle f, \pi(\lambda)g_1 \rangle|^2 \leq C_{\Lambda}^2 \|g_1\|_{S_0}^2$. By the continuous embedding of S_0 in \mathbf{L}^2 , we have $\|g_2\|_2 \leq \|g_2\|_{S_0}$, and thus:

$$\|\mathbf{G}_{g_1, g_2, \Lambda, \mathbf{m}}(f)\|_2 \leq C_{\Lambda} \|g_1\|_{S_0} \|g_2\|_{S_0} \|f\|_2.$$

□

The subscripts g_1, g_2 and Λ will be omitted if they are not crucial for the discussion. If $g_1 = g_2$, we write $\mathbf{G}_{g_1, g_2, \Lambda, \mathbf{m}} = \mathbf{G}_{g, \Lambda, \mathbf{m}}$. Unless otherwise stated, $g_1 = g_2$ will be assumed for most of the rest of this chapter. Hence, $f \mapsto \langle f, \pi(\lambda)g \rangle \pi(\lambda)g$ are the projections (orthogonal projections if $\|g\|_2 = 1$) onto the one-dimensional subspaces of \mathbf{L}^2 generated by the time-frequency shifted versions of g .

Figure 5.1 shows an example for the application of a Gabor multiplier. A signal comprising a chirp, two sinusoids at distinct frequencies and a Dirac impulse has been synthesized. The short-time Fourier transform (STFT) of the composite signal is shown in the first plot. The second plot shows the multiplier \mathbf{m} , which is a 0/1-mask in this example. The chirp has been filtered out, which can be seen in the third plot. This example shows that with Gabor multipliers time-varying filtering can be realized. A second example, obtained from a music signal, is shown in Figure 5.2. The signal is a short segment from a piece performed by a double-bass and drums. The first plot shows the STFT of the signal. The note played by the bass is well recognizable with its harmonics in the low frequency region. The second plot shows a 0/1-mask which was used to extract the bass note. The STFT of the resulting signal is shown in

Figure 5.1: *Gabor multiplier applied to synthesized signal*Figure 5.2: *Gabor multiplier applied to real signal*

the last plot.¹ Clearly, the noisy components, originating mainly from the drums, have been eliminated. It is hard to evaluate, however, the quality of the extracted signal component. Human perception must be seen as the ultimate criterion in audio signal processing, as differences between signal which may seem crucial in a mathematical sense, can be inaudible. For the given example (Figure 5.2), the result of the extraction seems satisfying to the listener, i.e., the instrument, the pitch and the quality of the extracted note are perfectly recognizable.

The close examination of the properties of Gabor multipliers is motivated by the desire to quantify as accurately as possible the dependence of the action of $\mathbf{G}_{\mathbf{m}}$ on the shape of the windows, the lattice parameter and the symbol \mathbf{m} itself.

The following lemma states some basic facts on the global behavior of Gabor multipliers which are deduced from assumptions on the symbol \mathbf{m} . We have already seen that $\mathbf{G}_{g,\Lambda,\mathbf{m}}$ is a bounded operator on $\mathbf{L}^2(\mathbb{R}^d)$ whenever \mathbf{m} is essentially bounded. Additional assumptions on \mathbf{m} yield refinements of this statement.

A linear operator \mathbf{K} may be described by its (distributional) kernel $\kappa(\mathbf{K})$ via an integral equation:

$$\mathbf{K}f(t) = \int \kappa(\mathbf{K})(t, y) f(y) dy.$$

This is a consequence of the famous Schwartz kernel theorem, see [40, Theorem 14.3.4].² Clearly, this is a generalization of the matrix representation of a linear operator in the (finite) discrete case, to which it reduces in the distributional case of a discrete measure.

Proposition 3. *Let $g \in S_0(\mathbb{R}^d)$.*

If $\mathbf{m} \in c_0(\Lambda)$, then $\mathbf{G}_{g,\Lambda,\mathbf{m}}$ is compact.

If \mathbf{m} is real-valued, then $\mathbf{G}_{g,\Lambda,\mathbf{m}}$ is self-adjointness.

If $\mathbf{m} \in \ell^2(\Lambda)$, then $\mathbf{G}_{g,\Lambda,\mathbf{m}}$ is a Hilbert-Schmidt operator on $L^2(\mathbb{R}^d)$.

Proof. The proof of compactness of Gabor multipliers with $\mathbf{m} \in c_0(\Lambda)$ is analogous to the proof of Theorem 6, the image of the unit ball in $\mathbf{L}^2(\mathbb{R}^{2d})$ is compact even in S_0 .

To see $\mathbf{G}_{\mathbf{m}} = \mathbf{G}_{\mathbf{m}}^*$ for real-valued \mathbf{m} , note that

$$\begin{aligned} \langle f, \mathbf{G}_{\mathbf{m}} h \rangle &= \langle f, \sum_{\lambda \in \Lambda} m(\lambda) \langle h, g_\lambda \rangle g_\lambda \rangle \\ &= \sum_{\lambda \in \Lambda} \overline{m(\lambda)} \langle f, \langle h, g_\lambda \rangle g_\lambda \rangle = \sum_{\lambda \in \Lambda} m(\lambda) \overline{\langle h, g_\lambda \rangle} \langle f, g_\lambda \rangle \\ &= \sum_{\lambda \in \Lambda} m(\lambda) \langle \langle f, g_\lambda \rangle g_\lambda, h \rangle = \langle \mathbf{G}_{\mathbf{m}} f, h \rangle \end{aligned}$$

The Hilbert-Schmidt property of Gabor multipliers with upper symbol in ℓ^2 follows from the fact that Hilbert-Schmidt operators correspond to \mathbf{L}^2 -kernels. The kernel of

¹Here, the mask was found by visual inspection. However, we hope that for an automatized extraction routine, image recognition tools might be applied to find corresponding signal components.

²In particular, for operators from S_0 to S'_0 the kernel is contained in S_0 , see [40, Theorem 14.4.1].

$\mathbf{G}_{g,\Lambda,\mathbf{m}}$ is given by

$$\kappa(\mathbf{G}_{g,\Lambda,\mathbf{m}})(x, \xi) = \sum_{\lambda \in \Lambda} m(\lambda) g_\lambda(x) g_\lambda(\xi).$$

It's trivial to see that $\kappa(\mathbf{G}_{g,\Lambda,\mathbf{m}})$ is square integrable if $\mathbf{m} \in \ell^2$. \square

As we will see below, for some considerations of interest it is advantageous to replace $\kappa(\mathbf{K})$ by a *symbol* corresponding to \mathbf{K} , which can shed light on different aspects of the operator. The next section will introduce several possible ways to describe and characterize a Gabor multiplier by means of different classes of symbols.

5.2 The Kohn-Nirenberg Symbol

Definition 11 (Kohn-Nirenberg Symbol). *The Kohn-Nirenberg Symbol (KNS) $\sigma(\mathbf{K})$ of an operator \mathbf{K} on $\mathbf{L}^2(\mathbb{R}^d)$, with kernel $\kappa(\mathbf{K})$ in $\mathbf{L}^2(\mathbb{R}^d \times \mathbb{R}^d)$ is defined on $\mathbb{R} \times \widehat{\mathbb{R}^d}$ by*

$$\sigma(\mathbf{K})(x, \xi) = \mathcal{F}_2 \kappa(\mathbf{K})(x, x - t) = \int_{\mathbb{R}^d} \kappa(\mathbf{K})(x, x - t) e^{-2\pi i \xi t} dt.$$

Remark 11. The KNS has been defined for quite general classes of operators, in particular for operators with kernels in S_0 or S'_0 in [29], leading to the *generalized Kohn-Nirenberg correspondence*. The KNS features the following properties, which are taken from [29], where proofs can be found.

1. $\sigma(\mathbf{K})$ defines an invertible mapping between the kernels of operators defined in $S_0(\mathbb{R}^{2d})$ and their KNS in $S_0(\mathbb{R}^d \times \widehat{\mathbb{R}^d})$. The inversion is given by

$$\kappa(\mathbf{K})(x, y) = \int_{\widehat{\mathbb{R}^d}} \sigma(\mathbf{K})(x, \xi) e^{2\pi i \xi(x-y)} d\xi.$$

On the Hilbert space level $\mathbf{L}^2(\mathbb{R}^{2d}) \longleftrightarrow \mathbf{L}^2(\mathbb{R}^d \times \widehat{\mathbb{R}^d})$, this is a unitary isomorphism.

2. (Shift-covariance) The action of $\pi_2(\lambda)$ on \mathbf{K} corresponds to a translation of the symbol $\sigma(\mathbf{K})$, i.e.,:

$$[\sigma(\pi_2(\lambda)\mathbf{K})] = T_\lambda[\sigma(\mathbf{K})]$$

3. (Trace formula) The trace of an operator \mathbf{K} with $\kappa(\mathbf{K}) \in S_0(\mathbb{R}^{2d})$ can be obtained by total integration over the KNS:

$$tr(\mathbf{K}) = \int_{\mathbb{R}^d} \kappa(\mathbf{K})(x, x) dx = \int_{\mathbb{R}^d \times \widehat{\mathbb{R}^d}} \sigma(\mathbf{K})(\lambda) d\lambda.$$

5.3 The Spreading Function

The spreading function $\eta(\mathbf{K})$ of an operator \mathbf{K} can be seen as the coefficient function of an expansion of \mathbf{K} by means of the unitary time-frequency shift operators. A linear operator acting on $\mathbf{L}^2(\mathbb{R}^d)$ can thus be written as:

$$\mathbf{K} = \int_{\mathbb{R}^d} \int_{\widehat{\mathbb{R}}^d} \eta(\mathbf{K})(t, \nu) M_\nu T_t d\nu dt, \quad (5.3)$$

with

$$\kappa(\mathbf{K})(x, y) = \int_{\mathbb{R}^d} e^{2\pi i \nu x} \eta(\mathbf{K})(x - y, \nu) d\nu. \quad (5.4)$$

The operator kernel can be recovered from its spreading function by

$$\eta(\mathbf{K})(t, \nu) = \int_{\mathbb{R}^d} \kappa(\mathbf{K})(x, x - t) e^{-2\pi i \nu x} dx. \quad (5.5)$$

. It turns out, see [46], that the spreading function is related to the KNS via a symplectic Fourier transform:

$$\eta(\mathbf{K})(t, \nu) = \mathcal{F}_s[\sigma(\mathbf{K})](t, \nu) = \int_{\mathbb{R}^d} \int_{\widehat{\mathbb{R}}^d} \sigma(\mathbf{K})(x, \xi) e^{2\pi i(x\nu - \xi t)} dx d\xi.$$

The spreading function will have an important role in characterizing classes of operators which are well-approximated by Gabor multipliers. Furthermore, the spreading function can be consulted to investigate the completeness of families of projection operators, see 6.3. It is hence a useful tool in the study of multi-window frames.

5.4 The Lower and Upper Symbol of a Gabor Multiplier

In this section we study two more classes of symbols, which are especially suited to handle the properties of Gabor multipliers. Intuitively, a Gabor multiplier should act on a signal by suppressing or deleting TF-localised signal components. In contrast, the displacement of components in the TF-plane would be considered as an undesired influence on the signal's time-frequency characteristics. Since the Gauss function g is optimally and functions $g \in S_0$ are at least nicely concentrated in a time-frequency sense, we will expect them to behave like (approximate) eigenfunctions of \mathbf{G}_m . Thus, for an operator \mathbf{K} , which is well represented by a Gabor multiplier, the coefficients $\langle \mathbf{K}\pi(\lambda)g, \pi(\lambda)g \rangle$ should capture the main part of the operator. In an operator sense this expression can be written as a Hilbert-Schmidt inner product, which is defined as the inner product of the operator kernels. These are, by definition, in $\mathbf{L}^2(\mathbb{R}^{2d})$, such that

$$\langle \mathbf{K}_1, \mathbf{K}_2 \rangle_{\mathcal{HS}} = \langle \kappa(\mathbf{K}_1), \kappa(\mathbf{K}_2) \rangle = \text{tr}(\mathbf{K}_1 \mathbf{K}_2^*)$$

is well-defined. This yields:

$$\begin{aligned} \langle \mathbf{K}\pi(\lambda)g, \pi(\lambda)g \rangle &= \int_x \int_t \kappa(\mathbf{K})(x, t) \pi(\lambda)g(t) dt \overline{\pi(\lambda)g(x)} dx \\ &= \int_x \int_t \kappa(\mathbf{K})(x, t) \overline{g_\lambda(x)} \overline{g_\lambda(t)} dt dx \\ &= \langle \mathbf{K}, g_\lambda \otimes g_\lambda^* \rangle = \langle \mathbf{K}, P_\lambda \rangle, \end{aligned}$$

where we write $g_\lambda = \pi(\lambda)g$ and P_λ for the rank one operator $g_\lambda \otimes g_\lambda^*$. This leads to the following definition:

Definition 12 (Lower Symbol). *The lower symbol of an operator \mathbf{K} with respect to a window $g \in S_0$ and a lattice Λ is defined as*

$$\sigma_L(\mathbf{K})(\lambda) = \langle \mathbf{K}, g_\lambda \otimes g_\lambda^* \rangle = \langle \mathbf{K}, P_\lambda \rangle$$

Remark 12. As the KNS, cf. Remark 2.2, the lower symbol of an operator is shift-covariant and obeys the following estimate (hence the term lower symbol):

$$\|\sigma_L(\mathbf{K})\|_\infty \leq \|\mathbf{K}\|.$$

Again, the definition of the lower symbol is valid for quite general operators with kernel in S'_0 , i.e., operators in $\mathcal{L}(S_0, S'_0)$, see [30, Corollary 5.8.2 and Theorem 5.8.3] and [24] for more details on *Gelfand triples*.

Example 4 (Lower Symbol of an STFT multiplier). TF-localization operators can be obtained by multiplying the STFT $V_g(f)$ with some 0/1-function describing an area of interest. The resulting operators are called STFT-multipliers, see Theorem 6.

Definition 13. An operator \mathbf{K} defined as

$$\mathbf{K}f = \mathcal{V}_g^* \mu \mathcal{V}_g f,$$

where $\mu \in \mathbf{L}^\infty(\mathbb{R}^d \times \widehat{\mathbb{R}^d})$ is the multiplier, is a STFT-multiplier.

STFT-multipliers can be seen as a special case of Gabor multipliers. Consider the issue of approximating an STFT multiplier by a Gabor multiplier $\mathbf{G}_{g, \Lambda, \mathbf{m}}$, where $\Lambda = a\mathbb{Z} \times b\mathbb{Z}$. f and $\mathbf{K}f$ clearly have a Gabor transform with respect to a given, tight Gabor system $\mathcal{G} = (g_t, \Lambda)$, hence we can define an operator $\mathcal{W}_m : \ell^2(\Lambda) \mapsto \ell^2(\Lambda)$, mapping $T_{g_t, \lambda} f$ to $T_{g_t, \lambda} \mathbf{K}f$. For tight systems we have $\text{Id} = T_{g_t}^* T_{g_t}$, hence, \mathcal{W}_m is given by

$$\mathcal{W}_m(\lambda) = [T_{g_t} \mathcal{V}_g^* \mu \mathcal{V}_g T_{g_t}^*](\lambda).$$

Generally, \mathcal{W}_m is a linear operator, which can be written as a matrix $(\mathcal{W}_m)(i, j)_{i \in \Lambda, j \in \Lambda}$ with non-zero off-diagonal entries. In order to obtain a Gabor multiplier, we have to

set all off-diagonal entries to 0, hence only keeping $(\mathcal{W}_m)(i, i)$ as multiplier sequence. Investigating $(\mathcal{W}_m)(i, i)$ more closely, we find that:

$$\begin{aligned}\mathcal{W}_m(i, i) &= \int_{z \in \mathbb{R}^d \times \widehat{\mathbb{R}^d}} \mu(z) \langle \pi(\lambda_i)g_t, \pi(z)g \rangle \langle \pi(z)g, \pi(\lambda_i)g_t \rangle dz \\ &= \int_{z \in \mathbb{R}^d \times \widehat{\mathbb{R}^d}} \mu(z) \langle \pi_2(z)P_g, \pi_2(\lambda_i)P_{g_t} \rangle_{\mathcal{HS}} dz = \langle \mathbf{K}, \pi_2(\lambda_i)P_{g_t} \rangle_{\mathcal{HS}},\end{aligned}$$

which shows that the diagonal of the operator \mathcal{W}_m is just the lower symbol of the given STFT-multiplier with respect to \mathcal{G} .

Once the lower symbol is known, we can ask the question whether and how the operator \mathbf{K} can be recovered from its lower symbol. Investigating the definition of Gabor multipliers, we find that they are composed of projections onto time-frequency shifted versions of g . This means, that $\mathbf{G}_{g, \Lambda, \mathbf{m}}$ can be written as $\sum_{\lambda \in \Lambda} \mathbf{m}(\lambda)P_\lambda$. The estimate in (5.2) suggests the following synonym for the multiplier $\mathbf{m}(\lambda)$:

Definition 14 (Upper Symbol). *For a Gabor multiplier $\mathbf{G}_{g, \Lambda, \mathbf{m}}$, the multiplier symbol $\mathbf{m}(\lambda)$ is also called upper symbol for $\mathbf{G}_{g, \Lambda, \mathbf{m}}$ with respect to a window $g \in S_0$ and a lattice Λ and denoted by $\sigma_U(\mathbf{G}_{g, \Lambda, \mathbf{m}})(\lambda)$, or just $\sigma_U(\lambda)$.*

Remark 13. Note that the upper symbol is a priori only defined for Gabor multipliers. We will see later on, however, that also an upper symbol for more general operators can be obtained as an inner product with respect to TF-shifted versions of a basic operator.

Upper and lower symbol of an operator are uniquely determined if and only if the system $(P_\lambda)_{\lambda \in \Lambda}$ forms a Riesz basis within the Hilbert space \mathcal{HS} of all Hilbert-Schmidt operators. In this case, an isomorphism between upper and lower exists, which will be further described in Theorem 13.

An important question is the invertibility of the map $\mathbf{K} \mapsto \sigma_L(\mathbf{K})$ which, if a bijection between upper and lower symbol exists, is equivalent to the invertibility $\mathbf{K} \mapsto \sigma_U(\mathbf{K})$. As specified to some extent in the next proposition, this topic relates to the classification of operators which are representable as Gabor multipliers. The proposition shows how the KNS of a Gabor multiplier relates to its upper symbol, will be an important tool in answering these questions.

Proposition 4. *The KNS of $\mathbf{G}_{g, \Lambda, \mathbf{m}}$ is given by the convolution over Λ between the upper symbol $\sigma_U(\mathbf{G}_{g, \Lambda, \mathbf{m}})$ and the KNS of $P_0 = g_0 \otimes g_0^*$.*

Proof.

$$\begin{aligned}\sigma(\mathbf{G}_{g, \Lambda, \mathbf{m}})(x, \xi) &= \int_{\mathbb{R}^d} \kappa(\mathbf{G}_{g, \Lambda, \mathbf{m}})(x, x - t) \overline{e^{2\pi i x t}} dt \\ &= \int_{\mathbb{R}^d} \sum_{(x', \xi') \in \Lambda} \sigma_U(x', \xi') \kappa(P_{(x', \xi')})(x, x - t) \overline{e^{2\pi i x t}} dt \\ &= \sum_{(x', \xi') \in \Lambda} \sigma_U(x', \xi') \sigma(\pi_2(x', \xi')P_0)(x, \xi)\end{aligned}$$

Now we set $\lambda' = (x', \xi')$, and obtain:

$$\sigma(\mathbf{G}_{g,\Lambda,\mathbf{m}})(z) = \sum_{\lambda' \in \Lambda} \sigma_U(\lambda') T_{\lambda'} \sigma(P_0)(z) = \sum_{\lambda' \in \Lambda} \sigma_U(\lambda') \sigma(P_0)(z - \lambda'),$$

where the shift-covariance of the KNS has been used in the last reformulation. Hence,

$$\sigma(\mathbf{G}_{g,\Lambda,\mathbf{m}}) = \left[\sigma_U(\mathbf{G}_{g,\Lambda,\mathbf{m}}) *_\Lambda \sigma(P_0) \right]. \quad (5.6)$$

□

Corollary 2. *As a consequence of the Proposition 4, a given operator \mathbf{K} can be exactly represented as a Gabor multiplier with respect to $\mathcal{G} = (g, \Lambda)$, if and only if $\mathcal{V}_g g|_\Lambda$ is bounded away from 0 on the support of the spreading function $\eta(\mathbf{K})$.*

Proof. By symplectic Fourier transform (5.6) can be written as

$$\eta(\mathbf{K}) = [\mathcal{F}_s \sigma_U(\mathbf{K})] \cdot \eta(P_0)$$

A straightforward calculation shows that $\eta(P_0) = \mathcal{V}_g g$. Hence the upper symbol is well-defined if and only the given support condition holds. □

In [29, Theorem 7.7.5] it is shown that for Λ -invariant operators the spreading function is discretely supported on Λ° , hence the previous result seems to indicate that exact representation of an operator is a concept too restrictive in the context of Gabor multipliers. We may thus turn to the issue of best-approximation of an operator. As discussed before, the influence of the windows g_1 and g_2 and the lattice Λ , or the time- and frequency-shift parameters may be crucial, but is difficult to quantify. One of the central questions about Gabor multipliers is which operators can be realized or approximated by a Gabor multiplier and how the quality of approximation depends on the primary Gabor system (g, Λ) . The consideration that Gabor multipliers are a practically tractable generalization of STFT-multipliers suggests the assumption that it might be favorable to use *tight* systems in the first place. This supposition is reinforced by numerical simulations, in which the approximation of STFT-multiplier by Gabor multipliers is investigated, see Section 5.7.1. The treatment of approximation of general linear operators becomes more tractable, by considering the properties of the family of projection operators $(P_\lambda)_{\lambda \in \Lambda}$ in more detail: If we look at $\mathbf{G}_{g,\Lambda,\mathbf{m}}$ as a weighted sum of projection operators, then \mathcal{GM}_2 , the space of Gabor multipliers with $\ell^2(\Lambda)$ -symbol, can be understood as the closed linear span of the projection operators $(P_\lambda)_{\lambda \in \Lambda}$ in \mathcal{HS} .

5.4.1 $(P_\lambda)_{\lambda \in \Lambda}$ as Riesz basis

On the space of Hilbert-Schmidt operators an inner product, hence orthogonal projection and thus the notion of best approximation of operators are well defined. We can formalize the search for the best representation \mathbf{K}_{app} of a general Hilbert-Schmidt

operator \mathbf{K} as a Gabor multiplier (with $\ell^2(\Lambda)$ -multiplier) as follows. If $(P_\lambda)_{\lambda \in \Lambda}$ is a Riesz basis for its closed linear span within the Hilbert space \mathcal{HS} , then

$$\mathbf{K}_{app} = \sum_{\lambda \in \Lambda} \mathbf{c}_{app}(\lambda) P_\lambda,$$

where the sequence \mathbf{c}_{app} minimizes the error $\epsilon(\mathbf{c})$ given by

$$\epsilon(\mathbf{c}) = \left\| \sum_{\lambda \in \Lambda} \mathbf{c}(\lambda) P_\lambda - \mathbf{K} \right\|_{\mathcal{HS}},$$

is the best approximation of \mathbf{K} in \mathcal{GM}_2 . The optimal coefficient sequence \mathbf{c}_{app} can be determined by means of inner products with a biorthogonal basis $(Q_\lambda)_{\lambda \in \Lambda}$. If in addition $(Q_\lambda)_{\lambda \in \Lambda} \subseteq \overline{\text{span}((P_\lambda)_{\lambda \in \Lambda})}$ is assumed, $(Q_\lambda)_{\lambda \in \Lambda}$ is even uniquely determined. The next theorem gives a criterion for deciding upon the Riesz basis-property for the special case $P_\lambda = g_\lambda \otimes g_\lambda^*$.

Theorem 7. *Assume that (g, Λ) generates an Gabor frame for $L^2(\mathbb{R}^d)$, $g \in \mathbf{L}^2$ with $\|g\|_2 = 1$. Then the family (P_λ) is a Riesz basis for its closed linear span within the Hilbert space \mathcal{HS} of all Hilbert-Schmidt operators on $L^2(\mathbb{R}^d)$ if and only if the Λ -Fourier transform of $(|STFT_g(g)(\lambda)|^2)_{\lambda \in \Lambda}$ is bounded away from 0 on all Λ .*

Proof. By definition $(P_\lambda)_{\lambda \in \Lambda}$ is a Riesz basis if there exist constants $A > 0$ and $B < \infty$, such that for all $\mathbf{c} \in \ell^2$:

$$A\|\mathbf{c}\|_2^2 \leq \left\| \sum_{\lambda \in \Lambda} \mathbf{c}(\lambda) P_\lambda \right\|_2^2 \leq B\|\mathbf{c}\|_2^2$$

We reformulate the inner expression as follows:

$$\begin{aligned} \left\| \sum_{\lambda \in \Lambda} \mathbf{c}(\lambda) P_\lambda \right\|_2^2 &= \sum_{\lambda} \sum_{\lambda'} \mathbf{c}(\lambda) \overline{\mathbf{c}(\lambda')} \langle g_\lambda \otimes g_\lambda^*, g_{\lambda'} \otimes g_{\lambda'}^* \rangle \\ &= \sum_{\lambda} \sum_{\lambda'} \mathbf{c}(\lambda) \overline{\mathbf{c}(\lambda')} \int_t \int_x \pi(\lambda) g(t) \overline{\pi(\lambda) g(x)} \overline{\pi(\lambda') g(t)} \pi(\lambda') g(x) dx dt \\ &= \sum_{\lambda} \sum_{\lambda'} \mathbf{c}(\lambda) \overline{\mathbf{c}(\lambda')} \int_t \pi(\lambda) g(t) \overline{\pi(\lambda') g(t)} dt \int_x \pi(\lambda') g(x) \overline{\pi(\lambda) g(x)} dx \\ &= \sum_{\lambda} \sum_{\lambda'} \mathbf{c}(\lambda) \overline{\mathbf{c}(\lambda')} |\langle g, \pi(\lambda' - \lambda) g \rangle|^2 \\ &= \sum_{\lambda'} \overline{\mathbf{c}(\lambda')} \sum_{\lambda} \mathbf{c}(\lambda) |\langle g, \pi(\lambda' - \lambda) g \rangle|^2 \end{aligned}$$

Now we have $\phi(\mu) = |STFT_g(g)(\mu)|^2 = |\langle g, \pi(\mu) g \rangle|^2$ and obtain

$$\begin{aligned} \left\| \sum_{\lambda \in \Lambda} \mathbf{c}(\lambda) P_\lambda \right\|_2^2 &= \langle \mathbf{c} * \phi, \mathbf{c} \rangle_{\ell^2(\Lambda)} \\ &= \langle \hat{\mathbf{c}} \cdot \hat{\phi}, \hat{\mathbf{c}} \rangle_{\ell^2(\Lambda)} \\ &= \int_{\mu} \hat{\phi}(\mu) |\hat{\mathbf{c}}(\mu)|^2 d\mu \end{aligned} \tag{5.7}$$

Clearly, we have $\|c\|_2^2 = \int_\mu |\hat{c}(\mu)|^2 d\mu$, hence (5.7) is bounded below by $A\|c\|_2^2$ if and only if $\mathcal{F}_\Lambda(|STFT_g(g)(\mu)|^2) \geq A > 0$ for all $\mu \in \Lambda$.

The upper bound is provided by the fact that any $g \in S_0$ is a Bessel atom for \mathbf{L}^2 . \square

Remark 14. Note that the proof shows that the Gramian matrix of the system $(P_\lambda)_{\lambda \in \Lambda}$ is given by the circulant matrix

$$\langle P_\lambda, P_{\lambda'} \rangle = |STFT_g g(\lambda' - \lambda)|^2,$$

it is therefore diagonalized by the Fourier transform, which yields the eigenvalues of $(\langle P_\lambda, P_{\lambda'} \rangle)_{\lambda \in \Lambda}$.

Definition 15. A Gabor system $\mathcal{G} = (g, \gamma, \Lambda)$ is called *well-balanced*, if (g, Λ) is a frame and $(P_\lambda)_{\lambda \in \Lambda}$, where $P_\lambda = g_\lambda \otimes \gamma_\lambda^*$, forms a Riesz basis for its closed linear span within \mathcal{HS} .

Remark 15. An operator \mathbf{K} belongs to the closed linear span of this Riesz basis if and only if it belongs to \mathcal{GM}_2 , the space of Gabor multipliers with $\ell^2(\Lambda)$ -symbol.

One question that may arise in the context of representing operators by means of Gabor multipliers is how the identity operator can be represented as a Gabor multiplier. The following result shows, however, that only constant multipliers can yield the identity.

Theorem 8. Let $\mathcal{G} = (g_1, g_2, \Lambda)$ be well-balanced, with $g_1, g_2 \in S_0$. The Gabor multiplier $\mathbf{G}_{g_1, g_2, \Lambda, \mathbf{m}}$ is equal to a multiple of the identity operator on \mathbf{L}^2 if and only if the upper symbol \mathbf{m} is a constant function.

Proof. First note that the Kohn-Nirenberg symbol of the identity operator Id is the constant function $\mathbf{1}$, as the kernel of Id is a Dirac impulse. Hence, $T_\mu \sigma(\text{Id}) = \sigma(\text{Id})$ for all μ . As shown in Lemma 4, the KNS of the Gabor-multiplier $\mathbf{G}_{g_1, g_2, \Lambda, \mathbf{m}}$ is given by $\sum_{\lambda' \in \Lambda} \mathbf{m}(\lambda') T_{\lambda'} \sigma(P_0)$, where P_0 denotes $g_1 \otimes g_2^*$. Thus, if

$$\mathbf{1} = \sum_{\lambda' \in \Lambda} \mathbf{m}(\lambda') T_{\lambda'} \sigma(P_0)(\lambda), \quad (5.8)$$

we also have

$$\begin{aligned} T_\mu \mathbf{1} &= T_\mu \sum_{\lambda' \in \Lambda} \mathbf{m}(\lambda') T_{\lambda'} \sigma(P_0)(\lambda) \\ &= \sum_{\lambda' \in \Lambda} \mathbf{m}(\lambda') \sigma(P_0)(\lambda - \lambda' - \mu) \\ &= \sum_{\lambda' \in \Lambda} \mathbf{m}(\lambda' + \mu) T_{\lambda'} \sigma(P_0)(\lambda), \end{aligned} \quad (5.9)$$

and because $\sigma(P_0)$ is not equal to 0, (5.8) and (5.9) imply $\mathbf{m}(\lambda') = \mathbf{m}(\lambda' + \mu)$ for all $\mu \in \Lambda$, hence $\mathbf{m} \equiv c$. Thus we obtain:

$$\text{Id } f = c \sum_{\lambda \in \Lambda} \langle f, \pi(\lambda) g_1 \rangle \pi(\lambda) g_2. \quad (5.10)$$

\square

Remark 16. It follows immediately from (5.10) that (g_1, Λ) and $(\frac{1}{c}g_2, \Lambda)$ are dual systems. Therefore, if $\mathbf{G}_{g_1, g_2, \Lambda, \mathbf{m}} = \text{Id}$, then (g_1, Λ) and (g_2, Λ) are dual frames up to a constant. In particular, if $g_1 = g_2 = g$, the Gabor frame (g, Λ) has to be tight.

As mentioned before, any Riesz basis in a Hilbert space possesses a biorthogonal basis $(Q_\lambda)_{\lambda \in \Lambda} \subseteq \text{span}((P_\lambda)_{\lambda \in \Lambda})$. The next theorem states that this biorthogonal basis will be of the same, coherent form as $(P_\lambda)_{\lambda \in \Lambda}$.

Theorem 9. *Let $(P_\lambda)_{\lambda \in \Lambda}$ be a Riesz basis in \mathcal{HS} . Then the uniquely determined biorthogonal basis $(Q_\lambda)_{\lambda \in \Lambda} \subseteq \text{span}((P_\lambda)_{\lambda \in \Lambda})$ is of the form $(Q_\lambda)_{\lambda \in \Lambda} = \pi_2(\lambda)Q_0$.*

Remark 17. Due to a result on spline-type spaces, see [24], Q_0 has an S_0 -kernel, whenever $g \in S_0$.

Note that biorthogonality is a *symmetric* relation between systems of functions or vectors, i.e., by definition the two systems $P_i, i \in \mathcal{I}$ and $Q_j, j \in \mathcal{J}$ are biorthogonal if (and only if) $\langle P_i, Q_j \rangle = \delta_{i-j}$, for all $i \in \mathcal{I}$ and $j \in \mathcal{J}$. Due to the *coherence* of both systems, the biorthogonality follows already from the verification of $\langle Q_0, P_\lambda \rangle_{\mathcal{HS}} = \delta_\lambda$.

Proof. From the biorthogonality of $(P_\lambda)_{\lambda \in \Lambda}$ and $(Q_\lambda)_{\lambda \in \Lambda}$ we have that $\langle Q_0, P_\lambda \rangle_{\mathcal{HS}} = \delta_\lambda$. From this we deduce by

$$\langle \pi_{\lambda'} Q_0 \pi_{\lambda'}^*, P_\lambda \rangle_{\mathcal{HS}} = \langle Q_0, \pi_{-\lambda'} P_\lambda \pi_{-\lambda'}^* \rangle_{\mathcal{HS}} = \langle Q_0, P_{\lambda-\lambda'} \rangle = \delta_{\lambda-\lambda'},$$

and the group structure of Λ , that $(\pi_2(\lambda)Q_0)$ is a biorthogonal system for $(P_\lambda)_{\lambda \in \Lambda}$. The statement then follows from the uniqueness of $(Q_\lambda)_{\lambda \in \Lambda}$. \square

Remark 18. If $(g_\lambda)_{\lambda \in \Lambda}$ is a redundant frame and $(P_\lambda)_{\lambda \in \Lambda}$ is a system of rank-1 operators, then Q_0 cannot have rank 1, i.e., there do not exist functions g, γ , such that $Q_0 = \gamma_1 \otimes \gamma_2^*$.

Proof. First note that

$$\pi(\lambda')\gamma_1 \otimes \gamma_2^* \pi(\lambda')^* = (\pi(\lambda')\gamma_1) \otimes (\pi(\lambda')\gamma_2)^*$$

by a straightforward calculation. By definition of biorthogonality $\langle Q_{\lambda'}, P_\lambda \rangle_{\mathcal{HS}} = \delta_{\lambda-\lambda'}$ for all $\lambda, \lambda' \in \Lambda$. Assume that $Q_0 = \gamma_1 \otimes \gamma_2^*$ is rank one, hence:

$$\begin{aligned} \langle Q_{\lambda'}, P_\lambda \rangle_{\mathcal{HS}} &= \langle \pi(\lambda')\gamma_1, g_\lambda \rangle \langle g_\lambda, \pi(\lambda')\gamma_2 \rangle \\ &= \overline{\langle g_\lambda, \pi(\lambda')\gamma_1 \rangle} \langle g_\lambda, \pi(\lambda')\gamma_2 \rangle \\ &= \langle g_\lambda, \langle g_\lambda, \pi(\lambda')\gamma_1 \rangle \pi(\lambda')\gamma_2 \rangle = \delta_{\lambda-\lambda'}, \end{aligned}$$

and thus $(\langle g_\lambda, \pi(\lambda')\gamma_1 \rangle \pi(\lambda')\gamma_2)_{\lambda' \in \Lambda}$ would be a biorthogonal system for $(g_\lambda)_{\lambda \in \Lambda}$, which is a contradiction to the assumption that $(g_\lambda)_{\lambda \in \Lambda}$ is a redundant frame. \square

The following theorem does not only structurally describe the operator Q_0 generating the biorthogonal system for $(P_\lambda)_{\lambda \in \Lambda}$, it also yields a method for obtaining Q_0 numerically.

Theorem 10. *The operator Q_0 generating the biorthogonal basis $(Q_\lambda)_{\lambda \in \Lambda} = \pi_2(\lambda)Q_0$ is given formally by its KNS as*

$$\sigma(Q_0) = \mathcal{F}_\Lambda^{-1} \left(\frac{1}{\mathcal{F}_\Lambda(|\mathcal{V}_g g|_\Lambda|^2)} \right) *_\Lambda \sigma(P_0),$$

where $\mathcal{V}_g g|_\Lambda$ is the restriction of $\mathcal{V}_g g$ to Λ .

Proof. $Q_0 \in \text{span}((P_\lambda)_{\lambda \in \Lambda})$, hence $Q_0 = \sum_{\lambda \in \Lambda} c_\lambda P_\lambda$ for some $\mathbf{c} = (c_\lambda)$ in $\ell^1(\Lambda)^3$. Then we have, by Lemma 4, that

$$\sigma(Q_0)(\lambda) = [\sigma_U(Q_0) * \sigma(P_0)](\lambda),$$

such that only the upper symbol $\sigma_U(Q_0)(\lambda) = c_\lambda$ has to be determined. Note that by definition of biorthogonality we have $\delta_{\lambda,0} = \langle Q_0, P_\lambda \rangle$, hence

$$\begin{aligned} \delta_{\lambda,0} &= \sum_{\lambda' \in \Lambda} c_{\lambda'} \langle P_\lambda, P_{\lambda'} \rangle \\ &= \sum_{\lambda' \in \Lambda} c_{\lambda'} |STFT_g(\lambda' - \lambda)|^2 \\ &= \mathbf{c} *_\Lambda |\mathcal{V}_g g|_\Lambda|^2 \end{aligned} \tag{5.11}$$

From (5.11) we get via the Fourier transform over Λ :

$$\mathbf{1} \equiv \mathcal{F}_\Lambda \mathbf{c} \cdot \mathcal{F}_\Lambda |\mathcal{V}_g g|_\Lambda|^2,$$

such that

$$\mathbf{c} = \mathcal{F}_\Lambda^{-1} \left(\frac{1}{\mathcal{F}_\Lambda(|\mathcal{V}_g g|_\Lambda|^2)} \right).$$

□

Remark 19. Heuristically, the shape of the sequence $\alpha_\lambda = |\mathcal{V}_g g|_\Lambda|^2$ tends towards the sequence $\delta_{\lambda,0}$ for $(a, b) \rightarrow (\infty, \infty)$ if $g \in S_0$. Consequently, in a heuristic sense, $Q_0 \rightarrow P_0$ in S_0 for decreasing lattice density.

The result of the previous theorem suggests a fast way to calculate the biorthogonal operator. A realization of the procedure in MATLAB can be found in the appendix.

5.5 Best-Approximation of General Linear Operators

The following, main statement of this section follows from the results in the last section and general facts about projection in Hilbert spaces.

³The fact that the coefficients $\mathbf{c} = (c_\lambda)$ are in $\ell^1(\Lambda)$ and thus Q_0 again has an S_0 -kernel, is a non-trivial consequence of the theory of spline-type spaces, as described in [24, Theorem 4.13].

Theorem 11. *For a given Hilbert Schmidt operator $\mathbf{K} \in \mathcal{HS}$ the best approximation by Gabor multipliers with $g \in S_0$ and $\Lambda \subset \mathbb{R}^d \times \widehat{\mathbb{R}}^d$ is given by*

$$\mathbf{K}_{app} = \sum_{\lambda \in \Lambda} \langle \mathbf{K}, Q_\lambda \rangle_{\mathcal{HS}} P_\lambda = \sum_{\lambda \in \Lambda} \langle \mathbf{K}, P_\lambda \rangle_{\mathcal{HS}} Q_\lambda. \quad (5.12)$$

For fixed (g, Λ) the mapping $\mathbf{K} \mapsto \mathbf{K}_{app}(T)$ is the orthogonal projection from the Hilbert space \mathcal{HS} onto the closed subspace of Gabor multipliers with $\ell^2(\Lambda)$ -symbols.

5.5.1 Numerical realization and examples

In this section we briefly describe how Gabor multipliers can be handled in a finite discrete setting. The highly structured elements involved in the numerical realization of Gabor multipliers suggest fast algorithms, which are described in detail in [26]. Here we only give a comprehensible description of the numerical setting and some examples of realization.

Let the signal length be denoted by n , the number of lattice points by $k = \frac{n}{a} \frac{n}{b}$. The operators $(P_\lambda)_{\lambda \in \Lambda}$ are matrices of dimension $n \times n$. By writing them as row-vectors of size $1 \times n^2$, we can build the matrix \mathcal{A} of size $k \times n^2$, representing the system of projection operators $(P_\lambda)_{\lambda \in \Lambda}$:

$$\mathcal{A}(i, j) = P_{\lambda_i}(j) \text{ for } i = 1, \dots, k \text{ and } j = 1, \dots, n^2.$$

We denote the pseudo-inverse of an operator (matrix) \mathbf{K} by \mathbf{K}^+ . Then, writing the operator \mathbf{K} and its best-approximation \mathbf{K}_{app} in the system \mathcal{A} , both $n \times n$ -matrices, as $1 \times n^2$ -vectors, we have the following representation of \mathbf{K}_{app} :

$$\mathbf{K}_{app} = \mathbf{K} \cdot \mathcal{A}^+ \cdot \mathcal{A}.$$

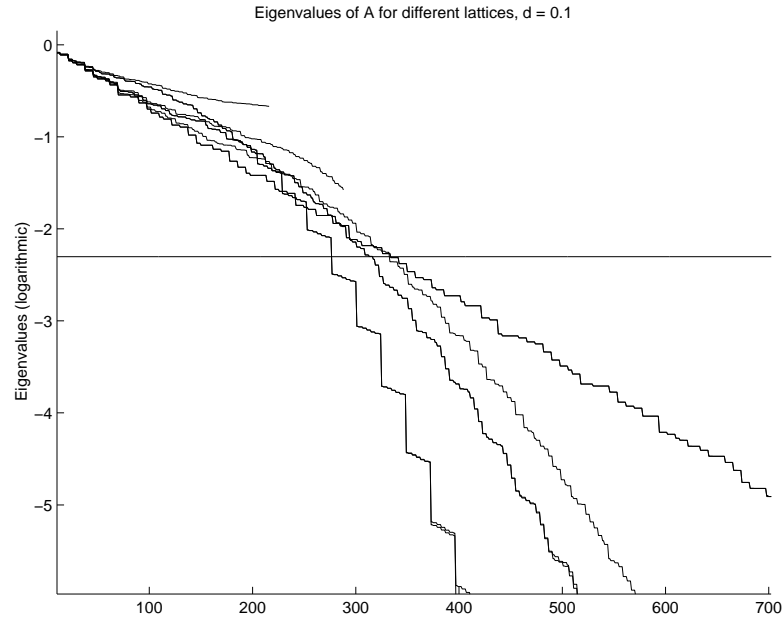
Now we have that $\mathcal{A}^+ = \mathcal{A}^* \cdot (\mathcal{A} \cdot \mathcal{A}^*)^+$, and as \mathcal{A} is assumed to have full rank, $(\mathcal{A} \cdot \mathcal{A}^*)$ is invertible, such that $\mathcal{A}^+ = \mathcal{A}^* \cdot (\mathcal{A} \cdot \mathcal{A}^*)^{-1}$. Hence we obtain:

$$\mathbf{K}_{app} = \mathbf{K} \cdot \mathcal{A}^* \cdot (\mathcal{A} \cdot \mathcal{A}^*)^{-1} \cdot \mathcal{A}.$$

Apparently, $(\mathcal{A} \cdot \mathcal{A}^*)$ is the Gramian matrix of $(P_\lambda)_{\lambda \in \Lambda}$, which is a circulant matrix, see Eemark 14 in Section 5.4.1. Hence, its inverse can be calculated at low computational cost via the Fourier transform of the convolution kernel given by $|STFT_g g(\lambda' - \lambda)|^2$, see the Appendix, Section A.5 for a MATLAB realization.

On the other hand, the row vector $\mathbf{K} \cdot \mathcal{A}^*$, size $1 \times k$, clearly contains the lower symbol of the operator \mathbf{K} with respect to \mathcal{A} , whereas $[\mathbf{K} \cdot \mathcal{A}^* \cdot (\mathcal{A} \cdot \mathcal{A}^*)^{-1}]$ is a row vector of the same size representing the upper symbol, which are the coefficients \mathbf{c} of the best-approximation in the expansion

$$\mathbf{K}_{app} = \sum_{\lambda \in \Lambda} \mathbf{c}(\lambda) P_\lambda.$$

Figure 5.3: *Eigenvalues of \mathcal{A} for different Gabor systems*

Thus, $(\mathcal{A} \cdot \mathcal{A}^*)$ is the matrix representing the mapping from upper to lower symbol, see Theorem 13, which can immediately be seen to be invertible if and only if \mathcal{A} has full rank.

We give some interesting examples for the numerical realization of the facts discussed so far.

The dimension of the space spanned by $(P_\lambda)_{\lambda \in \Lambda}$

Theorem 7 yields a criterion for deciding upon the Riesz basis property of $(P_\lambda)_{\lambda \in \Lambda}$, which is particularly easy to handle in the finite discrete case. As discussed above, we can determine the rank of \mathcal{A} using the fact that $(\mathcal{A} \cdot \mathcal{A}^*)$ is a circulant matrix. Recalls that $(\mathcal{A} \cdot \mathcal{A}^*)$ is generated by the modulus squared of $stft(g, g, a, b)$. Via a two-dim FFT of this matrix, we even obtain the eigenvalues at the same time. This fact yields a useful tool to determine the number of *salient* eigenvectors, i.e., eigenvectors corresponding to eigenvalues above a given threshold, of the matrix $(\mathcal{A} \cdot \mathcal{A}^*)$. A corresponding MATLAB code can be found in Appendix A.3. Figure 5.3 shows that the number of salient eigenvectors is relatively independent of the redundancy of the Gabor frame \mathcal{G} , as long as the system is well-balanced. The plot shows the eigenvalues for 9 different systems with redundancies between 1.5 and 24. The number of eigenvalues above the threshold $d = 0.1$ in dependence on the system's redundancy is given as follows:

Redundancy	1.5	2.0	3.0	4.0	6.0	6.0	8.0	12.0	24.0
Number of eigenvalues > 0.1	216	276	276	288	316	316	332	333	333

The results clearly support the fact that the growth of the dimension of the space spanned by $(P_\lambda)_{\lambda \in \Lambda}$ is by far slower than the increment of the number of Gabor atoms inside the mask, corresponding to the increment of redundancy. Consequently, in the choice of a system \mathcal{G} for the approximation of an operator by means of a Gabor multiplier, the increase in computation time is disproportionately higher than the improvement in approximation quality.

Synthesizing a Gabor multiplier

In this section we discuss the issue of calculating the Gabor multiplier if the upper symbol and the Gabor system \mathcal{G} are given. As shown in Lemma 4, the KNS of the Gabor-multiplier is just the convolution of the upper symbol (b) with the KNS of the projection operator P_0 . Hence, the KNS of the operator kernel of the Gabor multiplier can be obtained from the inverse Fourier transform of the product of the Fourier transforms of b and the KNS of P_0 , respectively:

$$\mathcal{F}(\sigma(\mathbf{G}_m)) = \mathcal{F}(b) \cdot \mathcal{F}(\sigma(P_0)).$$

The next section shows that the KNS is calculated by FFT as well, hence the whole procedure is numerically very effective. See Appendix A.6 for the corresponding MATLAB code.

Calculating the KNS and the spreading function

According to the definition of the KNS (Definition 11) and the spreading function, see (5.4, both representations (and their inverses) can be obtained by a simple transformation on the columns or rows of the matrix kernel, followed by n Fourier transforms of length n . A summary of the corresponding MATLAB code, due to M.Hampejs, [26], is given in Appendix A.7.

5.6 Changing the Parameters

Once the approximation procedure has been established, we face the obvious question: how does the choice of the Gabor system used for approximation influence the performance? In the next two sections the relation of Gabor multipliers given by different systems is investigated and some numerical results are presented.

5.6.1 Changing the window

In this section we investigate the effect of changing the window g on the resulting Gabor multiplier. In particular, we are interested in the best approximation of a given Gabor multiplier in the system given by a different window. The next theorem will shed light on this issue. In the sequel we denote by σ_L^g and σ_U^g the lower and upper symbols, respectively, of the Gabor multipliers with respect to the systems (g, Λ) and by P_0^g and

P_0^γ the projection kernels $g \otimes g^*$ and $\gamma \otimes \gamma^*$, respectively, and the biorthogonal kernels as Q_0^g and Q_0^γ .

Theorem 12. *Let a Gabor multiplier $K_g = G_{g,\Lambda,\sigma_U^g}$ be given. Then $\sigma_U^\gamma(K_g)$, the upper symbol of the best approximation K_γ of K_g within the system (γ, Λ) is given by the Λ -convolution of σ_U^g , the upper symbol defining K_g and $\sigma_U^\gamma(P_0^g)$, the upper symbol of P_0^g with respect to the new system (γ, Λ) .*

Proof. The upper symbol of the best approximation of $K_g = \sum_{\lambda' \in \Lambda} \sigma_U^g(\lambda') P_{\lambda'}^g$ with respect to the system (γ, Λ) is given as

$$\begin{aligned} \sigma_U^\gamma(K_g)(\lambda) &= \langle K_g, Q_\lambda^\gamma \rangle \\ &= \sum_{\lambda' \in \Lambda} \sigma_U^g(\lambda') \langle P_{\lambda'}^g, Q_\lambda^\gamma \rangle \\ &= \sum_{\lambda' \in \Lambda} \sigma_U^g(\lambda') \langle P_0^g, Q_{\lambda-\lambda'}^\gamma \rangle \\ &= \sum_{\lambda' \in \Lambda} \sigma_U^g(\lambda') \sigma_U^\gamma(P_0^g)(\lambda - \lambda') \\ &= \sigma_U^g * \sigma_U^\gamma(P_0^g) \end{aligned}$$

□

It is obvious that $\sigma_U^g(P_0^g)$ is simply a δ -function. We also have that $g \longrightarrow \gamma$ in S_0 implies the convergence of Q_0^γ to Q_0^g in S_0 , therefore $\sigma_U^\gamma(P_0^g)$ tends towards a δ -function for $g \longrightarrow \gamma$. Thus, for $g \longrightarrow \gamma$, $\sigma_U^\gamma(K_g) \longrightarrow \sigma_U^g(K_g)$.

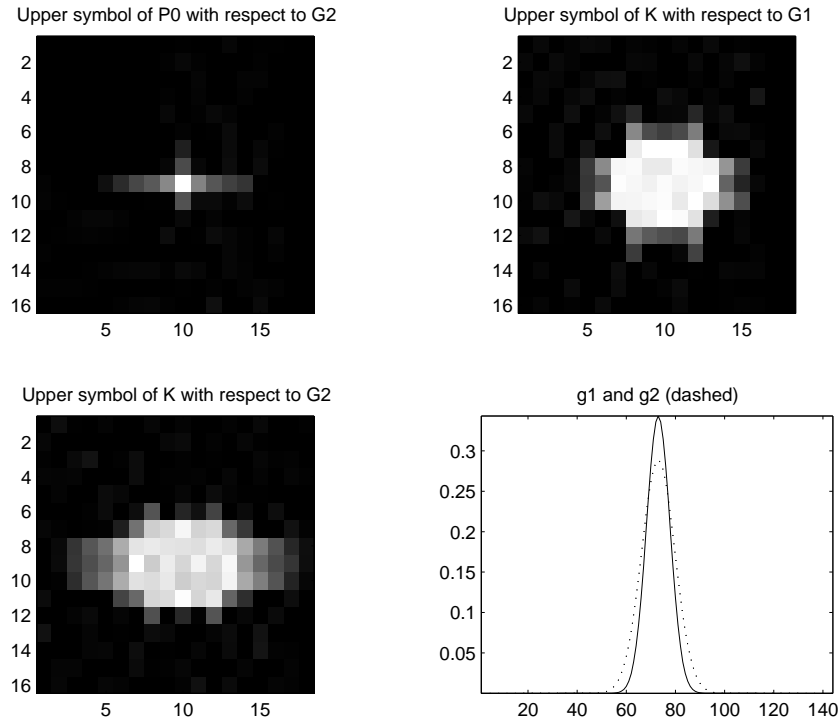
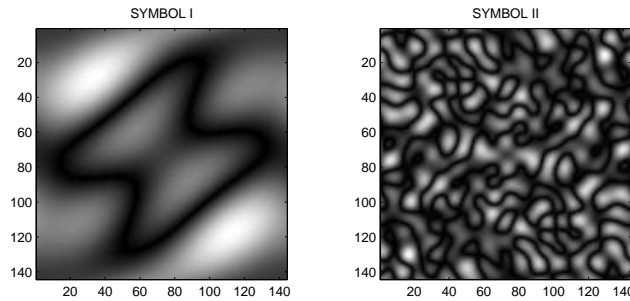
Example

Figure 5.4 illustrates the results of Theorem 12 for an operator H defined as the projection onto the first few eigenvectors of a localization operator. $K = K_g$ is its best approximation by means of the system $G1 = (g, \Lambda)$. The plot first shows the upper symbol of the best approximation of P_0^g in the system $G2 = (\gamma, \Lambda)$, where γ is derived from g by a dilation. The second and third plots show $\sigma_U^g(K_g)$ and $\sigma_U^\gamma(K_g)$, respectively. The effect of the convolution is clearly visible. The last plot depicts the two window $g_1 = g$ and $g_2 = \gamma$.

Tight windows

As shown in Theorem 8, the only way to represent the identity operator by a Gabor multiplier is to make use of a tight Gabor system together with a constant multiplier. This suggests the assumption that at least for smooth symbols, which locally resemble a constant multiplier, it might be advantageous to use the tight versions of weakly oversampled systems.⁴ The following numerical results strongly support this expectation.

⁴Note that $g_t \longrightarrow g$ for $\text{red}(\Lambda) \longrightarrow n$, see [32].

Figure 5.4: *Upper symbols*Figure 5.5: *Upper symbols with different smoothness*

Two experiments have been carried out with the same basic parameters: The signal length was assumed to be 144, hence the dimension of the operators was 144×144 . The same discrete Gaussian window was chosen as original window. The redundancies varied between 2 and 144. In the first experiment, the upper symbol generating the Gabor multipliers was chosen to be very smooth (with frequencies up to $2/144$), whereas in the second experiment, frequencies up to $9/144$ occur in the multiplier of the second experiment, see Figure 5.5. In both experiments, the approximation quality of the tight systems was compared the approximation quality of the systems using the original window for all redundancies. The STFT- multiplier, i.e., the Gabor multiplier with the highest redundancy, corresponding to the time- and frequency-shift parame-

Table 5.1: **CASE I: Smooth upper symbol**

Redundancy	Error with tight window	Error with original window
2	0.0938	0.2963
4	0.0734	0.2367
16	0.0734	0.2367
3	0.0491	0.1242
6	0.0034	0.0064
24	0.0034	0.0064
18	0.0489	0.1238
36	0.0000	0.0000
144	0.0000	0.0000

Table 5.2: **CASE II: Higher frequency upper symbol**

Redundancy	Error with tight window	Error with original window
2	1.1097	1.1305
4	1.0167	1.0320
16	1.0167	1.0320
3	0.7059	0.7196
6	0.1465	0.1460
24	0.1465	0.1459
18	0.6982	0.7128
36	0.0006	0.0006
144	0.0000	0.0000

ters $a = 1$ and $b = 1$, served as the prototype operator to be approximated.

The results are presented in Table 5.1 and 5.2. The error of the approximation was measured as the operator norm of the difference of the prototype operator and its approximation.

The approximation quality is clearly improved by the choice of the systems, especially in the cases of low redundancy, which are most commonly used in applications.

The second experiment shows that for less smooth symbols, the STFT-multiplier is generally less exactly reproducible by systems with low redundancy. In addition, the improvement introduced by the choice of a tight system is less momentous.

5.6.2 The relation between upper and lower signal

Theorem 13. *A bounded and invertible linear mapping between upper and lower symbol of a Gabor multiplier exists if and only if $(P_\lambda)_{\lambda \in \Lambda}$ is a Riesz basis, in which case the bijection is given by the Gram matrix of the system $(P_\lambda)_{\lambda \in \Lambda}$.*

Proof. Let a Gabor multiplier be given as

$$K = \sum_{\lambda \in \Lambda} \sigma_U(\lambda) P_\lambda.$$

Thus we have

$$\begin{aligned}\sigma_L(\lambda') &= \left\langle \sum_{\lambda \in \Lambda} \sigma_U(\lambda) P_\lambda, P_{\lambda'} \right\rangle \\ &= \sum_{\lambda \in \Lambda} \langle P_\lambda, P_{\lambda'} \rangle \sigma_U(\lambda).\end{aligned}$$

□

$\langle P_\lambda, P_{\lambda'} \rangle$ was shown to be equal to $|STFT_g g(\lambda' - \lambda)|^2$ in the proof of Theorem 7, hence the lower symbol σ_L is obtained by a *convolution* over Λ between $|STFT_g g|^2$ and σ_U .

5.6.3 Varying the lattice

Recall Example 4, which can be seen as a special case of approximating a Gabor multiplier given in a system \mathcal{G}_1 by means of a different system \mathcal{G}_2 . Similarly, we find the lower symbol for the best-approximation $\mathbf{G}_{app}^{\mathcal{G}_2}$ of a Gabor multiplier $\mathbf{G} = G_{g_1, \Lambda_1}$ in a system $\mathcal{G}_2 = (g_2, \Lambda_2)$ by a convolution on Λ_1 :

$$\sigma_L^{\mathcal{G}_2}(\mathbf{G})(\mu) = \sum_{\lambda \in \Lambda_1} \sigma_U^{\mathcal{G}_1}(\mathbf{G})(\lambda) |STFT_{g_1 g_2}|^2(\mu - \lambda), \mu \in \Lambda_2.$$

According to Theorem 13 above, the upper symbol of $\mathbf{G}_{app}^{\mathcal{G}_2}$ can then be recovered by:

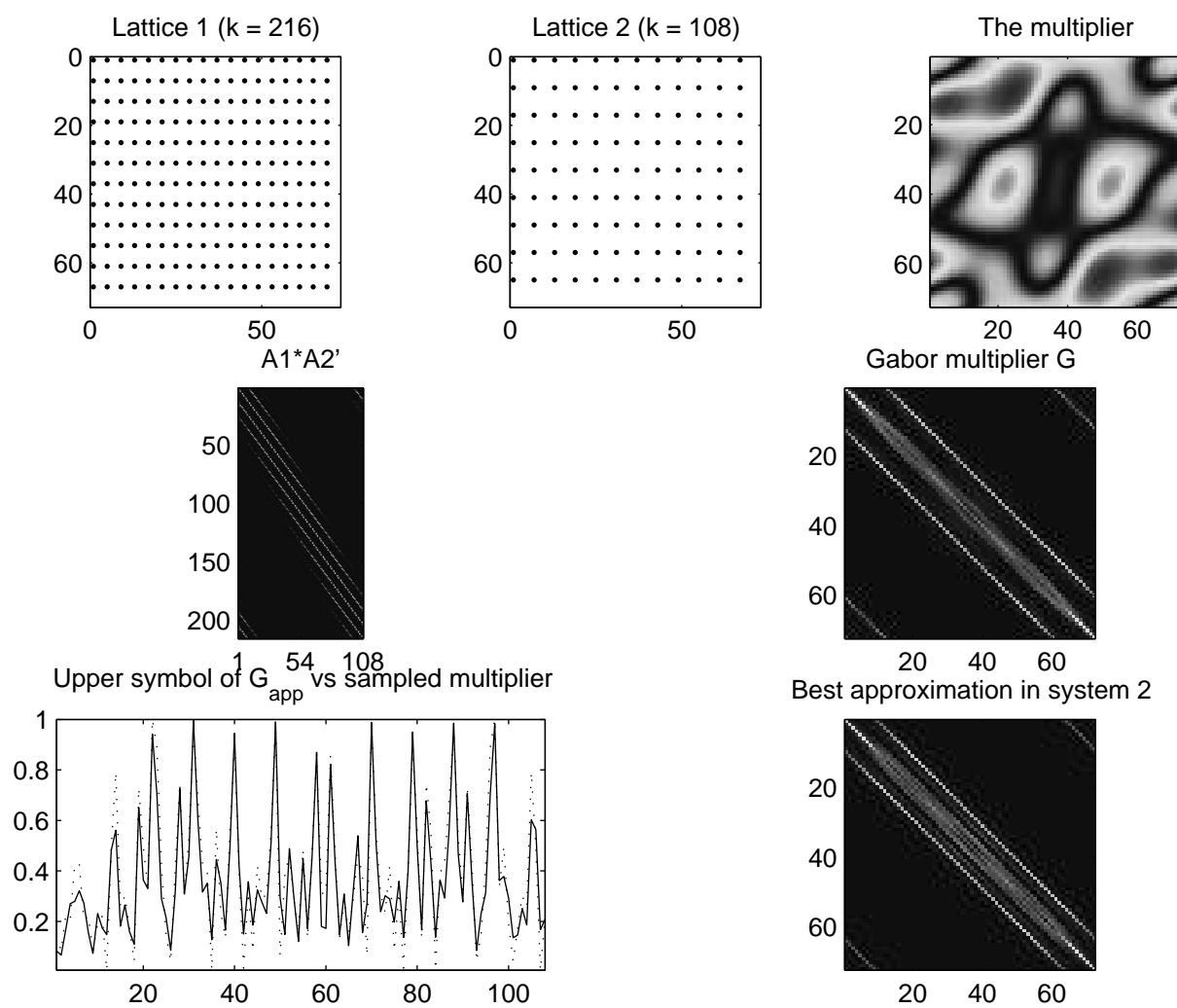
$$\sigma_U^{\mathcal{G}_2}(\mathbf{G}) = \sigma_U^{\mathcal{G}_2}(\mathbf{G}_{app}) = \mathcal{F}^{-1} \left[\mathcal{F}(\sigma_L^{\mathcal{G}_2}) / \mathcal{F}(|STFT_{g_2 g_2}|^2) \right]. \quad (5.13)$$

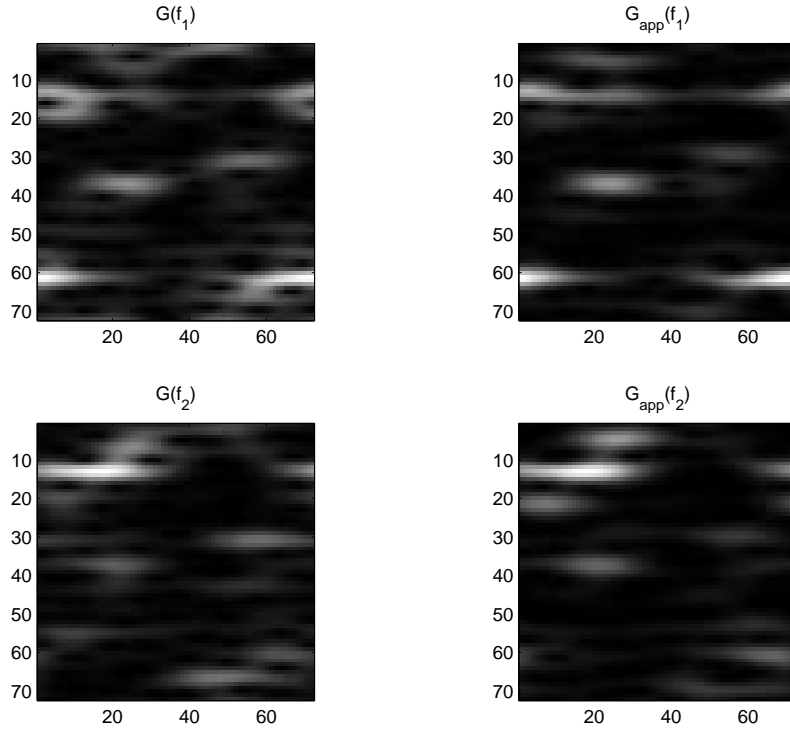
Example

Numerically, if we denote by \mathcal{A}_1 the matrix of size $k_1 \times n^2$, $k_1 = |\Lambda_1|$, comprised of the projection operators corresponding to system \mathcal{G}_1 and analogously by \mathcal{A}_2 the matrix corresponding to \mathcal{G}_2 , the necessary calculations for obtaining $\sigma_U^{\mathcal{G}_2}(\mathbf{G})$ can be written as:

$$\sigma_U^{\mathcal{G}_2}(\mathbf{G}) = \sigma_U^{\mathcal{G}_1}(\mathbf{G}) \cdot \mathcal{A}_1 \cdot \mathcal{A}_2^+ = \sigma_U^{\mathcal{G}_1}(\mathbf{G}) \cdot \mathcal{A}_1 \cdot \mathcal{A}_2^* \cdot (\mathcal{A}_2 \mathcal{A}_2^*)^{-1},$$

where $\mathcal{A}_1 \cdot \mathcal{A}_2^*$ is a $k_1 \times k_2$ matrix and $\sigma_U^{\mathcal{G}_1}(\mathbf{G}) \cdot \mathcal{A}_1 \cdot \mathcal{A}_2^*$ represents the *lower* symbol of the approximation. Figure 5.6 shows the result of this procedure. In the first two plot, the two lattices under consideration can be seen. Here, the signal length n is 72. The third plot shows the multiplier \mathbf{m} before being sampled. In the next plot the matrix $\mathcal{A}_1 \cdot \mathcal{A}_2^*$, "transferring" the symbol from system \mathcal{G}_1 to \mathcal{G}_2 , is shown. The remaining plots show the Gabor multiplier \mathbf{G} and the best approximation $\mathbf{G}_{app}^{\mathcal{G}_2}$, as well as a comparison between the upper symbol of $\mathbf{G}_{app}^{\mathcal{G}_2}$, obtained from (5.13) and the symbol arising from simple downsampling of \mathbf{m} . Figure 5.7 shows results of the action of both \mathbf{G} and \mathbf{G}_{app} on two random signals f_1 and f_2 by means of their short-time Fourier transform .

Figure 5.6: *Changing the lattice*

Figure 5.7: *Effect of lattice change on TF-concentration*

Higher order approximation

Clearly, using a different lattice, especially if the second lattice has a lower redundancy, entails some sort of loss in approximation quality. The class of operators which are *exactly* reproducible in a certain Gabor system is quite restricted. On the other hand, any function f and its image under an operator \mathbf{G} have a Gabor representation from which they can be recovered. In particular, for tight systems we even have $f = \sum_{\lambda \in \Lambda} \langle f, \pi(\lambda)g \rangle \pi(\lambda)g$. Hence, as in Example 4, a linear operator $\mathcal{W} : T_g f \mapsto T_g \mathbf{G}f$ exists. The restriction to Gabor multipliers corresponds to ignoring all entries off the diagonal of this operator, whereas incorporating these entries in the operator corresponds to extending the system of projection operators $(P_\lambda)_{\lambda \in \Lambda}$ to operators of the form $g_\lambda \otimes g_\mu^*$, where μ and λ are in Λ with $\lambda \neq \mu$.

Theorem 14. *Let two tight Gabor systems $\mathcal{G}_1 = (g_1, \Lambda_1)$ and $\mathcal{G}_2 = (g_2, \Lambda_2)$ and a multiplier $\mathbf{m} \in \ell^2(\Lambda_1)$ be given. The operator $\mathbf{G} : \mathbf{L}^2 \mapsto \mathbf{L}^2$, given by $\mathbf{G} = \sum_{\lambda \in \Lambda_1} \mathbf{m}(\lambda) P_\lambda^{g_1}$, can be represented as follows:*

$$\mathbf{G} = \sum_{\mu \in \Lambda_2} \sum_{\nu \in \Lambda_2} c_{\mathbf{m}}(\mu, \nu) (\pi(\mu)g_2) \otimes (\pi(\nu)g_2)^*,$$

where the coefficient sequence $c_{\mathbf{m}}$ is given by

$$c_{\mathbf{m}}(\mu, \nu) = \sum_{\lambda \in \Lambda_1} \mathbf{m}(\lambda) \left(STFT_{g_1} \pi(\mu)g_2 \right)(\lambda) \overline{\left(STFT_{g_1} \pi(\nu)g_2 \right)(\lambda)}.$$

Proof. We denote the Gabor analysis operator corresponding to the system \mathcal{G}_i by T_{g_i} , hence, as the systems are tight, we have $f = T_{g_i}^* T_{g_i} f$ for all $f \in \mathbf{L}^2$. Then, as $T_{g_2} \mathbf{G} f = T_{g_2} \mathbf{G} T_{g_2}^* T_{g_2} f$, we write the operator \mathcal{W} mapping $T_{g_2} f \in \ell^2(\Lambda_2)$ to $T_{g_2} \mathbf{G} f \in \ell^2(\Lambda_2)$ as

$$\mathcal{W} = T_{g_2} T_{g_1}^* \mathbf{m} T_{g_1} T_{g_2}^*.$$

Expanding \mathcal{W} , we find:

$$\begin{aligned} \mathcal{W}(\mu, \nu) &= \sum_{\lambda \in \Lambda_1} \mathbf{m}(\lambda) \langle \pi(\mu) g_2, \pi(\lambda) g_1 \rangle \langle \pi(\lambda) g_1, \pi(\nu) g_2 \rangle \\ &= \sum_{\lambda \in \Lambda_1} \mathbf{m}(\lambda) (STFT_{g_1} \pi(\mu) g_2)(\lambda) \overline{(STFT_{g_1} \pi(\nu) g_2)(\lambda)} \end{aligned}$$

As \mathcal{W} maps the Gabor transform with respect to \mathcal{G}_2 of f to the Gabor transform of $\mathbf{G}f$, we have in fact that

$$\mathbf{G}f = \sum_{\mu \in \Lambda_2} \mathcal{W}(T_{g_2} f)(\mu) \pi(\mu) g_2,$$

hence, substituting $\langle f, \pi(\nu) g_2 \rangle$ for $T_{g_2} f(\nu)$, we obtain

$$\begin{aligned} \mathbf{G}f &= \sum_{\nu \in \Lambda_2} \sum_{\mu \in \Lambda_2} \mathcal{W}(\langle f, \pi(\nu) g_2 \rangle)(\mu) \pi(\mu) g_2 \\ &\quad \sum_{\nu \in \Lambda_2} \sum_{\mu \in \Lambda_2} \mathcal{W}(\pi(\mu) g_2 \otimes (\pi(\nu) g_2)^*) f, \end{aligned}$$

from which the representation claimed in the theorem follows. \square

Remark 20. Here, the operators $P_{\mu, \nu} = (\pi(\mu) g_2 \otimes (\pi(\nu) g_2)^*)_{\mu, \nu \in \Lambda}$ form an overcomplete system in \mathcal{HS} . Apparently, if the original Gabor frame is chosen to be tight, $(P_{\mu, \nu})_{\mu, \nu \in \Lambda}$ is a tight frame in \mathcal{HS} again. $\mathcal{W}(\mu, \nu)$ are exactly the expansion coefficients with respect to this frame.

5.7 Characterizing the Operator by its Eigenvectors

It is a natural approach to try to describe the behavior of Gabor multipliers through their eigenvectors, which represent an orthonormal basis for the range of the operators. In this section, for simplicity we always assume that tight Gabor systems are used. This assumption makes the eigenanalysis of Gabor multipliers more comprehensible. First note that for tight Gabor systems, a constant upper symbol (or multiplier \mathbf{m}) generates a multiple of the identity operator. Whenever the multiplier \mathbf{m} takes values between 0 and c , the eigenvalues of the resulting Gabor multiplier lie in the interval $[0, c]$, see [30].

Another motivation for studying the eigen-behavior of Gabor multipliers is the application to time-varying filtering tasks. Often a 0/1 multiplier, i.e., a characteristic function corresponding to a (usually bounded) region in the time-frequency plane, will be a first choice for a time-varying filtering task. However, as the Gabor system under inspection is redundant, the process of filtering by means of the corresponding Gabor multiplier cannot be a projection and in particular it is not idempotent. It can even be shown that for multiplier sequences with compact support repeated application of the operator to any given signal even yields a series of resulting signals converging to zero. This can be seen by noting that in this case all eigenvalues of \mathbf{G}_m must be less than 1, as $\|\mathbf{G}_m\| \leq 1$. See [68] for details.

We hope to achieve better concentration inside a given masking region than with conventional methods like the LSE (least square error) filter and with less computational effort than the iteration filter suggested by Qian and Chen in [55]. For a 0/1 multiplier, for instance, we expect the eigenvectors corresponding to the eigenvalues close to 1 to be well concentrated inside the mask. Hence a projection onto the eigenvectors corresponding to eigenvalues above a certain threshold ρ should generate a good result, i.e., a signal which is nicely concentrated inside the region of interest and close to 0 outside. In Section 5.8 numerical examples will be presented which confirm the applicability of this approach.

We give a precise mathematical description of the situation next: Let a tight Gabor system (g, Λ) with $g \in S_0$ be given. Denote by M_R a masking region, centered around $\lambda = 0$ without restriction of generality⁵, with $M_R \subseteq B_R(0)$. Let the finite-dimensional approximation of the frame operator S be given as

$$S_R f = \sum_{\lambda \in M_R \cap \Lambda} \langle f, g_\lambda \rangle g_\lambda, \quad (5.14)$$

which is a compact, self-adjoint operator. Let φ_k^R be the eigenvectors of S_R corresponding to its eigenvalues α_k^R . We fix a threshold $\rho > 0$ and define the following subspaces of $L^2(\mathbb{R}^d)$.

Definition 16. • $H_R = \text{range}(S_R)$

- $E_R = \text{span}\{\varphi_k^R | k \in \mathcal{I}_R^e\}$, where $\mathcal{I}_R^e = \{k : |\alpha_k^R| \geq \rho\}$.
- $R_R = \text{span}\{\varphi_k^R | k \in \mathcal{I}_R^e\}$, where $\mathcal{I}_R^e = \{k : |\alpha_k^R| < \rho\}$.

Note that due to the spectral theorem for compact, self-adjoint operators, $H_R = E_R \oplus R_R$ and with $\mathcal{I}_R = \mathcal{I}_R^e \cup \mathcal{I}_R^e$, we can write the finite-dimensional approximation of the frame operator as $S_R = \sum_{k \in \mathcal{I}_R} \alpha_k^R \langle f, \varphi_k^R \rangle \varphi_k^R$. We first prove a lemma also of interest by itself.

Lemma 3. Fix $R_0 > 0$. For any $\varepsilon > 0$, there exists R_1 such that for all $f \in H_{R_0}$

$$\|f - S_R f\|_2^2 < \varepsilon \|f\|_2^2 \text{ for all } R > R_1.$$

⁵All results in the sequel can be stated and proved analogously for any $\lambda \in \Lambda$ due to Λ -invariance of the essential properties of the operators.

Proof. First note that $S_R \rightarrow \text{Id}$ in the strong operator topology for $R \rightarrow \infty$, i.e., $\|S_R f - f\|_2 \rightarrow 0$. As $|\mathcal{I}_{R_0}| < K$, there exists R_1 , such that for all $k \in \mathcal{I}_{R_0}$ the estimate $\|S_R \varphi_k^{R_0} - \varphi_k^{R_0}\|_2 < \varepsilon$ holds whenever $R > R_1$. Any $f \in H_{R_0}$ can be written as $f = \sum_{k \in \mathcal{I}_{R_0}} \langle f, \varphi_k^{R_0} \rangle \varphi_k^{R_0}$, thus we have:

$$\begin{aligned} \|f - S_R f\|_2^2 &\leq \left\| \sum_{k \in \mathcal{I}_{R_0}} \langle f, \varphi_k^{R_0} \rangle \varphi_k^{R_0} - \sum_{k \in \mathcal{I}_{R_0}} \langle f, \varphi_k^{R_0} \rangle S_R \varphi_k^{R_0} \right\|_2^2 \\ &\leq \underbrace{\sum_{k \in \mathcal{I}_{R_0}} |\langle f, \varphi_k^{R_0} \rangle|^2}_{\|f\|_2^2} \underbrace{\|\varphi_k^{R_0} - S_R \varphi_k^{R_0}\|_2^2}_{\varepsilon}, \end{aligned}$$

for all $R > R_1$ and all $f \in H_{R_0}$. \square

Remark 21. Apparently, as the convergence is uniform on compact sets, a similar estimate can be given even if $\widetilde{H_{R_0}}$ is defined by means of a different Gabor frame.

Now we are ready to prove the following theorem.

Theorem 15. *For any fixed ρ , $0 < \rho < \|S\|$, the union of E_R as defined in Definition 16 is dense in $\mathbf{L}^2(\mathbb{R}^d)$, i.e.,*

$$\overline{\bigcup_{R>0} E_R} = \mathbf{L}^2(\mathbb{R}^d).$$

Proof. The frame property of $(g_\lambda)_{\lambda \in \Lambda}$ implies that $\overline{\bigcup_{R>0} H_R} = \mathbf{L}^2(\mathbb{R}^d)$, and thus it suffices to show that for any fixed R_0 , we can find R_1 such that $H_{R_0} \subseteq \overline{E_R}$ for $R \geq R_1$. To see this, we show that for any $\varepsilon > 0$, R_1 can be determined such that

$$\left\| \sum_{k \in \mathcal{I}_R^e} \langle f, \varphi_k^R \rangle \varphi_k^R \right\|_2^2 \leq \varepsilon \|f\|_2^2,$$

for all $f \in H_{R_0}$ whenever $R > R_1$.

Let $f \in H_{R_0}$, with

$$1 = \|f\|_2^2 = \sum_{k \in \mathcal{I}_R} |\langle f, \varphi_k^R \rangle|^2 = \sum_{k \in \mathcal{I}_R^e} |\langle f, \varphi_k^R \rangle|^2 + \sum_{k \in \mathcal{I}_R^i} |\langle f, \varphi_k^R \rangle|^2. \quad (5.15)$$

From Lemma 3 it follows that for $\gamma = \varepsilon(1 - \rho^2)$, we can choose $R_1 > R_0$, such that

$$\|f - S_{R_1} f\|_2^2 \leq \gamma \text{ for all } f \in H_{R_0} \text{ with } \|f\|_2 = 1.$$

Hence,

$$1 \leq \|S_{R_1} f\|_2^2 + \|f - S_{R_1} f\|_2^2,$$

such that $\|S_{R_1} f\|_2^2 \geq 1 - \gamma$ for all $f \in H_{R_0}$ with $\|f\|_2 = 1$. We also have

$$\begin{aligned} \|S_{R_1} f\|_2^2 &= \sum_{k \in \mathcal{I}_{R_1}} |\alpha_k^{R_1}|^2 |\langle f, \varphi_k^{R_1} \rangle|^2 \\ &= \sum_{k \in \mathcal{I}_e^{R_1}} |\alpha_k^{R_1}|^2 |\langle f, \varphi_k^{R_1} \rangle|^2 + \sum_{k \in \mathcal{I}_e^{R_1}} |\alpha_k^{R_1}|^2 |\langle f, \varphi_k^{R_1} \rangle|^2 \\ &\leq \sum_{k \in \mathcal{I}_e^{R_1}} |\langle f, \varphi_k^{R_1} \rangle|^2 + \rho^2 \sum_{k \in \mathcal{I}_e^{R_1}} |\langle f, \varphi_k^{R_1} \rangle|^2 \end{aligned}$$

because $\alpha_k^{R_1} \leq 1$ for all k . We obtain:

$$\begin{aligned}
1 - \gamma &= \sum_{k \in \mathcal{I}_R^e} |\langle f, \varphi_k^R \rangle|^2 + \sum_{k \in \mathcal{I}_R^e} |\langle f, \varphi_k^R \rangle|^2 - \gamma \leq \|S_{R_1} f\|_2^2 \\
&\leq \sum_{k \in \mathcal{I}_e^{R_1}} |\langle f, \varphi_k^{R_1} \rangle|^2 + \rho^2 \sum_{k \in \mathcal{I}_e^{R_1}} |\langle f, \varphi_k^{R_1} \rangle|^2 \\
(5.15) &\implies \\
(1 - \rho^2) \sum_{k \in \mathcal{I}_e^{R_1}} |\langle f, \varphi_k^{R_1} \rangle|^2 &\leq \gamma,
\end{aligned}$$

and thus for all $f \in H_{R_0}$ with $\|f\|_2 = 1$:

$$\sum_{k \in \mathcal{I}_e^{R_1}} |\langle f, \varphi_k^{R_1} \rangle|^2 \leq \varepsilon,$$

hence

$$\sum_{k \in \mathcal{I}_e^{R_1}} |\langle f, \varphi_k^{R_1} \rangle|^2 \leq \varepsilon \|f\|_2^2,$$

which shows that any $\overline{E_{R_1}}$ is dense in H_{R_0} . \square

In particular, we have shown the following:

Corollary 3. *Any $f \in H_{R_0}$ can be approximated arbitrarily well by $\tilde{f} \in E_R$ for $R > R_1$, where R_1 is chosen according to the proof of Theorem 15.*

Corollary 4. *In the situation of Theorem 15, define the operator*

$$\tilde{S}_{R,\rho} f = \sum_{k \in \mathcal{I}_R^e} \frac{1}{\alpha_k^R} \langle f, \varphi_k^R \rangle \varphi_k^R$$

and let $\tilde{g}_\lambda^{R,\rho} = \tilde{S}_{R,\rho} g_\lambda$, $\lambda \in M$. Then we have $f = \tilde{S}_{R,\rho} S_R f = S_R \tilde{S}_{R,\rho} f$ i.e.,

$$f = \sum_{\lambda \in M_R \cap \Lambda} \langle f, \tilde{g}_\lambda^{R,\rho} \rangle g_\lambda = \sum_{\lambda \in M_R \cap \Lambda} \langle f, g_\lambda \rangle \tilde{g}_\lambda^{R,\rho} \quad (5.16)$$

for all $f \in E_R$.

Proof. This result follows from the theory on atomic systems for subspaces of Hilbert spaces, see [31].

As $f \in E_R$, it can be written as $f = \sum_{j \in \mathcal{I}_e^R} \langle f, \varphi_j^R \rangle \varphi_j^R$, hence

$$\begin{aligned}
\sum_{\lambda \in M_R \cap \Lambda} \langle f, \tilde{g}_\lambda^{R,\rho} \rangle g_\lambda &= \sum_{\lambda \in M_R \cap \Lambda} \sum_{j \in \mathcal{I}_e^R} \langle f, \varphi_j^R \rangle \sum_{k \in \mathcal{I}_R^e} \frac{1}{\alpha_k^R} \overline{\langle g_\lambda, \varphi_k^R \rangle} \langle \varphi_j^R, \varphi_k^R \rangle g_\lambda \\
&= \sum_{\lambda \in M_R \cap \Lambda} \left\langle \sum_{j \in \mathcal{I}_e^R} \langle f, \varphi_j^R \rangle \varphi_j^R, \sum_{k \in \mathcal{I}_R^e} \frac{1}{\alpha_k^R} \langle g_\lambda, \varphi_k^R \rangle \varphi_k^R \right\rangle g_\lambda \\
&= \sum_{k \in \mathcal{I}_e^R} \frac{1}{\alpha_k^R} \langle f, \varphi_k^R \rangle \underbrace{\sum_{\lambda \in M_R \cap \Lambda} \langle \varphi_k^R, g_\lambda \rangle g_\lambda}_{\alpha_k^R \varphi_k^R} = f.
\end{aligned}$$

\square

Discussion

Note that the $\tilde{g}_\lambda^{R,\rho}$ as defined in Corollary 4 can be seen as a *local* dual basis, as well as $\tilde{S}_{R,\rho}$ may be understood as a local inverse of the Gabor multiplier $\sum_{\lambda \in M_R \cap \Lambda} \langle f, g_\lambda \rangle g_\lambda$. As discussed before, local dual bases may be used for the reconstruction in multiple Gabor systems.

5.7.1 Simulation examples

As described to some detail in [68], the calculation of the eigenspaces of Gabor multipliers can be realized with a numerical effort corresponding to the size of the masked area rather than the signal-length. The numerical realization relies on the fact that for rectangular matrices G with size $k \times n$, where k is the number of building blocks inside the masking area and n is the signal length, the eigenvectors of the frame operator $S = G^*G$ can be obtained from the eigenvectors of the Gramian matrix $\Gamma = GG^*$. As we assume $k \ll n$ here, this is numerically a lot cheaper than calculating the eigenvectors of S directly. In fact, let $v_j, j = 1, \dots, k$ be the eigenvectors of S such that $Sv_j = \alpha_j v_j$. If $\Gamma \omega_j = \alpha_j \omega_j$, then

$$v_j = \frac{1}{\sqrt{\alpha_j}} \sum_{i=1}^k \omega_j(i) g_i$$

A MATLAB code for these calculations can be found in the Appendix, Section A.4. Figure 5.8 shows the typical behavior of the eigenvectors corresponding to eigenvalues close to 1 of a Gabor multiplier with a rectangular 0/1 mask. In this and all subsequent examples, the signal length is 144. Here, a Gaussian window was chosen as an original window, the system used for the analysis was (g_t, Λ) , $\Lambda = \mathbb{Z}_{\frac{144}{8}} \times \mathbb{Z}_{\frac{144}{6}}$. The masking area, with diameter 62, the eigenvalues of G_{g_t, Λ, χ_M} and the absolute values of the first 4 eigenvectors are shown in the plot.

Any numerical realization of practically interesting tasks requires the choice of systems with low redundancy. The choice of the lattice Λ and the choice of the window thus entail certain parameters of freedom whose influence on the behavior of the eigenvalues and eigenvectors of the resulting operators will be investigated in the sequel. It will be shown that the eigenspaces are relatively independent of these parameters, which is a desired feature of the approach.

1. Dependence on the lattice

In [28] it has been shown, that for any reasonably time-frequency concentrated window g , namely for any $g \in S_0$, the behavior of the frame operator and hence the dual atoms depend continuously on the lattice constants (a, b) . In particular, whenever the lattice parameters are slightly changed, the frame property is not lost, i.e., the set of lattice parameters generating a frame for a given $g \in S_0$ is open in $\mathbb{R} \times \mathbb{R}$.⁶

⁶Note that this innocent sounding result is in fact quite remarkable, as for windows in \mathbf{L}^2 , the property of generating a frame may depend in a chaotic way on the lattice constants, see [27].

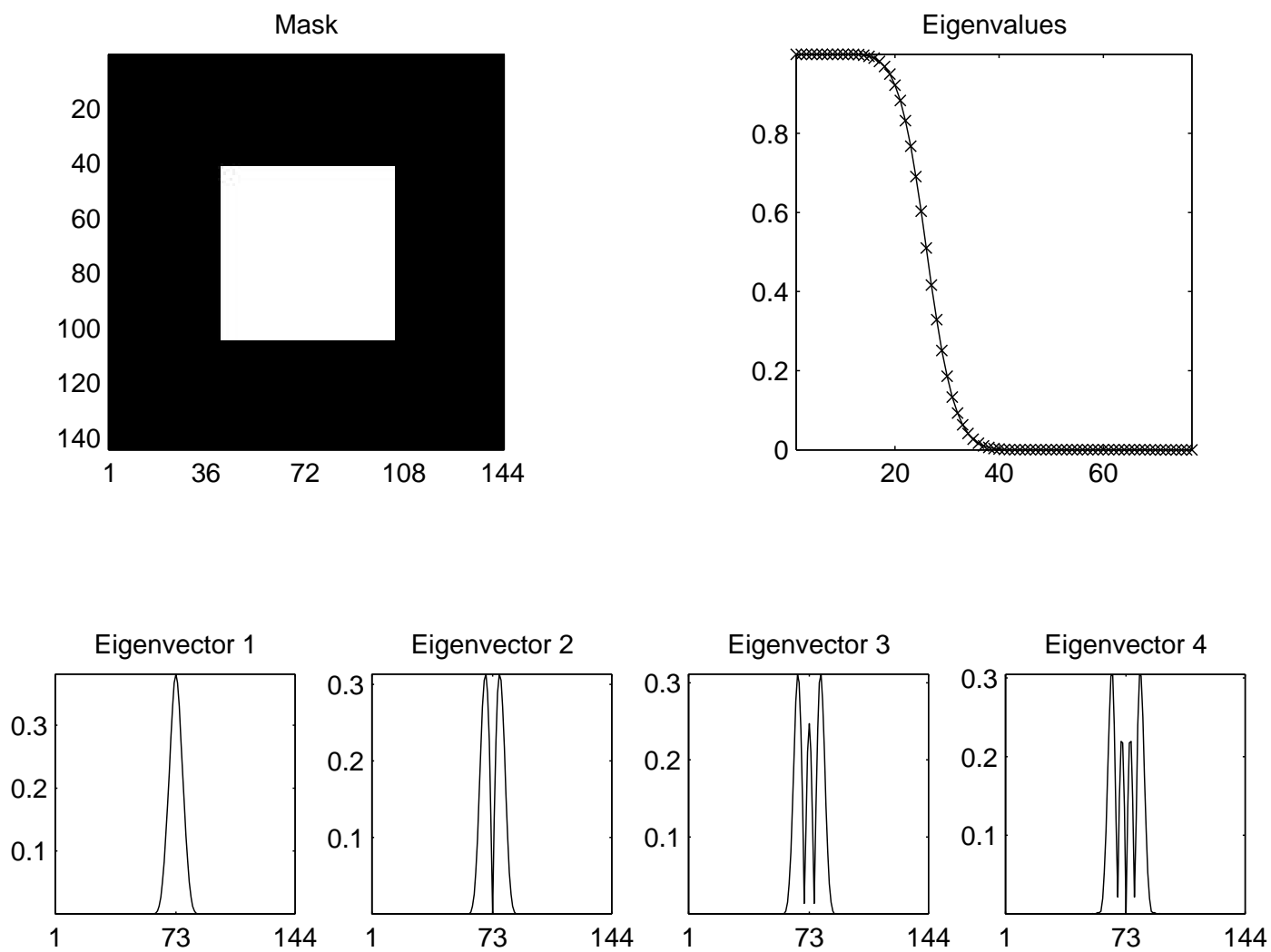


Figure 5.8: *Eigenvectors and eigenvalues of a 0/1 Gabor multiplier*

Another result ([30, Theorem 6.4]) draws a conclusion from the above-mentioned statement for Gabor-multipliers defined with $g \in S_0$. It states that at least for S_0 -symbols (\mathbb{R}^{2d}), the Gabor-multipliers generated via some TF-lattices (a_k, b_k) converge in trace-class norm to the Gabor multiplier corresponding to the lattice given by (a_0, b_0) , whenever $(a_k, b_k) \rightarrow (a_0, b_0)$ for $k \rightarrow \infty$. To achieve this result, the symbol \mathbf{m} is sampled on the respective lattice.

In the present section we want to study the TF-localization behavior on a more quantitative level. We are interested in the connection between eigenspaces generated by a certain number of eigenfunctions of Gabor-multipliers obtained from different Gabor systems and the same symbol (mask). According to Theorem 15, in the limiting case the eigenspaces become independent of the lattice. However, in the case of small masking areas, the dependence can become quite considerable, as the following example shows.

The first example compares 2 Gabor systems with redundancy 3 and 2.6667, respectively. The number of lattice points inside the mask was 63 for both systems, this corresponds to a diameter of the masking area of 54. However, due to different eccentricity of the lattices, $\Lambda_1 = 8\mathbb{Z} \times 6\mathbb{Z}$ and $\Lambda_2 = 6\mathbb{Z} \times 9\mathbb{Z}$, the resulting eigenspaces do not coincide. The lower plots in Figure 5.9 show the short-time Fourier transform of the projections onto specific eigenspaces of the Gabor multipliers with the mask depicted in the first plot. These results suggest that the eigenspaces are better concentrated in the direction with higher sampling density.

Figure 5.10, on the other hand, shows similar results for a smaller masking area and for two lattices with $a = b$. Here, Λ_1 was the full lattice $\mathbb{Z} \times \mathbb{Z}$ and $\Lambda_2 = 4\mathbb{Z} \times 4\mathbb{Z}$. The similarity of the results is obvious.

Encouraged by the statement of Corollary 3, we have the following conjecture, for which numerical evidence will be given below:

Conjecture 1. For given tight Gabor frames $\mathcal{G}_i = (g_i, \Lambda_i)_{i=1, \dots, k}$ and a multiplier \mathbf{m} in $\ell^\infty(\lambda)$, consider the subspace E_N^i generated by the first N eigenvectors of the operator $G_{g_i, \Lambda_i, \mathbf{m}}$. Then for a fixed error ε , any function f_i in a N_1 -dimensional subspace spanned by the first N_1 eigenfunctions of $G_{g_1, \Lambda_1, \mathbf{m}}$ can be represented up to the error ε as a linear combination of N_2 eigenfunctions of $G_{g_i, \Lambda_i, \mathbf{m}}$, $i = 2, \dots, k$, with $N_2 = N_1 + E(\varepsilon, N_1, m)$.

Numerical evidence: We carry out the following experiment: 6 tight Gabor systems with lattice parameters $(a_i, b_i)_{i=1, \dots, 6}$ are considered, the length of the signals is $n = 144$. The mask is cone-shaped, centered around 0 and restricted to the area 71×71 .

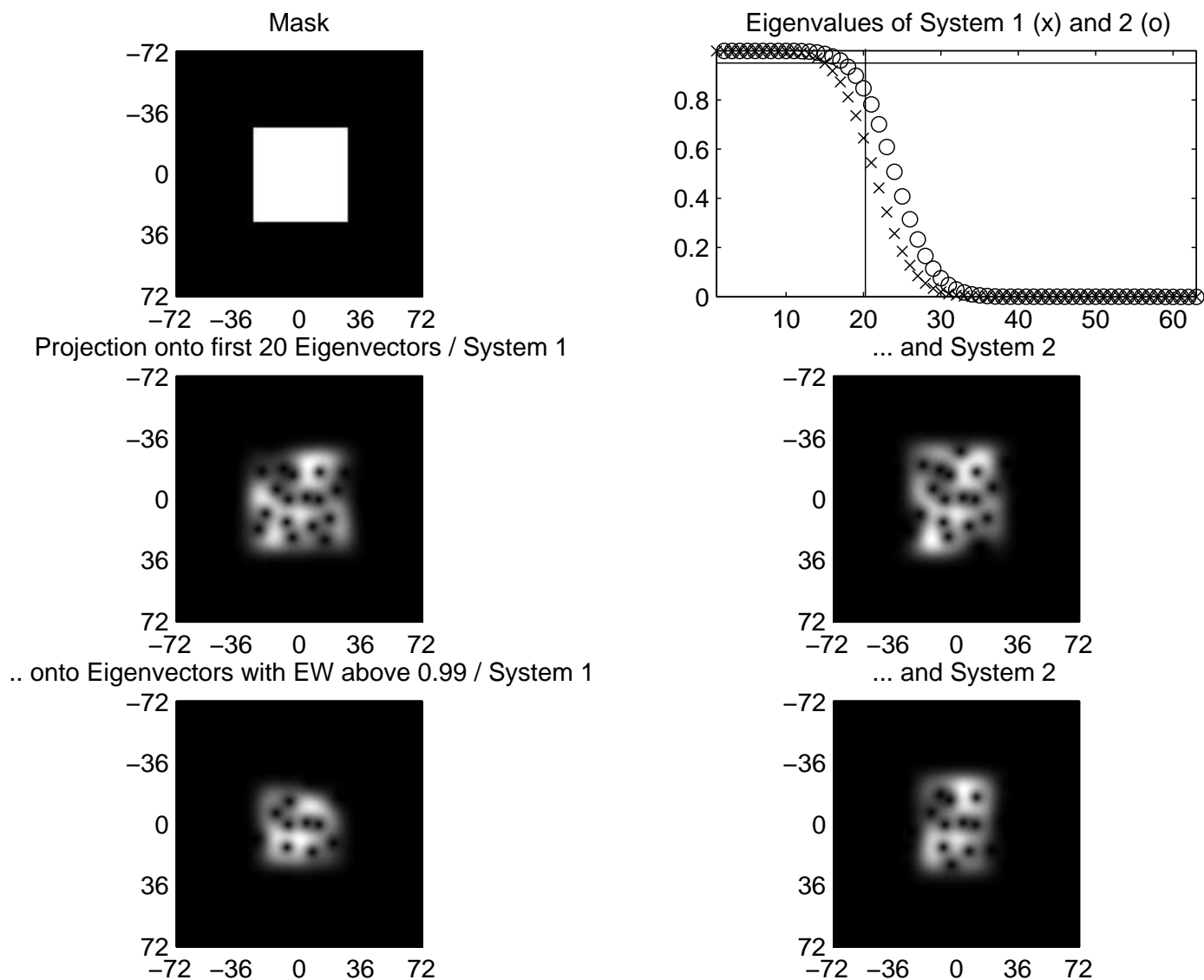
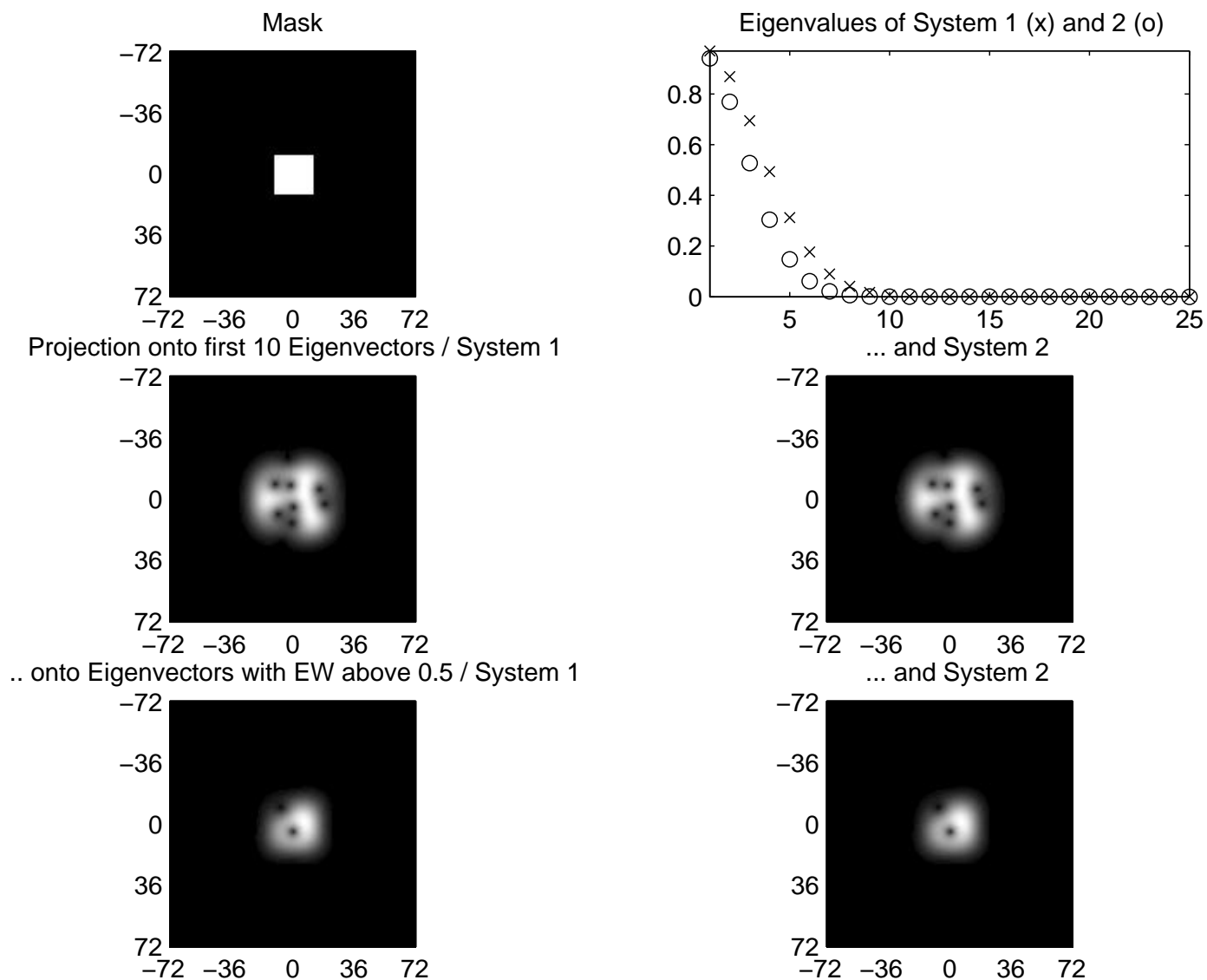


Figure 5.9: *Projection onto eigenspaces*

Figure 5.10: *Projection onto eigenspaces*

a	b	Redundancy	Lattice points inside the mask
9	3	5.3333	161
9	4	4	119
4	3	12	391
4	4	9	289
2	3	24	805
2	4	18	595

By the choice of the shape of the mask, the eigenvalues are strictly decreasing, and as a consequence the TF-concentration of the eigenfunctions is nicely centered around 0, see Figure 5.13 for typical examples. Hence, the size of the area covered by the eigenspace spanned by eigenfunctions v_1, \dots, v_N grows in a concentric manner. Now, for all systems, the projections onto the first 20, 25 and 30, respectively, eigenfunctions were determined, denoted by P_N^i , where N is the dimension of the eigenspace, hence the rank of the operator, and i is the respective Gabor system from which the operator has been derived. The following measure for the error in approximation was then introduced:

$$err_N^i(j) = \frac{1}{M} \sum_{k=1:M} \|P_N^i v_k^j - v_k^j\|_2,$$

where N is the rank of the projection operator P_N^i , i is the system from which it is derived. $v_k, k = 1 \dots M$ are the eigenvectors derived from the System \mathcal{G}_j and M is the dimension of the eigenspace we wish to represent. In our experiment, M was chosen to be 20, and the approximation quality for $N = 20, 25, 30$ was investigated. The results can be found in Table 5.3. The indexes $i = 1, \dots, 6$ run from top to bottom and $j = 1, \dots, 6$ from left to right, i.e., in the first row and second column the approximation error of the first system approximating the second can be read.

Figure 5.11 compares the TF-concentration of the three subspaces E_{20}^i, E_{25}^i and E_{30}^i for $i = 1$ and $i = 5$, respectively, i.e., for the systems with $(a_1, b_1) = (9, 3)$ and $(a_5, b_5) = (2, 3)$.

2. Dependence on the window

The continuous dependence of properties of a Gabor multiplier on the window g or the two windows, g_1 used for analysis and g_2 for the synthesis operator, respectively, are well established, cf. [32, section 3.3] and will not be discussed in detail here. It is remarkable, however, that for multipliers with compact support centered around 0 in the case of a strictly decreasing sequence of eigenvalues, the eigenvector corresponding to the biggest eigenvalue, seems to have the same shape as the given window g , in the tight case.

3. Dependence on the size of mask

Conjecture 2. Let a tight Gabor system $\mathcal{G} = (g, \Lambda)$, $\Lambda = \frac{n}{b}\mathbb{Z} \times \frac{n}{a}\mathbb{Z}$, i.e., with redundancy $\varrho = \frac{1}{ab}$ be given. Furthermore, assume a 0/1 mask such that k

Table 5.3: **Results of Experiment**

$err_{20}^i(j)$	System1	System2	System3	System4	System5	System6
System 1	0.0000	0.0247	0.0334	0.0057	0.0275	0.0360
System 2	0.0246	0.0000	0.0108	0.0230	0.0053	0.0135
System 3	0.0325	0.0104	0.0000	0.0313	0.0095	0.0052
System 4	0.0058	0.0230	0.0317	0.0000	0.0248	0.0336
System 5	0.0276	0.0054	0.0097	0.0247	0.0000	0.0108
System 6	0.0347	0.0130	0.0053	0.0327	0.0105	0.0000

$err_{25}^i(j)$	System1	System2	System3	System4	System5	System6
System 1	0.0000	0.0100	0.0126	0.0008	0.0101	0.0128
System 2	0.0094	0.0000	0.0014	0.0094	0.0004	0.0015
System 3	0.0096	0.0006	0.0000	0.0096	0.0005	0.0004
System 4	0.0009	0.0100	0.0125	0.0000	0.0101	0.0127
System 5	0.0095	0.0005	0.0011	0.0094	0.0000	0.0013
System 6	0.0097	0.0009	0.0006	0.0096	0.0005	0.0000

$err_{30}^i(j)$	System1	System2	System3	System4	System5	System6
System 1	0.0000	0.0042	0.0043	0.0005	0.0042	0.0043
System 2	0.0049	0.0000	0.0000	0.0049	0.0000	0.0000
System 3	0.0051	0.0000	0.0000	0.0051	0.0000	0.0000
System 4	0.0005	0.0043	0.0044	0.0000	0.0043	0.0044
System 5	0.0050	0.0000	0.0000	0.0050	0.0000	0.0000
System 6	0.0052	0.0000	0.0000	0.0052	0.0000	0.0000

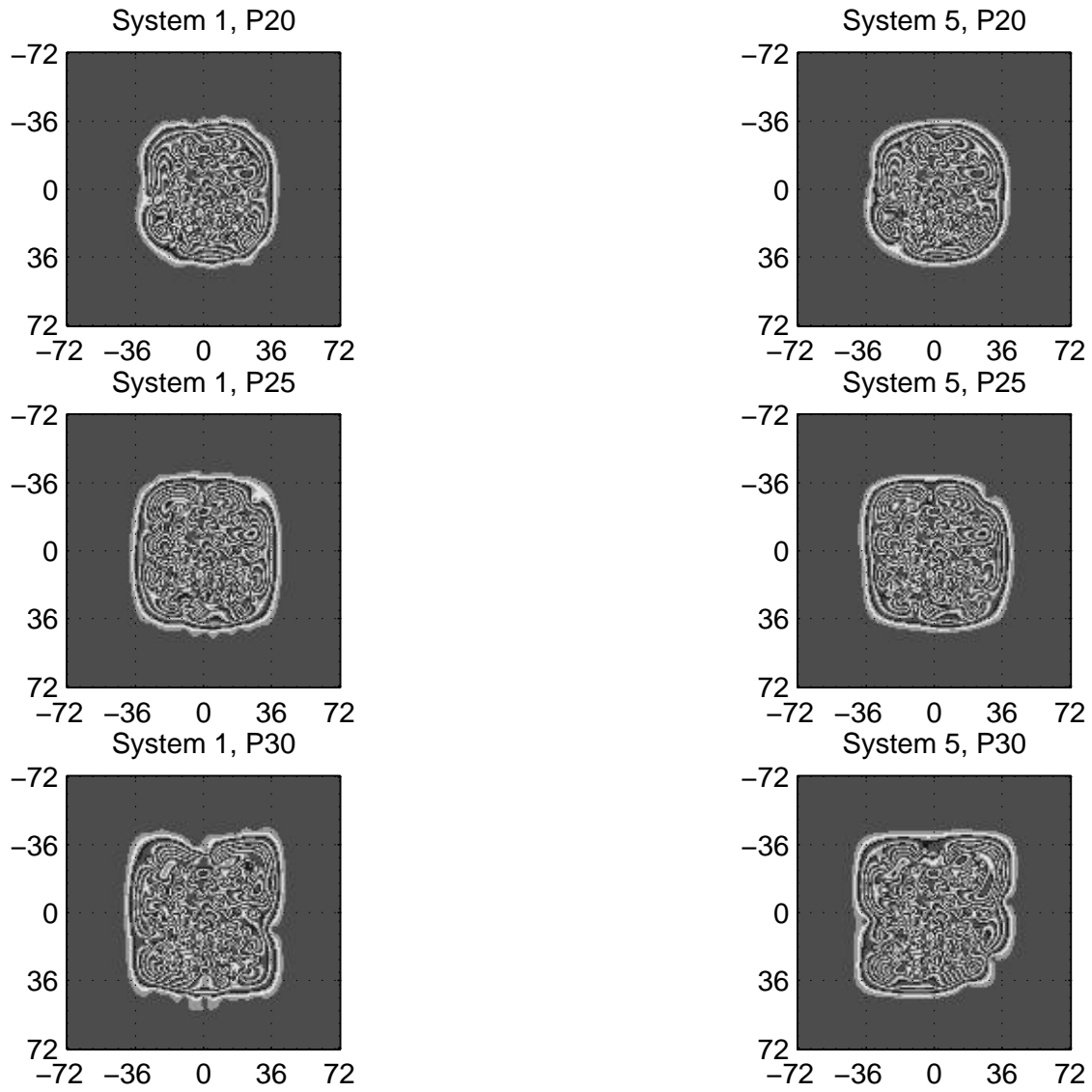
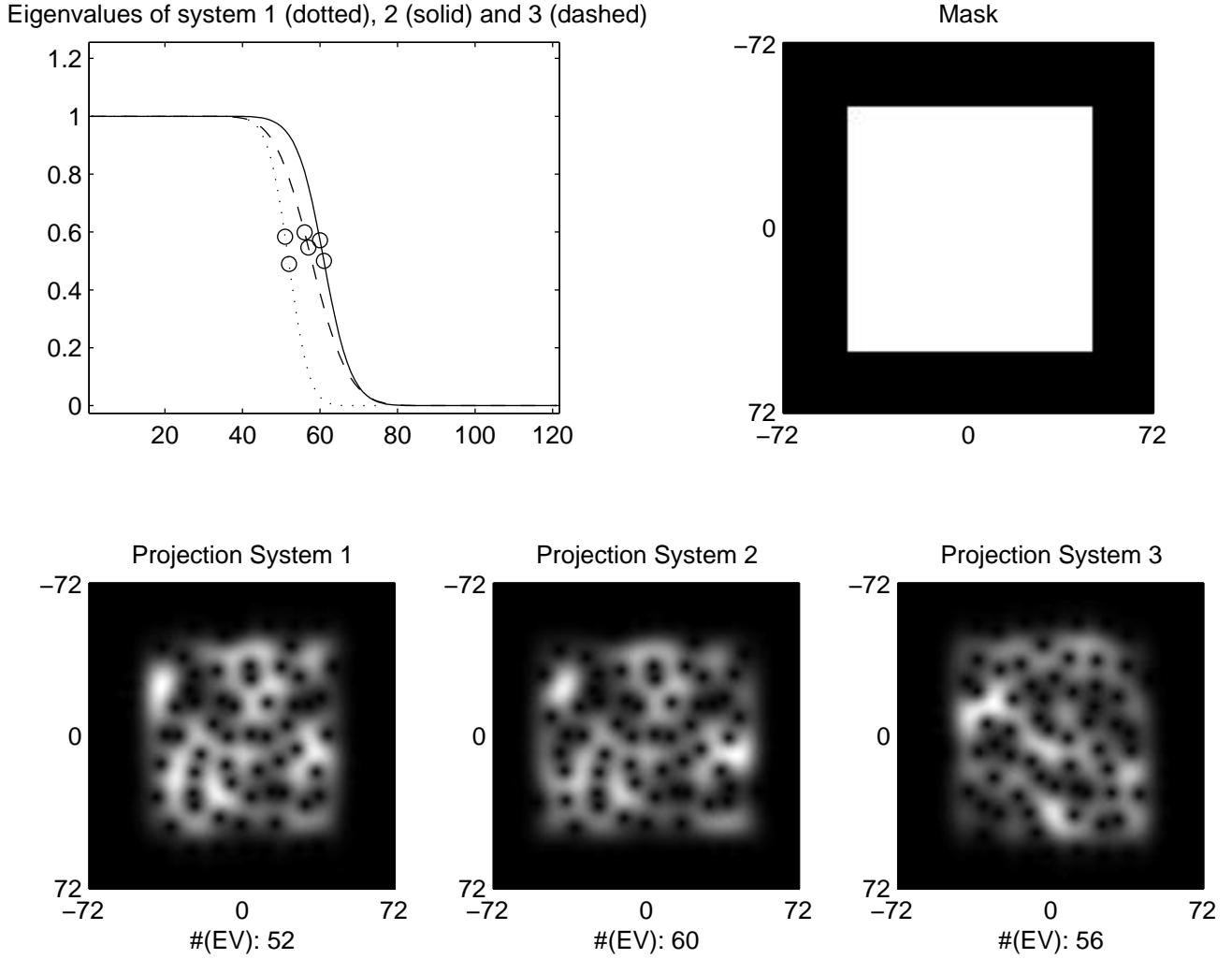


Figure 5.11: *Typical action of the operators P_N*

Figure 5.12: *Number of eigenvectors inside a mask*

sampling points of Λ fall inside the mask. The number K of eigenvectors concentrated in the masked region of the time-frequency plane can be estimated by $K = \frac{k}{\rho}$. This number corresponds to the number of eigenvalues greater than or equal to 0.5.

Numerical evidence:

Figure 5.12 shows the results of eigenanalysis of three different tight systems $\mathcal{G}_i, i = 1, \dots, 3$. The systems have redundancy 1.5, 2 and 6, respectively. Again, the signal length n was 144, and the mask was a square of size 94×94 , centered about $(0, 0)$. For the three systems, 77, 121 and 345 points, respectively, fall into the masked region, hence the number of eigenvectors concentrated in the masked region can be approximated by $\frac{77}{1.5} = 51.333$, $\frac{121}{2} = 60.5$ and $\frac{345}{6} = 57.5$. The first plot shows the eigenvalues of the Gabor multipliers corresponding to the

three systems. The critical values, corresponding to the numbers of eigenvectors above 0.5 (rounded to the closest integers), are marked. Note that the systems' redundancies differ rather crucially, leading to different actual mask sizes. Still the distribution of eigenvalues is very similar.

The next plots show the mask and the time-frequency concentration of the action of the projections onto the eigenvectors of rank K , $K = 52, 60, 57$, for the systems 1, 2, 3, respectively.

The number of eigenvalues $\alpha_i \geq 0.5$ was 51, 60 and 56, respectively, for the three systems.

4. Dependence on the shape of the mask

If the 0/1-mask is replaced by a symbol with value 1 in the origin and decreasing radial-symmetrically, then the eigenvectors' time-frequency concentration takes the form of increasing rings around the origin. Figure 5.13 compares the eigenvalues and eigenvectors of a Gabor multiplier with 0/1-mask with those of a Gabor multiplier with a cone-shaped mask of the same size, i.e., the same number of Gabor atoms contribute. The cone-shaped mask is shown in the first plot. The second plot shows the eigenvalues of both operators, the solid line corresponds to the 0/1-mask whereas the dotted line depicts the eigenvalues of the Gabor multiplier defined by the cone-shaped mask. The remaining plots present the time-frequency behavior of the first few eigenvectors of both operators.

5.8 Summary: Approximation in different classes of operators

In this concluding section we recapitulate some of the findings of this chapter by investigating the ability of Gabor multipliers to approximate operators from three classes of operators of special interest.

Underspread operators

Underspread operators have been defined by W.Kozek in [46], where details can be found. Basically, the definition of underspread operators implies that these operators can only be slowly time-varying. This is achieved by restricting the support of the spreading function $\eta(\mathbf{K})$, as defined in (5.4), of the operator \mathbf{K} to a certain compact region centered around 0 and hence enforcing a smooth KNS $\sigma(\mathbf{K})$. From (5.3) it becomes obvious that underspread operators exert limited time-frequency shifts. Note that operators which represent slowly time-varying systems and hence deviate from strict translation invariance, appear in many important application, e.g., in the investigation of quasistationary processes. It is thus remarkable that underspread operators can be well approximated by Gabor multipliers as we will see next.

We consider the following numerical setting for the experiments. Again we assume a

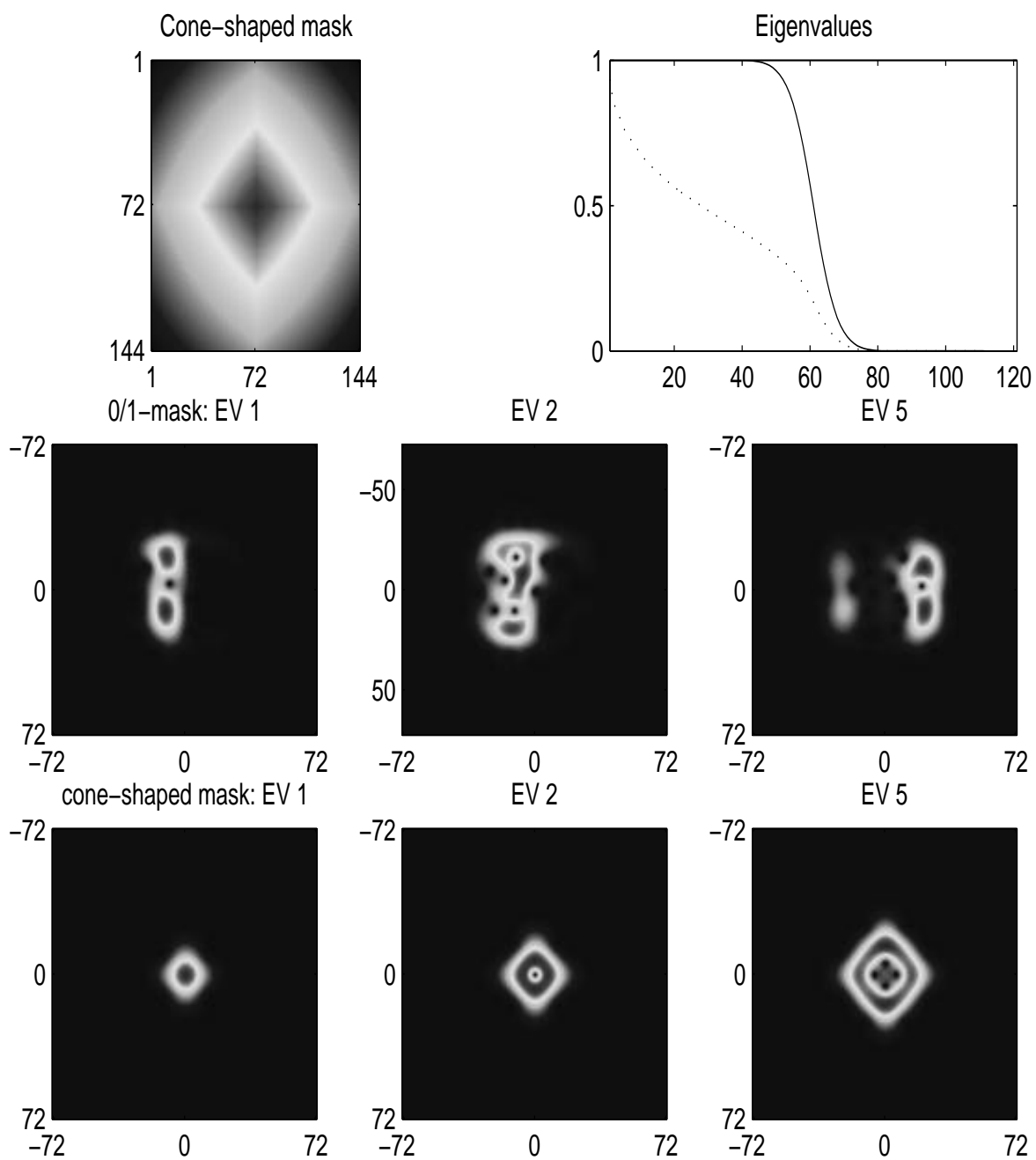
Figure 5.13: *Dependence on the shape of the multiplier*

Table 5.4: **Results of Experiment**

System	Lattice constants	Redundancy	Approximation error	Calculation time
System 1	(8,8)	2.25	0.0193	0.6
System 2	(9,12)	1.333	0.0738	0.55
System 3	(4,3)	12	1.0463e-006	1.5400
System 4	(8,9)	2	0.0308	0.61
System 5	(6,12)	2	0.0681	0.77

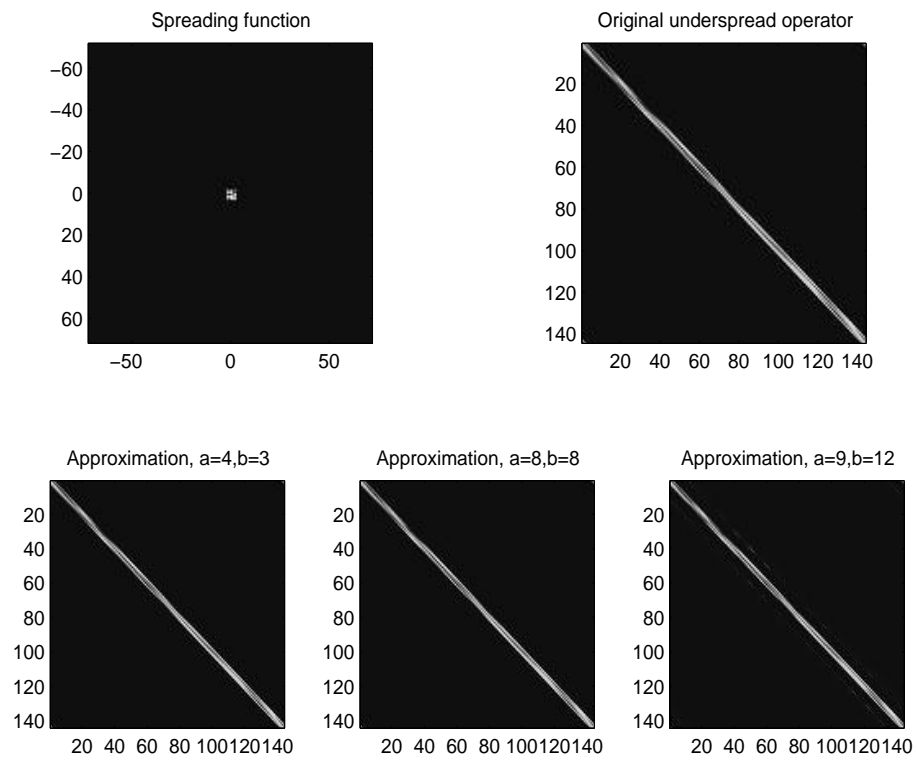
Table 5.5: **Results of Experiment**

System	Lattice constants	Redundancy	Approximation error
System 1	(4,12)	3	0.1485
System 2	(12,4)	3	0.0607

signal length 144 and a Gaussian window g . We numerically generate an underspread operator as follows. The spreading function is generated as random values assigned to a compact region centered around 0, then the operator is calculated according to (5.5). We first chose a spreading function with symmetric, compact support of size 5×5 and five lattices with lattice constants (8, 8), (9, 16), (4, 3), (8, 9) and (6, 12), respectively. For the approximation of operators we always apply the corresponding tight windows as suggested before. The results of the approximation by Gabor multipliers with respect to these systems are shown in Figure 5.14 and Table 5.4. The approximation quality is very good even for the system with low redundancy. Figure 5.14 shows the spreading function and the kernels of the original operator and the approximations, respectively. Note that for the last two lattices investigated, the redundancy was the same, but the eccentricity was different, which apparently leads to quite different approximation quality. It seems advantageous to use lattices with eccentricity similar to the eccentricity of the support of the spreading function. The second experiment confirms this expectation. Here, we generated a rectangular spreading function of size 3×9 , the resulting operator was then approximated in two systems with same redundancy but opposite eccentricity of the lattice. The results are given in table 5.5. The difference in approximation quality is obvious.

Iterated localization operators and projections onto orthonormal bases

We finally give a comparison of different methods that have been suggested for tackling time-varying filtering tasks. As mentioned before, in [55] Qian and Chen propose iterated localization operators in order to increase the concentration of the resulting signal inside a given masking region. We now investigate the ability of Gabor multipliers to

Figure 5.14: *Approximation of an underspread operator*

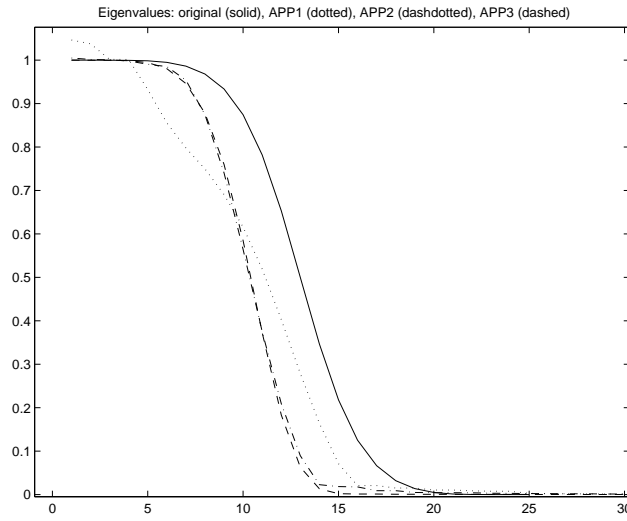


Figure 5.16: *Eigenvalues of common and iterated Gabor multiplier*

Gabor systems were applied to a random signal. The remaining plots show the STFT of the resulting signals. Whereas the TF-concentration of the best approximation of the iterated operator with respect to the *same* Gabor frame is still visibly poorer than the TF-concentration of the iterated localization operator, approximations 2 and 3 show comparable TF-concentration and the error is indeed negligible. It is instructive to have a look at the eigenvalues of the approximation operators, as shown in Figure 5.16. The eigenvalues of the approximation in the original system show a behavior quite different from the behavior characteristic of Gabor multipliers. The eigenvalues of the approximations in the systems with denser lattices, however, possess the typical trend. This leads to the following conclusion.

Conjecture 3. Whereas the iterated time-frequency operators originating from a certain low-redundancy Gabor frame are only poorly approximated with respect to the same frame, increasing the redundancy leads to the same quality of TF-concentration that can be achieved by means of iterations.

We next investigate the concentration of the projection onto the most salient eigenvectors of a Gabor multiplier as suggested by Conjecture 2. P is the projection onto the first 12 most salient eigenvectors of the Gabor multiplier generated by the Gabor frame with lattice constants $a = 8, b = 9$ (Redundancy 2) with a 0/1 mask as shown in Figure 5.17. Obviously the concentration achieved by projection onto salient eigenvectors is indeed comparable to the result achieved by the iteration method. The projection operator was again approximated by means of Gabor multipliers with respect to the frame generated on the same and a denser lattice. The results are similar to the result achieved in the previous experiment: similar concentration demands a higher density of the Gabor frame for the approximation: here, the second approximation was achieved by using the frame with lattice constants $a = 3, b = 3$.

In conclusion, it seems fair to say that in order to achieve good time-frequency concen-

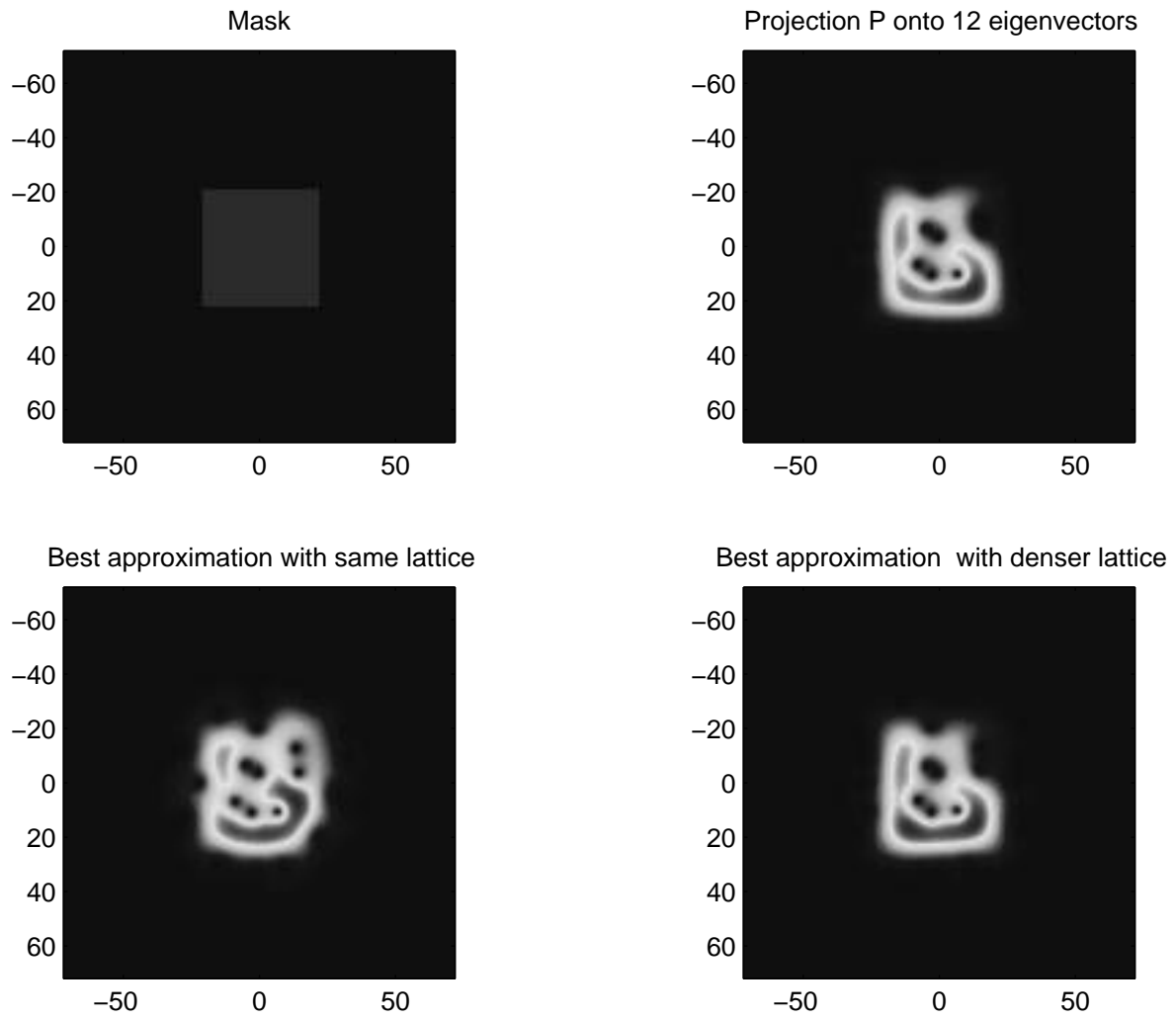


Figure 5.17: *TF-concentration of common and iterated Gabor multiplier*

tration, higher computational effort is necessary. Either iterations of a low-redundancy Gabor multiplier must be performed, eigenvectors have to be obtained, or a Gabor frame with a higher redundancy must be chosen in the first place. It will be the topic of future research to classify the necessary computational effort and the resulting improvement in more detail and with respect to specific time-varying filtering tasks.

Conclusions - Why are the results useful?

In this section we gave a summary of the theory of Gabor multipliers with an emphasis on the facets of significance for application. In particular, it seems important to understand the operators' behavior in dependence on the free variables, such as the window, the lattice or the chosen multiplier-symbol, such that the ambiguity inherent in redundant representations, as pointed out in [57], are better understood. We gave a first account for the influence of these parameters' choice on the properties of the resulting operators. These results will aid to clarify and solve issues in the application of Gabor multipliers, particularly time-varying filtering tasks. Using different representations on the symbol-level, we were able to explicitly derive the relations between operators corresponding to variable parameters. Furthermore, an explicit method for calculating the best approximation of a (time-varying filtering) operator within a class of Gabor multipliers was derived. A fast implementation of this method is possible due to the highly structured matrices involved.

By means of analysis of the eigenvalues and eigenvectors of Gabor-multipliers, we investigated the concentration in the time-frequency plane, which can be achieved by application of time-varying filtering operators. With the aid of these results, we will be able to develop methods tailored to filtering tasks in certain signal classes, such as music signals comprising contributions from different instruments.

Chapter 6

Time-Frequency BUPUs in Modulation Spaces

This chapter presents some results on partitions of unity in the time-frequency plane. More specifically, it will be shown that under certain conditions equivalent norms for $\mathbf{L}^2(\mathbb{R}^d)$ and S_0 are obtained by cutting a given function $f \in \mathbf{L}^2(\mathbb{R}^d)$ or $f \in S_0$, respectively, in time-frequency concentrated pieces. The resulting localized functions are then measured in an appropriate norm and the resulting sequence is evaluated in the according sequence norm. The approach is clearly inspired by the theory of Wiener amalgam spaces, which were briefly introduced in Section 1. As opposed to the partitioning of functions in one domain, time or frequency, only, partitioning in the time-frequency plane can never lead to compactly supported localized functions.

6.1 Partitioning Operators over the Time-Frequency Plane

In analogy to the definitions given in Section 3.1.2, we define a BUPU in the time-frequency plane:

Definition 17. *Given an admissible covering $\Omega = (\Omega_r)_{r \in \mathcal{I}}$ of \mathbb{R}^{2d} , a family $(\psi_r)_{r \in \mathcal{I}}$ is called a **bounded uniform partition of unity (BUPU)** in $L^2(\mathbb{R}^{2d})$ if the following is satisfied:*

- $0 \leq \psi_r(z) \leq 1$
- $\psi_r(z) = 0$ for all $z \in \mathbb{R}^{2d} \setminus \Omega_r$
- $\psi_r = T_r \psi_0$, i.e., the members of the BUPU are transformed into each other by translation.
- $\sum_{r \in \mathcal{I}} \psi_r(z) = 1$ for all $z \in \mathbb{R}^{2d}$.

Again, ψ_{r^*} will denote $\sum_{r \in r^*} \psi$.

Definition 18 (Time-frequency concentration operator). *Let g be a given window-function in S_0 , and $\psi \in \mathbf{L}_0^\infty(\mathbb{R}^{2d})$, a bounded function with compact support. Then for all $f \in \mathbf{L}^2(\mathbb{R}^d)$ or $f \in \mathbf{M}_m^{p,q}(\mathbb{R}^d)$, respectively, the time-frequency concentration operator H_ψ corresponding to g and ψ is defined as*

$$H_\psi f = \mathcal{V}_g^* \psi \mathcal{V}_g f.$$

Lemma 4.

Under the given assumptions, the operators H_ψ are compact operators.

Proof. Follows from Theorem 6 in Section 4.3. □

Lemma 5. *The operators H_ψ are regularizing, i.e., $H_\psi f$ is in S_0 for all $f \in \mathbf{L}^2(\mathbb{R}^d)$.*

Proof. Let $f \in \mathbf{L}^2(\mathbb{R}^d)$ be given. Note that

$$|\mathcal{V}_g \mathcal{V}_g^*(\psi \mathcal{V}_g f)| \leq |\mathcal{V}_g g| * |(\psi \mathcal{V}_g f)|, \quad (6.1)$$

see [40, Proposition 11.3.2.], hence, writing $G = \mathcal{V}_g g$,

$$\begin{aligned} \|H_\psi f\|_{S_0} &= \|\mathcal{V}_g \mathcal{V}_g^*(\psi \mathcal{V}_g f)\|_1 \\ &\leq \| |G| * |(\psi \mathcal{V}_g f)| \|_1 \\ &\leq \|G\|_1 \|(\psi \mathcal{V}_g f)\|_1 \\ &\leq \|g\|_{S_0} \|\psi\|_1 \|\mathcal{V}_g f\|_\infty \\ &\leq \|g\|_{S_0} |\Omega| \|f\|_2 \|g\|_2 \\ &\leq \|g\|_{S_0}^2 |\Omega| \|f\|_2, \end{aligned} \quad (6.2)$$

$$(6.3)$$

where Ω is the support of ψ . □

Remark 22. Note that as a consequence, the operator norm of H_ψ is bounded above by $\|g\|_{S_0}^2 |\Omega|$.

Lemma 6. *If ψ_λ is given by a shift of ψ_0 on Λ , i.e., $\psi_\lambda = T_\lambda \psi_0$, then the resulting operator $H_\lambda = H_{\psi_\lambda}$ is the operator-shifted version of $H_0 = H_{\psi_0}$, i.e.,*

$$\pi_2(\lambda) H_0 = H_\lambda.$$

Proof. Note that, with $z = (x, \xi)$, $\lambda = (t, \omega)$, $\mathcal{V}_g(\pi^*(\lambda)f) = (\mathcal{V}_g f)(z + \lambda)e^{2\pi i t \xi}$. Furthermore, $\pi(\lambda)\pi(z) = e^{-2\pi i t \xi}\pi(z + \lambda)$. Therefore,

$$\begin{aligned}
 \pi_2(\lambda)H_0f &= \pi(\lambda)\mathcal{V}_g^*\psi_0\mathcal{V}_g\pi^*(\lambda)f \\
 &= \pi(\lambda) \int_z [\psi_0\mathcal{V}_g(\pi^*(\lambda)f)](z)\pi(z)g(t)dz \\
 &= \int_z e^{2\pi i t \xi}\psi_0(z)\mathcal{V}_g f(z + \lambda)\pi(\lambda)\pi(z)g(t)dz \\
 &= \int_z e^{2\pi i t \xi}\psi_0(z)\mathcal{V}_g f(z + \lambda)e^{-2\pi i t \xi}\pi(z + \lambda)g(t)dz \\
 &= \int_z \psi_0(z - \lambda)\mathcal{V}_g f(z)\pi(z)g(t)dz \\
 &= (\mathcal{V}_g^*\psi_\lambda\mathcal{V}_g)f = H_\lambda f.
 \end{aligned}$$

□

We give some preliminary results on partitions in the time-frequency plane next. In the sequel we always assume a BUPU (ψ_λ) , where $\psi_\lambda = T_\lambda\psi_0$ and $\lambda \in \Lambda$. Hence, as shown in Lemma 6, $H_{\psi_\lambda} = \pi_2(\lambda)H_{\psi_0}$.

Lemma 7. $\sum_\lambda \|H_\lambda f\|_{S_0}$ defines an equivalent norm on S_0 .

Proof. Note that $\sum_\lambda H_\lambda f = f$, with absolute convergence in S_0 , because, with f and g in S_0 , $\mathcal{V}_g f$ is in $\mathcal{W}(C^0, \ell^1)$, see [32, Lemma 3.2.15]. This yields:

$$\sum_\lambda \|H_\lambda f\|_{S_0} \leq \|g\|_{S_0} \sum_\lambda \|\psi_\lambda \mathcal{V}_g f\|_1 \leq \|g\|_{S_0} \sum_\lambda \|\psi_\lambda \mathcal{V}_g f\|_\infty < \infty.$$

Thus, with $\sum_\Lambda \psi_\lambda \equiv 1$ on \mathbb{R}^{2d} , it follows trivially, that

$$\sum_\lambda \|H_\lambda f\|_{S_0} \leq \|g\|_{S_0} n_0 \|f\|_{S_0}.$$

Here, n_0 is the maximum number of overlapping members in the admissible covering, as defined in Definition 4. Conversely, by the triangle inequality:

$$\|f\|_{S_0} = \left\| \sum_\lambda H_\lambda f \right\|_{S_0} \leq \sum_\lambda \|H_\lambda f\|_{S_0}.$$

□

Lemma 8. $\sum_\lambda \|H_\lambda f\|_2^2$ defines an equivalent norm on $\mathbf{L}^2(\mathbb{R}^d)$.

Proof. Note that, as for $f \in \mathbf{L}^2(\mathbb{R}^d)$ and $g \in S_0$, $\mathcal{V}_g f$ is in $\mathcal{W}(C^0, \ell^2)$, the proof is analogous to the proof of Lemma 7. □

Lemma 9. For f in S_0 , the following inequality holds for some constant $C > 0$:

$$\sum_\lambda \|H_\lambda f\|_2 \leq C \|f\|_{S_0}$$

Proof. $S_0(\mathbb{R}^d)$ is continuously embedded in $\mathbf{L}^2(\mathbb{R}^d)$ ([32]), hence $\|f\|_2 \leq C\|f\|_{S_0}$ and the claim follows from Lemma 7. \square

The following lemma shows that a finite cluster of H_μ can be added to each λ in the series $\sum_\lambda \|H_\lambda f\|_2$ without affecting convergence.

Lemma 10. *If $\sum_\lambda \|H_\lambda f\|_2 < \infty$ and $F \subseteq \Lambda$ is a finite subset of Λ , then*

$$\sum_\lambda \left\| \sum_{\mu \in \lambda + F} H_\mu f \right\|_2 \leq C_F \sum_\lambda \|H_\lambda f\|_2,$$

where $C_F \leq n_0|F|$.

Proof.

$$\begin{aligned} \sum_\lambda \left\| \sum_{\mu \in \lambda + F} H_\mu f \right\|_2 &\leq \sum_\lambda \sum_{\mu \in \lambda + F} \|H_\mu f\|_2 \\ &\leq \sum_{\mu \in F} \sum_\lambda \|H_{\lambda + \mu} f\|_2 \\ &\leq n_0|F| \cdot \sum_\lambda \|H_\lambda f\|_2 \end{aligned}$$

\square

6.2 The S_0 Norm and Partitions in the TF-Domain

In view of the statements of Lemma 7 and Lemma 8, it is a natural next step to replace the norm of the localized pieces H_λ and investigate the resulting function spaces.

Lemma 11.

$$\mathbf{B}_H = \{f \in \mathbf{L}^2(\mathbb{R}^d) \mid \sum_\lambda \|H_\lambda f\|_2 < \infty\}$$

is a Banach space.

Proof. We verify completeness of the normed space \mathbf{B}_H . Note that for any absolutely convergent series $\sum_{n \in \mathbb{N}} \|f_n\|_{\mathbf{B}_H} \leq C < \infty$, the \mathbf{L}^2 -limit $f = \sum f_n$ is well-defined, as

$$\begin{aligned} \sum_{n \in \mathbb{N}} \|f_n\|_2 &= \sum_{n \in \mathbb{N}} \left\| \sum_{\lambda \in \Lambda} H_\lambda f_n \right\|_2 \\ &\leq \sum_{n \in \mathbb{N}} \sum_{\lambda \in \Lambda} \|H_\lambda f_n\|_2 \leq \sum_{n \in \mathbb{N}} \|f_n\|_{\mathbf{B}_H} \leq C \end{aligned}$$

Furthermore, $H_\lambda f = \sum_{n \in \mathbb{N}} H_\lambda f_n$ in \mathbf{L}^2 and

$$\|f\|_{\mathbf{B}_H} = \sum_{\lambda \in \Lambda} \|H_\lambda f\|_2 \leq \sum_{\lambda \in \Lambda} \sum_{n \in \mathbb{N}} \|H_\lambda f_n\|_2 \leq C$$

by assumption, hence $f \in \mathbf{B}_H$. \square

It turns out that for appropriately chosen partitions $(\psi_\lambda)_{\lambda \in \Lambda}$, the S_0 -norm in Lemma 7 can in fact be replaced by the \mathbf{L}^2 -norm.

Theorem 16. *Let $g \in S_0$ and $H_\lambda = H_{\psi_\lambda}$, where $\Psi = (\psi_\lambda)_{\lambda \in \Lambda}$ is a BUPU in \mathbb{R}^{2d} .*

$$\|f\|_{\mathbf{B}_H} = \sum_{\lambda} \|H_\lambda f\|_2$$

defines an equivalent norm on S_0 . Furthermore, if for some $C > 0$,

$$\sum_{\lambda \in \Lambda} \|\psi_\lambda \mathcal{V}_g f\|_2 \leq C \sum_{\lambda \in \Lambda} \|H_\lambda f\|_2 < \infty \quad (6.4)$$

for f in $\mathbf{L}^2(\mathbb{R}^d)$, then f is in S_0 . In particular, in this case, \mathbf{B}_H and S_0 coincide as Banach spaces.

Proof. Due to the results in Lemma 9 and Lemma 11, we only have to show that

$$\|f\|_{S_0} \leq C_1 \sum_{\lambda} \|H_\lambda f\|_2 \quad (6.5)$$

for all $f \in S_0$ in order to obtain

$$\frac{1}{C_1} \|f\|_{S_0} \leq \sum_{\lambda} \|H_\lambda f\|_2 \leq C_2 \|f\|_{S_0}$$

on \mathbf{B}_H . For any fixed $\mu \in \Lambda$, f will be split in a part $E_\mu f = \sum_{\lambda \in F^\mu} H_\lambda f$, essentially localized around μ and a residual part $R_\mu f = \sum_{\lambda \notin F^\mu} H_\lambda f$. With this notation we obtain

$$H_\mu f = H_\mu E_\mu f + H_\mu R_\mu f,$$

and therefore

$$\|f\|_{S_0} \leq \sum_{\mu} \|H_\mu f\|_{S_0} \leq \sum_{\mu} \|H_\mu E_\mu f\|_{S_0} + \sum_{\mu} \|H_\mu R_\mu f\|_{S_0} \quad (6.6)$$

The finite index sets F^μ have to be chosen judiciously, according to the following considerations.

Recall that the maximum number of overlapping members of a BUPU is bounded above by a constant n_0 . Fix $\varepsilon_1 = \frac{0.5}{n_0 \|g\|_{S_0}} > 0$. As $G = \mathcal{V}_g g \in \mathbf{L}^1(\mathbb{R}^d)$, it is possible to choose a radius R , such that

$$G = G_1 + G_2 \text{ with } \text{supp}(G_1) \subseteq B_R(0) \text{ and } \|G_2\|_1 < \varepsilon_1. \quad (6.7)$$

As $(\Omega_0 + B_R(0))$, where $\Omega_0 = \text{supp}(\psi_0)$, is a bounded and hence compact set in \mathbb{R}^{2d} , we can choose some finite index set F_0 , such that

$$\bigcup_{\lambda \notin F_0} \Omega_\lambda \cap (\Omega_0 + B_R(0)) = \emptyset.$$

Then, with $F_\mu = F_0 + \mu$, we also have

$$\bigcup_{\lambda \notin F_\mu} \Omega_\lambda \cap (\Omega_\mu + B_R(\mu)) = \emptyset,$$

for all $\mu \in \Lambda$ by uniformity of Ψ .

Now we show that by this choice the residual part in (6.6) strictly less than $\|f\|_{S_0}$ for all $f \in S_0$:

$$\begin{aligned} \|H_\mu R_\mu f\|_{S_0} &= \|\mathcal{V}_g^* \psi_\mu \mathcal{V}_g \sum_{\lambda \notin F_\mu} \mathcal{V}_g^* \psi_\lambda \mathcal{V}_g f\|_{S_0} = \\ &\|\mathcal{V}_g \mathcal{V}_g^* \psi_\mu \mathcal{V}_g \mathcal{V}_g^* \sum_{\lambda \notin F_\mu} \psi_\lambda \mathcal{V}_g f\|_1 \leq \|g\|_{S_0} \|\psi_\mu [\mathcal{V}_g g * (\sum_{\lambda \notin F_\mu} \psi_\lambda \mathcal{V}_g f)]\|_1 \end{aligned}$$

By the choice of $G = \mathcal{V}_g g = G_1 + G_2$ in (6.7), we have

$$\|\psi_\mu [G_1 * (\sum_{\lambda \notin F_\mu} \psi_\lambda \mathcal{V}_g f)]\|_1 = 0,$$

for F_μ and all finite index sets F with $F_\mu \subseteq F$. Thus,

$$\begin{aligned} \sum_{\mu \in \Lambda} \|H_\mu R_\mu f\|_{S_0} &\leq \|g\|_{S_0} \sum_{\mu \in \Lambda} \|\psi_\mu [G_2 * (\sum_{\lambda \notin F_\mu} \psi_\lambda \mathcal{V}_g f)]\|_1 \\ &\leq \|g\|_{S_0} \sum_{\mu \in \Lambda} \int_z |\psi_\mu(z)| \cdot |G_2 \sum_{\lambda \notin F_\mu} \psi_\lambda \mathcal{V}_g f| dz \\ &\leq \|g\|_{S_0} \sum_{\mu \in \Lambda} \int_{\omega_\mu} |G_2| \cdot |\sum_{\lambda \notin F_\mu} \psi_\lambda \mathcal{V}_g f| dz \\ &\leq \|g\|_{S_0} n_0 \|G_2\|_1 \|\sum_{\lambda \notin F_\mu} \psi_\lambda \mathcal{V}_g f\|_1 \\ &\leq \|g\|_{S_0} n_0 \cdot \varepsilon_1 \|f\|_{S_0} \leq 0.5 \|f\|_{S_0} \end{aligned} \tag{6.8}$$

If for a constant $C > 0$, (6.4) is fulfilled for $f \in \mathbf{L}^2$, then we choose $\varepsilon_1 = \frac{0.5}{C|\psi_0|n_0\|g\|_{S_0}^2} > 0$, to achieve as above:

$$\sum_{\mu \in \Lambda} \|H_\mu R_\mu f\|_{S_0} \leq \|g\|_{S_0} n_0 \|G_2\|_1 \|\sum_{\lambda \notin F_\mu} \psi_\lambda \mathcal{V}_g f\|_1$$

Now, we have $\|\psi F\|_1 \leq |\text{supp}(\psi)| \|\psi F\|_2$ for any ψ with compact support, hence

$$\begin{aligned} \sum_{\mu \in \Lambda} \|H_\mu R_\mu f\|_{S_0} &\leq \|g\|_{S_0} n_0 \varepsilon_1 |\psi_0| \|\sum_{\lambda \notin F_\mu} \psi_\lambda \mathcal{V}_g f\|_2 \\ &\leq \|g\|_{S_0} n_0 \varepsilon_1 |\psi_0| \|f\|_2 \\ &\leq \|g\|_{S_0}^2 n_0 \varepsilon_1 |\psi_0| \|f\|_{S_0} \leq 0.5 \|f\|_{S_0} \end{aligned}$$

Thus, from (6.6):

$$\|f\|_{S_0} \leq 2 \cdot \sum_{\mu} \|H_{\mu} E_{\mu} f\|_{S_0}, \quad (6.9)$$

for $f \in S_0$ and whenever (6.4) holds for $f \in \mathbf{L}^2$.

Next we derive an estimate for the right hand side of (6.9). For all $f \in \mathbf{L}^2$ we have

$$\|H_{\mu} H_{\mu} f - H_{\mu} f\|_{S_0} \leq \|H_{\mu} - \text{Id}\|_{S_0} \cdot \|H_{\mu} f\|_{S_0}.$$

Now, as $\|H_{\mu} f - f\| \leq \|g\|_{S_0} \|f\|_{S_0}$ for all $f \in S_0$, the operator norm of $H_{\mu} - \text{Id}$ is bounded by $\|g\|_{S_0}$. Hence, by Lemma 5, we obtain for all $f \in \mathbf{L}^2$:

$$\|H_{\mu} H_{\mu} f - H_{\mu} f\|_{S_0} \leq \|g\|_{S_0}^2 |\text{supp}(\psi_{\mu})| \|f\|_2. \quad (6.10)$$

For $f = E_{\mu} f$, this yields for all μ :

$$\begin{aligned} \|H_{\mu} E_{\mu} f\|_{S_0} &\leq \|H_{\mu}^2 E_{\mu} f - H_{\mu} E_{\mu} f\|_{S_0} + \|H_{\mu}^2 E_{\mu} f\|_{S_0} \\ &\leq \|g\|_{S_0}^2 |\text{supp}(\psi_0)| \|E_{\mu} f\|_2 + \|g\|_{S_0}^2 |\text{supp}(\psi_0)|^2 \|E_{\mu} f\|_2 \\ &\leq (1 + |\text{supp}(\psi_0)|) \|g\|_{S_0}^2 |\text{supp}(\psi_0)| \|E_{\mu} f\|_2. \end{aligned} \quad (6.11)$$

Substituting (6.11) into (6.9), we obtain:

$$\|f\|_{S_0} \leq 2(1 + |\text{supp}(\psi_0)|) \|g\|_{S_0}^2 |\text{supp}(\psi_0)| \sum_{\mu} \|E_{\mu} f\|_2$$

According to Lemma 10, $\sum_{\mu} \|E_{\mu} f\|_2 \leq C_F \sum_{\mu} \|H_{\mu} f\|_2$ hence we found the requested estimate 6.5 with $C_1 = 2(1 + |\text{supp}(\psi_0)|) \|g\|_{S_0}^2 |\text{supp}(\psi_0)| C_F$. \square

Remark 23. Condition (6.4) can be understood as a kind of converse of the usual inequality for convolutions. To see this, note that

$$\|H_{\lambda} f\|_2 = \|\mathcal{V}_g \mathcal{V}_g^* \psi_{\lambda} \mathcal{V}_g f\|_2 \leq \|\mathcal{V}_g g\|_1 \cdot \|\psi_{\lambda} \mathcal{V}_g f\|_2.$$

It has been shown in [21, Proposition 7.], that a partial converse of the convolution inequality can be given under certain conditions. It will be the topic of future research to characterize in detail the partitions $(\psi_{\lambda})_{\lambda \in \Lambda}$ for which (6.4) holds.

The following proposition will be useful in the construction of time-frequency adaptive multiple Gabor frames.

Proposition 5. *On compact sets in S_0 , particularly on $K_{\mu} = \overline{H_{\mu}(o\mathbf{L}^2)}$, the identity operator can be uniformly approximated by $\sum_{\lambda \in F} H_{\lambda}$, i.e., for any given $\varepsilon > 0$ there exists a finite index set F_{μ}^* , such that*

$$\left\| \sum_{\lambda \in F_{\mu}^*} H_{\lambda} h - h \right\|_{S_0} < \varepsilon_2 \text{ for all } h \in K_{\mu}. \quad (6.12)$$

Consequently, if $(\psi_{\lambda})_{\lambda \in \Lambda}$ is a BUPU and (6.12) is fulfilled for $\mu = 0$, F_0^* , then, with $F_{\mu}^* = F_0^* + \mu$, (6.12) holds for all μ .

Proof. We fix $\varepsilon > 0$ and F_0^* such that (6.12) is fulfilled for $\mu = 0$. We show that, with $F_\mu^* = F_0^* + \mu$, (6.12) holds for all μ :

Note that, by isometry of time-frequency shifts, $\|f\|_2 = \|\pi(\mu)f\|_2$ for all $\mu \in \Lambda$. Then,

$$\begin{aligned} \sum_{\lambda \in F_0^* + \mu} H_\lambda H_\mu f - H_\mu f &= \sum_{\lambda \in F_0^* + \mu} \pi(\lambda) H_0 \pi^*(\lambda) \pi(\mu) H_0 (\pi(-\mu)f) - \pi(\mu) H_0 (\pi(-\mu)f) = \\ &= \sum_{\lambda \in F_0^*} \pi(\lambda + \mu) H_0 \pi^*(\lambda + \mu - \mu) H_0 (\pi(-\mu)f) - \pi(\mu) H_0 (\pi(-\mu)f) = \\ &= \pi(\mu) \left(\sum_{\lambda \in F_0^*} \pi(\lambda) H_0 \pi^*(\lambda) H_0 (\pi(-\mu)f) - H_0 (\pi(-\mu)f) \right), \end{aligned}$$

and therefore

$$\left\| \sum_{\lambda \in F_0^* + \mu} H_\lambda H_\mu f - H_\mu f \right\|_{S_0} = \left\| \sum_{\lambda \in F_0^*} H_\lambda H_0 f - H_0 f \right\|_{S_0} < \varepsilon_2 \text{ for all } f \in \mathbf{oL}^2$$

We thus obtain for all $f \in \mathbf{L}^2$ and all μ :

$$\left\| \sum_{\lambda \in F_\mu^*} H_\lambda H_\mu f - H_\mu f \right\|_{S_0} \leq \left\| \sum_{\lambda \in F_\mu^*} H_\lambda H_\mu - H_\mu \right\|_{\mathbf{L}^2 \rightarrow S_0} \|f\|_2 \leq 0.1 \|f\|_2. \quad (6.13)$$

□

6.3 Frames of Finite-Rank Operators

In a discrete setting, the operators H_λ can best be simulated by the projection onto a finite family of linear independent, possibly orthonormal, functions v_n , $n = 1, \dots, N$. The salient eigenvectors of approximations of a frame operator, as given in (5.14), are typical candidates for a finite family of orthonormal functions. As discussed in Section 5.7, these functions would typically cover the support of ψ_μ , if ψ_μ was the multiplier in (5.14).

On the other hand, Gabor frames (g, Λ) can be interpreted as a family of projection operators P_{g_λ} onto one-dimensional subspaces spanned by the g_λ . Note that $\pi_2(\lambda)P_{g_0} = P_{g_\lambda}$. The rank-one operators can be replaced by any other projection operators, translated over the time-frequency plane on a coarser lattice Λ . Hence, we are interested in systems of the form

$$\mathcal{P} = (P_\lambda)_{\lambda \in \Lambda} = (\pi_2(\lambda)P_0)_{\lambda \in \Lambda}, \quad (6.14)$$

where $P_0 = \sum_{r=1}^R v^r \otimes (v^r)^*$. Here we give a criterion to determine completeness of the systems (6.14) in the following sense:

The system of projection operators $\mathcal{P} = (P_\lambda)_{\lambda \in \Lambda}$ is complete in \mathbf{L}^2 , if there exist constants $A, B > 0$, such that

$$A\|f\|_2^2 \leq \sum_{\lambda \in \Lambda} \|P_\lambda f\|_2^2 \leq B\|f\|_2^2. \quad (6.15)$$

This condition is equivalent to the frame condition for the family of functions

$$\bigcup_r \{v_\lambda^r, \lambda \in \Lambda\}, \quad (6.16)$$

because the $v^r, r = 1, \dots, R$ are orthonormal.

Theorem 17. *If*

$$\sum_r \sum_{\mu \in \Lambda^\circ, \mu \neq 0} |\mathcal{V}_{g^r} g^r| < R, \quad (6.17)$$

where Λ° is the adjoint lattice of Λ , see 1.4, then condition (6.15) is satisfied for the system (6.14).

Proof. The proof of this theorem makes use of properties of the Kohn-Nirenberg symbol and the spreading function, which have been introduced in Chapter 5. First note that the frame operator of (6.16) is given by $S_{\mathcal{P}} = \sum_{\lambda \in \Lambda} \pi_2(\lambda) P_0$. Hence, by the shift-covariance of the KNS, see Section 11, the KNS of $S_{\mathcal{P}}$ is given by

$$\sigma(S_{\mathcal{P}})(\mu) = \sum_{\lambda \in \Lambda} \sigma(P_0)(\mu - \lambda), \quad (6.18)$$

which shows that $\sigma(S_{\mathcal{P}})$ is Λ -periodic. Under The symplectic Fourier transform of a Λ -periodic function is supported on Λ° , see [58, p.141] and [29, Theorem 7.7.5.] for details. On the other hand, the symplectic Fourier transform of the KNS leads to the spreading function of $S_{\mathcal{P}}$, which is hence given by:

$$\eta(S_{\mathcal{P}})(\zeta) = \sum_{\lambda^\circ \in \Lambda^\circ} \delta(\lambda^\circ - \zeta) \eta(P_0)(\zeta). \quad (6.19)$$

As shown in [29, Theorem 7.7.6.], any Λ -invariant operator can be decomposed into time-frequency shifts on Λ° by means of its spreading function:

$$S_{\mathcal{P}} = \frac{1}{ab} \sum_{\lambda^\circ \in \Lambda^\circ} \eta(P_0)(\lambda^\circ). \quad (6.20)$$

Now, by a straightforward calculation, $\eta(P_0)(\mu) = \frac{1}{R} \sum_{r=1}^R \mathcal{V}_{v^r} v^r(\mu)$, such that

$$S_{\mathcal{P}} = \frac{1}{R \cdot ab} \sum_{\lambda^\circ \in \Lambda^\circ} \mathcal{V}_{v^r} v^r(\lambda^\circ).$$

Now, (6.15) holds if and only if $S_{\mathcal{P}}$ is invertible, which is guaranteed by the convergence of the Neumann series, $\sum_{n=0}^{\infty} (\text{Id} - S_{\mathcal{P}})^{-1}$. The follows from $\|\text{Id} - S_{\mathcal{P}}\| < 1$, see [14, Chapter VII, Corollary 2.3], for example. Now, as

$$\text{Id} - S_{\mathcal{P}} = \frac{1}{R \cdot ab} \sum_{\lambda^\circ \in \Lambda^\circ, \lambda^\circ \neq 0} \mathcal{V}_{v^r} v^r(\lambda^\circ)$$

(6.17) leads to completeness of \mathcal{P} . □

Implementation

The criterion presented in Theorem 17 allows a fast numerical determination of completeness of a given multi-window Gabor system. See Appendix, Section A.8, for an implementation in MATLAB.

Theorem 17 gives a useful criterion allowing to determine whether a given multi-window Gabor system is a frame. The criterion relies heavily on the group structure of the lattice Λ . In the last chapter we investigate Gabor-type systems for which the group structure of the sampling points is no longer present.

Chapter 7

Multiple Gabor Systems with Windows in S_0

This chapter generalises the result of Theorem 2 to certain families of windows in S_0 . The condition on the support of either g or \hat{g} to be compact is replaced by decay conditions on the class of window functions considered. First, the case of tight Gabor frames is discussed. We show that the any signal $f \in \mathbf{L}^2$ can be entirely reconstructed from the localised coefficients. We then discuss the issue of upper and lower frame bound for the joint systems. The statements are then generalised for the case of not necessarily tight Gabor frames. Finally, the case of arbitrary time-frequency tilings is discussed.

7.1 Varying the System in one Domain

The results of Chapter 3 can be generalized to the case of windows g which are not necessarily compact in one domain. We will see later in this chapter that this generalization paves the way for a globally flexible design of multiple Gabor frames.

In some respects, our approach resembles the pseudo-frames introduced by S. Li, [49], who suggests a generalized multiresolution structure. However, in Li's approach, the existence of a frame or pseudoframe for the generating subspace V_0 is assumed. Contrary to this assumption, we construct the local families from globally defined Gabor frame.

We assume that different Gabor systems are to be used in different frequency regions, we drop the compactness condition for the window and show that under certain conditions on the windows in use, frames can still be constructed. The conditions on the windows concern time-frequency localization and are intuitively obvious.

Let tight Gabor systems $(g_\lambda^r)_{\lambda \in \Lambda^r}$, $r \in \mathcal{I}$ be given. In addition consider a bounded admissible partition of unity (BAPU), as defined in Definition 4, on \mathbb{R} or $\hat{\mathbb{R}}$, respectively, with $\text{supp}(\psi_r) \subseteq \Omega_r$, where Ω_r is a compact interval in \mathbb{R} . The following lemma restates some facts from Chapter 6 which will be used in the sequel.

Lemma 12. $\psi_r f$ is in $\mathbf{L}^2(\mathbb{R}^d)$ and $\|f\psi_r\|_2 \leq \|f\|_2$.

Also,

$$\|f\|_2^2 \leq n_0 \sum_r \|f\psi_r\|_2^2$$

and

$$\sum_r \|f\psi_r\|_2^2 \leq \sum_r \int_{\Omega_r} |f(t)|^2 dt \leq n_0 \|f\|_2^2.$$

Lemma 13. Let a tight Gabor frame (g, Λ) , $\Lambda = (\lambda_i)_{i \in \mathbb{N}} = (x_i, \xi_i)_{i \in \mathbb{N}}$ for $\mathbf{L}^2(\mathbb{R})$, with $g \in S_0$ be given. For arbitrary $\psi \in \mathcal{K}(\mathbb{R})$ with $\text{supp}(\psi) \in x_0 + [-R, R]$ and any given $\varepsilon > 0$ a set $\mathcal{X} \subset \Lambda$ of sampling points of the form

$$\mathcal{X} = \{(x, \xi) \in \Lambda : |x_0 - x| \leq R + \delta\}$$

derived from a finite constant $\delta(\varepsilon, g) > 0$ can be found, such that for all $f \in \mathbf{L}^2(\mathbb{R})$:

$$\|f\psi - \sum_{\lambda \in \mathcal{X}} \langle f\psi, g_\lambda \rangle g_\lambda\|_2 \leq \varepsilon \|f\psi\|_2.$$

Equivalently, if $\hat{\psi} \in \mathcal{K}(\hat{\mathbb{R}})$, $\text{supp}(\hat{\psi}) \in \xi_0 + [-\hat{R}, \hat{R}]$, we can find a constant $\hat{\delta}$ such that for the sampling set

$$\hat{\mathcal{X}} = \{(x, \xi) \in \Lambda : |\xi_0 - \xi| \leq \hat{R} + \hat{\delta}\}$$

we obtain

$$\|f * \psi - \sum_{\lambda \in \hat{\mathcal{X}}} \langle f * \psi, g_\lambda \rangle g_\lambda\|_2 \leq \varepsilon \|f * \psi\|_2.$$

A proof of the above statement can be found in [32]. It follows as a special case from Lemma 15 below. In fact, it turns out, that the δ in the previous lemma depends on the decay properties of g . Hence, in order to be able to find a lower frame bound for a Gabor system consisting of different original (tight) Gabor frames in distinct parts of the time or frequency range, we need to impose common decay conditions on the windows g^r generating the different system. The following condition will guarantee compactness of the set of windows used and hence allow a uniform estimate for all $r \in \mathcal{I}$.

Lemma 14. For any $s > 2d$ and $C > 0$, let $w_s(z) = (1 + \|z\|^2)^{\frac{s}{2}}$ for all $z \in \mathbb{R}^{2d}$. Then the set

$$H_{s,C} = \{g \in S_0 : |\mathcal{V}_{g_0} g| \leq C w_s\},$$

is a relatively compact subset of S_0 .

Proof. This result was proved in [32], here we use Theorem 5 for a slightly shorter proof. Note that $w_{-s} \in \mathbf{L}^1(\mathbb{R}^d)$ for $s > 2d$, hence for $\varepsilon > 0$ a compact set $U \in \mathbb{R}^{2d}$ can be found such that

$$\int_{U^c} w_{-s}(z) dz < \frac{\varepsilon}{C}.$$

Thus for all $g \in H_{s,C}$ we have

$$\int_{U^c} |\mathcal{V}_{g_0} g|(z) dz \leq C \int_{U^c} w_{-s}(z) dz < \varepsilon,$$

which, by Theorem 5, implies compactness of $H_{s,C}$ in S_0 . \square

In addition to the decay conditions on the windows g^r we assume that the redundancy of the lattices Λ^r is bounded above in the following sense: Let Λ^r be given as $\alpha^r \mathbb{Z} \times \beta^r \mathbb{Z}$ for all r . Then we assume that there exist $\alpha, \beta > 0$ such that

$$\min_{r \in \mathcal{I}} \alpha^r \geq \alpha \text{ and } \min_{r \in \mathcal{I}} \beta^r \geq \beta. \quad (7.1)$$

Lemma 15. *Assume that for the lattices $\Lambda^r, r \in \mathcal{I}$, (7.1) holds for some $\alpha, \beta > 0$. Let the tight Gabor systems $(g^r, \Lambda^r)_{r \in \mathcal{I}}$ be given with $g^r \in H_{s,C}$ for all r , some $C > 0$ and $s > 2$. Additionally, consider a BAPU $(\psi_r)_{r \in \mathcal{I}}$ on \mathbb{R} with $\text{supp}(\psi_r) \subseteq B_{R^r}(x_r)$, with $R^r \leq R < \infty$ for $r \in \mathcal{I}$.*

Then, for all $\varepsilon > 0$ there exists a $\delta(s, C)$ such that for the sampling sets

$$\mathcal{X}^r = \{(x, \xi) \in \Lambda^r : |x_r - x| \leq |R + \delta|\}, r \in \mathcal{I},$$

the estimate

$$\|\psi_r f - \sum_{\lambda \in \mathcal{X}^r} \langle \psi_r f, g_\lambda^r \rangle g_\lambda^r\|_2 \leq \varepsilon \|\psi_r f\|_2$$

holds for all $r \in \mathcal{I}$.

According to the lemma, for every index r , the sampling points in a strip of uniform size around each Ω_r , are sufficient to guarantee reconstruction of functions with support (bandwidth) restricted to Ω_r .

Remark 24. Note that the essential step in the proof is to show the independence of δ of the specific index $r \in \mathcal{I}$. Apart from this, the statement is similar to Lemma 13. Note that in analogy to the second statement in Lemma 13, the claim of Lemma 15 can be reformulated for partition in the frequency domain. In order to avoid lengthy notation, we only prove Lemma 15 here. Similar to the statement in Lemma 13, however, the same holds for the frequency domain.

Proof. For the given BAPU $(\psi_r)_{r \in \mathcal{I}}$, let $f^r = \psi_r f$, i.e., f^r has compact support in $\Omega_r = B_{R^r}(x_r)$.

We know that for $g \in S_0$ the Gabor analysis operator $\mathbf{T}_g : f \mapsto (\langle f, g_\lambda \rangle)_{\lambda \in \Lambda}$ is a continuous operator mapping \mathbf{L}^2 functions to ℓ^2 sequences, i.e.,

$$\|\mathbf{T}_g f\|_{\ell^2} \leq C_\Lambda \|g\|_{S_0} \|f\|_2.$$

The constant C_Λ only depends on the lattice constants α, β , hence, due to (7.1), we can choose $C_\Lambda = \max_r C_{\Lambda^r}$. Now, as $\{g^r, r \in \mathcal{I}\}$ is relatively compact in S_0 , all g^r have the same essential support, see Theorem 3 in Chapter 4, hence for $\varepsilon = \frac{\varepsilon_1}{C_\Lambda \max_r \|g^r\|_2^2}$

there exists $\psi \in S_0$ with $\text{supp}(\psi) \subseteq B_\delta(0)$, such that $\|g^r - \psi g^r\|_{S_0} < \varepsilon$ for all $r \in \mathcal{I}$. We set $g_c^r = \psi g^r$ for all r to achieve:

$$\text{supp } g_c^r \subseteq B_\delta(0) \quad (7.2)$$

and

$$\|g^r - g_c^r\|_{S_0} < \varepsilon \quad (7.3)$$

for all $r \in \mathcal{I}$. The last inequality thus guarantees that $\|\mathbf{T}_{g^r - g_c^r} f\|_{\ell^2(\Lambda)} \leq C_\Lambda \varepsilon \|f\|_2$ for all $f \in \mathbf{L}^2$. With (7.2) and $\text{supp}(f^r) \subseteq B_R(x_r)$, we find that

$$\mathbf{T}_{g_c^r}(f^r)(x, \xi) = \langle f^r, M_\xi T_x g_c^r \rangle = 0 \quad \text{whenever } |x - x_r| > R + \delta. \quad (7.4)$$

Now, we set $\mathcal{X}^r = \{(x, \xi) \in \Lambda^r : |x_r - x| \leq |R + \delta|\}, r \in \mathcal{I}$, ${}^c\mathcal{X}^r = \Lambda^r \setminus \mathcal{X}^r$, such that

$$\|f^r - \sum_{\lambda \in \mathcal{X}^r} \langle f^r, g_\lambda^r \rangle g_\lambda^r\|_2 = \|\sum_{\lambda \in {}^c\mathcal{X}^r} \langle f^r, g_\lambda^r \rangle g_\lambda^r\|_2.$$

By (7.4), $\langle f^r, g_c^r \rangle = 0$ on ${}^c\mathcal{X}^r$, hence we have for all r and all $f \in \mathbf{L}^2$:

$$|\langle f^r, g_\lambda^r \rangle| = |\langle f^r, g_\lambda^r - g_c^r \rangle| \quad \text{for all } \lambda \in {}^c\mathcal{X}^r.$$

This yields:

$$\begin{aligned} \|f^r - \sum_{\lambda \in \mathcal{X}^r} \langle f^r, g_\lambda^r \rangle g_\lambda^r\|_2^2 &= \|\sum_{\lambda \in {}^c\mathcal{X}^r} \langle f^r, g_\lambda^r \rangle g_\lambda^r\|_2^2 \\ &\leq \sum_{\lambda \in {}^c\mathcal{X}^r} |\langle f^r, g_\lambda^r - g_c^r \rangle|^2 \cdot \|g_\lambda^r\|_2^2 \\ &\leq \sum_{\lambda \in \Lambda} |\langle f^r, g_\lambda^r - g_c^r \rangle|^2 \cdot \|g_\lambda^r\|_2^2 \\ &\leq \|\mathbf{T}_{g^r - g_c^r} f^r\|_{\ell^2(\Lambda)}^2 \|g^r\|_2^2 \\ &\leq \varepsilon \cdot C_\Lambda \|f^r\|_2^2 \cdot \|g^r\|_2^2 \\ &= \frac{\varepsilon_1}{C_\Lambda \max_r \|g^r\|_2^2} \cdot C_\Lambda \|f^r\|_2^2 \cdot \|g^r\|_2^2 < \varepsilon_1 \|f^r\|_2^2. \end{aligned}$$

for all r and all $f \in \mathbf{L}^2$, which proves the assertion. \square

Corollary 5. *As a consequence of Lemma 15 and under the same conditions, the following inequality holds with the index sets \mathcal{X}^r as chosen in Lemma 15 for all $r \in \mathcal{I}$:*

$$\|\sum_{\lambda \in \mathcal{X}^r} \langle f \psi_r, g_\lambda^r \rangle g_\lambda^r\|_2^2 \geq (1 - \varepsilon) \|f \psi_r\|_2^2$$

Proof. Note that

$$\|f^r\|_2^2 \leq \|\sum_{\lambda \in \mathcal{X}^r} \langle f^r, g_\lambda^r \rangle g_\lambda^r\|_2^2 + \|\sum_{\lambda \in {}^c\mathcal{X}^r} \langle f^r, g_\lambda^r \rangle g_\lambda^r\|_2^2.$$

By Lemma 15 we thus have

$$\|f^r\|_2^2 \leq \|\sum_{\lambda \in \mathcal{X}^r} \langle f^r, g_\lambda^r \rangle g_\lambda^r\|_2^2 + \varepsilon \|f^r\|_2^2,$$

hence

$$(1 - \varepsilon) \|f^r\|_2^2 \leq \|\sum_{\lambda \in \mathcal{X}^r} \langle f^r, g_\lambda^r \rangle g_\lambda^r\|_2^2.$$

\square

7.1.1 Reconstruction

Theorem 18. *Let $(g^r, \Lambda^r)_{r \in \mathcal{I}}$ be tight Gabor frames with $g^r \in H_{s,C}$ for all r , some $C > 0$ and $s > 2$, with $\max_r \|g^r\|_{S_0} = C_g$. Furthermore assume that (7.1) holds for some $\alpha, \beta > 0$. Then, with the index sets \mathcal{X}^r as chosen in Lemma 15 for a given $\varepsilon < n_0$ and all $r \in \mathcal{I}$, $\mathcal{G}_{g^r, \mathcal{I}^r}^\psi = \bigcup_{r \in \mathcal{I}} \{(\psi_r \cdot g_\lambda^r) : \lambda \in \mathcal{X}^r\}$ is a Bessel sequence and any $f \in \mathbf{L}^2$ can be completely reconstructed from*

$$\left(\langle f, \psi_r \cdot g_\lambda^r \rangle \right)_{r \in \mathcal{I}, \lambda \in \mathcal{X}^r}. \quad (7.5)$$

Proof. First note that

$$\sum_r \sum_{\lambda \in \mathcal{X}^r} |\langle \psi_r f, g_\lambda^r \rangle|^2 \leq \sum_r \|\psi_r f\|_2^2 \leq n_0 \|f\|_2^2,$$

because all Gabor systems are tight and by Lemma 12, hence $\mathcal{G}_{g^r, \mathcal{I}^r}^\psi$ is a Bessel sequence and the operator

$$\mathcal{A} : f \mapsto \sum_r \sum_{\lambda \in \mathcal{X}^r} \langle \psi_r f, g_\lambda^r \rangle g_\lambda^r$$

is bounded.

Now, according to Lemma 15, \mathcal{A} satisfies

$$\begin{aligned} \|f - \mathcal{A}f\|_2^2 &\leq \sum_r \|\psi_r f - \sum_{\lambda \in \mathcal{X}^r} \langle \psi_r f, g_\lambda^r \rangle g_\lambda^r\|_2^2 \\ &\leq \varepsilon \sum_r \|\psi_r f\|_2^2 \\ &\leq \varepsilon n_0 \|f\|_2^2. \end{aligned}$$

Thus \mathcal{A} is invertible and we can use the Neumann series, see [40, Appendix], to obtain the inverse operator $\mathcal{A}^{-1} = \sum_{k=0}^{\infty} (\text{Id} - \mathcal{A})^k$ which satisfies:

$$f = \mathcal{A}^{-1} \mathcal{A}f,$$

hence

$$f = \sum_r \sum_{\lambda \in \mathcal{X}^r} \langle \psi_r f, g_\lambda^r \rangle \mathcal{A}^{-1}(g_\lambda^r) = \sum_r \sum_{\lambda \in \mathcal{X}^r} \langle f, \psi_r g_\lambda^r \rangle \mathcal{A}^{-1}(g_\lambda^r),$$

which shows that f can be reconstructed from the set of coefficients (7.5). \square

Remark 25. According to the experiments discussed in Section 3.4, the set of atoms $\mathcal{A}^{-1}(g_\lambda^r)$ used in the reconstruction are well-approximated by the original Gabor atoms g^r inside the different regions in the time-frequency plane, corresponding to the sampling sets \mathcal{X}^r . The behavior in the regions of overlap has not yet been analytically described. An analytical characterization of the dual systems in the overlap regions is beyond the scope of this thesis and will be the topic of future research.

We next show that an analogous result can be achieved for Gabor frames (g^r, Λ^r) , with frame bounds $A^r \neq B^r$, i.e., for general systems which are not necessarily tight. Due to a result on the time-frequency concentration of dual frames ([40], Theorem 13.2.1), the result on systems derived from general Gabor frames is just an easy modification of Theorem 20.

Lemma 16. *If (g, a, b) is a Gabor frame for \mathbf{L}^2 , and $g \in S_0$ is in $H_{s,C}$, $C > 0$ and $s > 2$, then the dual window γ is in S_0 and there exists C' such that $H_{s,C'}$ as well.*

Remark 26. An even more general statement about the localization of dual frame was recently proved in [41]. An interesting open question is whether for a compact set of window functions, such as the family of g^r in Theorem 19, the dual windows form a compact set again, more specifically, whether the constant C' in Lemma 16 can be chosen simultaneously for all g^r .

Corollary 6. *Let $(g^r, \Lambda^r)_{r \in \mathcal{I}}$ be Gabor frames with $g^r \in H_{s,C}$ for all r , some $C > 0$ and $s > 2$ and dual windows γ^r . Furthermore assume that for the lower frame bounds A^r of $(g^r, \Lambda^r)_{r \in \mathcal{I}}$ we have $A^r \geq A$, $A > 0$. Then $\|\gamma^r\|_{S_0} \leq A^{-1}\|g^r\|_{S_0}$ for all r .*

Proof. The inverse frame operators are bounded above by $\frac{1}{(A^r)}$, hence, with $\gamma^r = S_r^{-1}g^r$ we obtain the result. \square

Theorem 19. *Let $(g^r, \Lambda^r)_{r \in \mathcal{I}}$ be Gabor frames with $g^r \in H_{s,C}$ for all r , some $C > 0$ and $s > 2$, with $\max_r \|g^r\|_{S_0} = C_g$. Furthermore assume that (7.1) holds for some $\alpha, \beta > 0$ and that the frame bounds A^r and B^r of $(g^r, \Lambda^r)_{r \in \mathcal{I}}$ are bounded below and above, respectively, i.e., $A^r \geq A$, $A > 0$ and $B^r \leq B$, $B > 0$. Then, in analogy to the result in Lemma 15, index sets \mathcal{X}^r can be chosen for a given $\varepsilon < n_0$ and all $r \in \mathcal{I}$, such that $\mathcal{G}_{g^r, \mathcal{I}^r}^\psi = \bigcup_{r \in \mathcal{I}} \{(\psi_r \cdot g_\lambda^r) : \lambda \in \mathcal{X}^r\}$ is a Bessel sequence and any $f \in \mathbf{L}^2$ can be completely reconstructed from*

$$\left(\langle f, \psi_r \cdot g_\lambda^r \rangle \right)_{r \in \mathcal{I}, \lambda \in \mathcal{X}^r}. \quad (7.6)$$

Proof. In analogy to Lemma 15 we can determine the index sets

$$\mathcal{X}^r = \{(x, \xi) \in \Lambda^r : |x_r - x| \leq R + \delta\}, r \in \mathcal{I},$$

where the δ is independent of r , such that

$$\|f^r - \sum_{\lambda \in \mathcal{X}^r} \langle f^r, g_\lambda^r \rangle \gamma_\lambda^r\|_2 \leq \varepsilon \|f^r\|_2$$

holds for all $r \in \mathcal{I}$. Hence

$$\begin{aligned} \|f\|_2^2 &\leq n_0 \sum_r \|\psi_r f\|_2^2 \\ &\leq n_0 (1 - \varepsilon)^{-2} \sum_r \sum_{\lambda \in \mathcal{I}^r} |\langle f \psi_r, g_\lambda^r \rangle|^2 \|S_r^{-1} g_\lambda^r\|_2^2, \end{aligned}$$

where S_r denotes the frame operator corresponding to $(g^r, \Lambda^r)_{r \in \mathcal{I}}$. By assumption, S_r is invertible for all r and the operator norm of the inverse operator S_r^{-1} is bounded above by $\frac{1}{A^r}$, hence $\|S_r^{-1} g_\lambda^r\|_2^2 \leq \frac{1}{A^r} \|g_\lambda^r\|_2^2$ for all r . Hence $\|S_r^{-1} g_\lambda^r\|_2^2 \leq C_g^2$ for all r and

$$\|f\|_2^2 \leq (A(1 - \varepsilon))^{-2} n_0 C_g^2 \sum_r \sum_{\lambda \in \mathcal{I}^r} |\langle f \psi_r, g_\lambda^r \rangle|^2.$$

The rest of the proof is analogous to the proof of Theorem 18. \square

The next sections discuss the question whether for multiple Gabor families which are not strictly localised by multiplication with ψ_r frame-bounds can still be found.

7.1.2 Lower frame bound

For the next theorem we assume that the index sets \mathcal{X}^r are chosen such that there exists $\theta > 0$ such that

$$\sum_r \sum_{\lambda \in \mathcal{X}^r} |\langle \psi_r f, g_\lambda^r \rangle|^2 \leq \theta \sum_r \sum_{\lambda \in \mathcal{X}^r} |\langle f, g_\lambda^r \rangle|^2. \quad (7.7)$$

Theorem 20. *Let $(g^r, \Lambda^r)_{r \in \mathcal{I}}$ be tight Gabor frames with $g^r \in H_{s,C}$ for all r , some $C > 0$ and $s > 2$. Furthermore assume that (7.1) holds for some $\alpha, \beta > 0$ and that $\max_r \|g^r\|_{S_0} = C_g$. Then, with the index sets \mathcal{X}^r as chosen in Lemma 15 for a given ε and all $r \in \mathcal{I}$, a lower frame bound for the system*

$$\mathcal{G}_{g^r, \mathcal{I}^r} = \bigcup_{r \in \mathcal{I}} \{(g_\lambda^r) : \lambda \in \mathcal{X}^r\} \quad (7.8)$$

is given by $\frac{(1-\varepsilon)}{\theta n_0 C_g^2}$, whenever (7.7) holds for $\theta > 0$.

Lemma 17. *For the index sets \mathcal{X}^r as chosen in Lemma 15, there exists $\theta > 0$ such that*

$$\sum_r \sum_{\lambda \in \mathcal{X}^r} |\langle \psi_r f, g_\lambda^r \rangle|^2 \leq \theta \sum_r \sum_{\lambda \in \mathcal{X}^r} |\langle f, g_\lambda^r \rangle|^2.$$

Discussion. Since a proper proof for the above statement could not yet be completed, we give an intuitive argument for the validity of (7.7) for some $\theta > 0$ for the system constructed in Lemma 15.

Note that

$$\sum_r \sum_{\lambda \in \mathcal{X}^r} \langle \psi_r f, g_\lambda^r \rangle g_\lambda^r = \sum_r \sum_{\lambda \in \mathcal{X}^r} \langle f, g_\lambda^r \rangle g_\lambda^r - \sum_r \sum_{\lambda \in \mathcal{X}^r} \langle (1 - \psi_r) f, g_\lambda^r \rangle g_\lambda^r,$$

hence

$$\sum_r \sum_{\lambda \in \mathcal{X}^r} |\langle \psi_r f, g_\lambda^r \rangle|^2 - \sum_r \sum_{\lambda \in \mathcal{X}^r} |\langle (1 - \psi_r) f, g_\lambda^r \rangle|^2 \leq \sum_r \sum_{\lambda \in \mathcal{X}^r} |\langle f, g_\lambda^r \rangle|^2.$$

Intuitively, since the \mathcal{X}^r are chosen to best represent the respective localized parts of the signal f given by $\psi_r f$, single components in the summation

$$\sum_r \sum_{\lambda \in \mathcal{X}^r} |\langle (1 - \psi_r)f, g_\lambda^r \rangle|^2$$

can only have more energy than the respective components on the right hand side, if the energy falls in the part of the signal represented by $\|(1 - \psi_r)f \cdot \psi_r^*\|_2^2$, where ψ_r^* denotes the sum of all members of the BUPU with non-empty intersection with any of the $\{\pi(\lambda)g_\lambda^r, \lambda \in \mathcal{X}^r\}$. However, this energy would also influence the size of the coefficients on the right hand side in the neighboring sampling sets. Hence, whenever the frequency-shift parameters b_r are small enough, the left hand side must be bounded away from zero, which suggests the existence of a constant θ , such that (7.7) holds. \square

Proof of the theorem.

$$\|f\|_2^2 \leq n_0 \sum_r \|\psi_r f\|_2^2 \leq n_0(1 - \varepsilon)^{-1} \sum_r \left\| \sum_{\lambda \in \mathcal{X}^r} \langle f \psi_r, g_\lambda^r \rangle g_\lambda^r \right\|_2^2 \quad (7.9)$$

$$\leq n_0(1 - \varepsilon)^{-1} \sum_r \sum_{\lambda \in \mathcal{X}^r} |\langle f \psi_r, g_\lambda^r \rangle|^2 \|g_\lambda^r\|_2^2 \quad (7.10)$$

$$\leq n_0(1 - \varepsilon)^{-1} \theta C_g^2 \sum_r \sum_{\lambda \in \mathcal{X}^r} |\langle f, g_\lambda^r \rangle|^2. \quad (7.11)$$

as $\|g^r\|_2 \leq \|g^r\|_{S_0}$, hence, by assumption, $\|g^r\|_2^2 \leq C_g^2$ for all r . This yields

$$\frac{(1 - \varepsilon)}{\theta n_0 C_g^2} \|f\|_2^2 \leq \sum_r \sum_{\lambda \in \mathcal{X}^r} |\langle f, g_\lambda^r \rangle|^2$$

which proves that $\frac{(1 - \varepsilon)}{\theta n_0 C_g^2}$ is a lower frame bound for (7.8). \square

7.1.3 Upper frame bound

For the proof that an upper frame bound for the system constructed in Theorem 20 exists, i.e., that (7.8) is a Bessel sequence, we will allow more general sampling schemes via so-called relatively separated sampling sets. We first prove a general statement on sampling of the short-time Fourier transform on relatively separate sampling sets. Then we show that the sampling sets leading to the systems constructed in Theorem 20 are relatively separated. From this we deduce the existence of an upper frame bound for $\mathcal{G}_{g^r, \mathcal{I}^r}$. The generality of this approach will find application in the situation of time-frequency adaptive mixed Gabor systems as well.

Definition 19 (Relatively separated sets). *A countable set*

$$\mathcal{X} = \{z_i = (x_i, \xi_i), i \in \mathcal{I}\}$$

in \mathbb{R}^{2d} is called separated, if $\inf_{j, k \in \mathcal{I}} |z_j - z_k| > 0$. A relatively separated set is a finite union of separated sets.

Lemma 18. *Let \mathcal{X} be a relatively separated set in \mathbb{R}^{2d} . If a function F on \mathbb{R}^{2d} is in $W(C^0, \ell^2)$, then $F|_{\mathcal{X}}$ is in $\ell^2(\mathcal{X})$ and*

$$\sum_{x_i \in \mathcal{X}} |F(x_i)|^2 \leq C(\mathcal{X}) \|F\|_{W(C^0, \ell^2)}, \quad (7.12)$$

where the constant $C(\mathcal{X})$ depends only on the structure of the sampling set \mathcal{X} .

Remark 27. The above lemma is true in a much more general situation, especially for any weighted sequence space ℓ_m^p , and more general shift-invariant Banach spaces Y , see [33, Lemma 3.8] for example.

Proof. Recall that $\|F\|_{W(C^0, \ell^2)} = \|a_{kn}\|_{\ell^2}$, where

$$a_{kn} = \text{ess sup}_{(x, \xi) \in [0, 1]^{2d}} |F(x + k, \xi + n)| = \|F \cdot T_{(k, n)} \chi_{[0, 1]^{2d}}\|_{\infty}.$$

By assumption, \mathcal{X} is the finite union of separate sets \mathcal{X}^r , $r = 1, \dots, n_0$ and there exists δ , such that $\min |z_j - z_k| \geq \delta > 0$ for any pair z_j, z_k in \mathcal{X}^r , $r = 1, \dots, n_0$. Hence, for all $r = 1, \dots, n_0$, we have at most $\frac{\sqrt{2d}}{\delta} + 1$ points $z_i \in \mathcal{X}^r$ in $(k, n) + [0, 1]^{2d}$, $(k, n) \in \mathbb{Z}^d \times \mathbb{Z}^d$, such that the number of $z_i \in \mathcal{X}$ in the box $(k, n) + [0, 1]^{2d}$, $(k, n) \in \mathbb{Z}^d \times \mathbb{Z}^d$ is bounded above by $n_0 \cdot (\frac{\sqrt{2d}}{\delta} + 1)$. Clearly

$$|F(x, \xi)| \leq \|F \cdot T_{(k, n)} \chi_{[0, 1]^{2d}}\| \text{ for all } (x, \xi) \in (k, n) + [0, 1]^{2d}.$$

Altogether, this yields:

$$\begin{aligned} \sum_{z_i \in \mathcal{X}} |F(z_i)|^2 &\leq n_0 \cdot \left(\frac{\sqrt{2d}}{\delta} + 1\right) \sum_{(k, n) \in \mathbb{Z}^{2d}} \|F \cdot T_{(k, n)} \chi_{[0, 1]^{2d}}\|_{\infty}^2 \\ &= n_0 \cdot \left(\frac{\sqrt{2d}}{\delta} + 1\right) \|F\|_{W(C^0, \ell^2)}^2 \end{aligned} \quad (7.13)$$

□

Lemma 19. *The union of points $\{\lambda = (x, \xi), \lambda \in \mathcal{X}^r\}$ in the index sets \mathcal{X}^r as chosen in Lemma 15 and Theorem 19 is relatively separated.*

Proof. Each of the lattices Λ^r determining the Gabor frames used in the construction of $\mathcal{G}_{g^r, \mathcal{I}^r}$ are of course separated. The admissibility condition for the BAPU $(\psi_r)_{r \in \mathcal{I}}$ allows only finite overlap between any pair of members in the BAPU. As a finite radius $\delta > 0$ of overlap is added to the compact support Ω_r of ψ_r , we have:

$$\sup_{r \in \mathcal{I}} \#\{r' : \text{supp}(\psi_r) + B_{\delta}(0) \cap \text{supp}(\psi_{r'}) + B_{\delta}(0)\} \leq n_0^*,$$

where $n_0^* = n_0 + n(\delta)$. Hence, for any $[0, 1]^{2d}$ at most n_0^* lattices Λ^r contribute to the sampling set $\bigcup_{r \in \mathcal{I}} \mathcal{X}^r$, which is therefore relatively separated. □

Theorem 21. *An upper frame bound for the family of functions (7.8) is given by $CC_{H_{s,C}}n_0 \cdot (\frac{\sqrt{2d}}{\delta} + 1)$.*

Proof. First note that

$$\sum_r \sum_{\lambda \in \mathcal{X}^r} |\langle f, g_\lambda^r \rangle|^2 = \sum_r \sum_{\lambda \in \mathcal{X}^r} |\mathcal{V}_{g^r} f(\lambda)|^2.$$

Now, fixing $g_0 \in S_0$, we have the following convolution relation (see [40, Lemma 11.3.3] for details):

$$|\mathcal{V}_{g^r} f(\lambda)| \leq \frac{1}{|\langle g^r, g_0 \rangle|} (|\mathcal{V}_{g_0} f| * |\mathcal{V}_{g^r} g^r|)(\lambda)$$

and thus, as $g^r \in H_{s,C}$ for all r , with $C_{H_{s,C}} = w_{-s}(0)$ we obtain :

$$\sum_r \sum_{\lambda \in \mathcal{X}^r} |\langle f, g_\lambda^r \rangle|^2 \leq C_{H_{s,C}}^2 \sum_r \sum_{\lambda \in \mathcal{X}^r} (|\mathcal{V}_{g_0} f| * Cw_{-s})^2(\lambda).$$

Now, for g_0 in S_0 and $f \in \mathbf{L}^2$, $|\mathcal{V}_{g_0} f|$ is in $W(C^0, \ell^2)$ and w_{-s} is in $W(C^0, \ell^1)$, see [32], Theorem 3.3.1 and Lemma 3.6.8. Hence $F(\lambda) = [|\mathcal{V}_{g_0} f| * Cw_{-s}](\lambda)$ is in $W(C^0, \ell^2)$ and as $\mathcal{X} = \bigcup_{r \in \mathcal{I}} \mathcal{X}^r$ was shown to be a relatively separated set Lemma 18 can be applied to obtain the following estimate:

$$\sum_r \sum_{\lambda \in \mathcal{X}^r} |\langle f, g_\lambda^r \rangle|^2 \leq C_{H_{s,C}}^2 n_0 \cdot \left(\frac{\sqrt{2d}}{\delta} + 1 \right) \|F\|_{W(C^0, \ell^2)}^2.$$

Now, as

$$\|F\|_{W(C^0, \ell^2)} = \| |\mathcal{V}_{g_0} f| * Cw_{-s} \|_{W(C^0, \ell^2)} \leq \|\mathcal{V}_{g_0} f\|_2 \|Cw_{-s}\|_{W(C^0, \ell^1)},$$

setting $C = \|Cw_{-s}\|_{W(C^0, \ell^1)}^2$, we achieve the final estimate for the upper frame bound of $\mathcal{G}_{g^r, \mathcal{I}^r}$ as follows:

$$\sum_r \sum_{\lambda \in \mathcal{X}^r} |\langle f, g_\lambda^r \rangle|^2 \leq C \|g_0\|_{S_0} C_{H_{s,C}}^2 n_0 \cdot \left(\frac{\sqrt{2d}}{\delta} + 1 \right) \|f\|_2^2$$

□

7.2 Outlook: Time-Frequency Adaptive Systems

As discussed in Section 3.4.2, we may look for a more flexible partitioning of the time-frequency plane by giving up the restriction that the systems in use may only vary in one domain. In this final section, we introduce the notion of *quilted Gabor frames* and collect some arguments developed in this work which suggest the construction of frames of this type.

Definition 20 (Quilted Gabor frames). *Let a bounded uniform or admissible partition of unity of \mathbb{R}^{2d} be given with the additional property that there exists a constant $\eta > 0$ such that $\Omega_r = \text{supp}(\psi_r) \subseteq B_{\eta_r}(\mu_r) \subseteq B_\eta(\mu_r)$, $\mu_r \in \mathbb{R}^{2d}$, for all r . To every Ω_r assign a Gabor frame $\mathcal{G}^r = (g^r, a_r, b_r)$. A family of the form*

$$\bigcup_r \{g_\lambda^r, \lambda \in \mathcal{X}^r\}, \quad (7.14)$$

where $\mathcal{X}^r = \{\lambda = (x, \xi) : |x_r - x| < \vartheta_1, |\xi_r - \xi| < \vartheta_2\}$ is called a quilted Gabor frame for $\mathbf{L}^2(\mathbb{R}^d)$ if there exist $A, B > 0$ such that

$$A\|f\|_2^2 \leq \sum_r \sum_{\lambda \in \mathcal{X}^r} |\langle f, g_\lambda^r \rangle|^2 \leq B\|f\|_2^2 \quad (7.15)$$

holds for all $f \in \mathbf{L}^2(\mathbb{R}^d)$.

Discussion

- As discussed in Section 6.1, if $H_r = H_{\psi_r}$ for the partition of unity $(\psi_r)_{r \in \mathcal{I}}$, we have

$$f = \sum_{r \in \mathcal{I}} H_r f$$

with absolute convergence for $f \in S_0$ and ℓ^2 -convergence for all $f \in \mathbf{L}^2$. Additionally, there exist constants $0 < C_1 \leq C_2 < \infty$, such that

$$C_1\|f\|_2^2 \leq \sum_\lambda \|H_\lambda f\|_2^2 \leq C_2\|f\|_2^2.$$

- As stated in Proposition 3, Section 5.7, on compact sets, in particular on $K_r = \overline{H_r(\circ \mathbf{L}^2)}$, the identity operator can be uniformly approximated by finite dimensional frame operators, i.e., for any given $\varepsilon > 0$ there exists a finite set of sampling points $\mathcal{X}^r = B_{R^r}(\mu_r) \cap \Lambda^r$ corresponding to the system \mathcal{G}^r , such that

$$\|h - \sum_{\lambda \in \mathcal{X}^r} \langle h, g_\lambda^r \rangle g_\lambda^r\|_2 < \varepsilon \text{ for all } h \in K_r, \quad (7.16)$$

hence,

$$\|H_r - \sum_{\lambda \in \mathcal{X}^r} \langle H_r f, g_\lambda^r \rangle g_\lambda^r\|_2 < \varepsilon \|H_r f\|_2 \text{ for all } f \in \mathbf{L}^2. \quad (7.17)$$

- In order to be able to construct a quilted Gabor frame similar to the construction of the multiple Gabor frames in Section 7.1.2, a constant δ has to be determined, such that with $R_r = \eta_r + \delta$ (7.16) holds for all r simultaneously. Practically this corresponds to choosing a rim of the same finite radius around every Ω_r , the resulting ball will have compact support again.
- Hence, if the local sampling sets \mathcal{X}^r can be chosen to be $\mathcal{X}^r = B_{\eta_r + \delta}(\mu_r) \cap \Lambda^r$, then, in analogy to the multiple Gabor case, an upper frame bound for the system (7.14) exists.

- The crucial open question is how to describe in detail common properties of the Gabor frames \mathcal{G}^r which allow a *uniform* determination of δ for any given ε .

Appendix A

MATLAB files

A.1 stftl.m

```
function stf = mostf(x,w,a);

% MOSTFT.M for LONG signals, M.D.
% determines the STFT of a LONG vector over a lattice
% with lattice constants a (time) and full frequency range
% STFTL(f)(ak,bm) is the output
% USAGE: MOSTFT(x,w,a) , w = window, x = signal
%          a = time gap

if nargin == 2; a = 1; end; x = x(:).'; w = w(:).';
l=length(x); lw = length(w);

tp = round(l/a)+lw/a-1; %number of time-points
stf = zeros(lw,tp); N = length(x); x = [zeros(1,lw-a) x
zeros(1,lw-a)];
for j = 1:tp ;
    y = w.*x((j-1)*a+1:(j-1)*a+lw);
    stf(:,j)=fft(y)';
end;

function srec = rec(S,wd,a);

% REC.M ... Gabor reconstruction for long signals, M.D.
% S is Gabor transform matrix calculated with mostft.m
% wd is the dual window of the analysis window g,
% calculated via gabop: wd = pinv(gabop(g,a,length(g)))
% and a must be the same time-shift as in the analysis
% USAGE: srec = rec(S,wd,a);

[m,n] = size(S); S=S(:); lw=length(wd); l = (n+1)*a-lw;
dum=zeros(1,l+2*lw-2*a);
for j = 1:n
    dum((j-1)*a+1:(j-1)*a+lw) = ...
    ... dum((j-1)*a+1:(j-1)*a+lw)+(fft(S((j-1)*lw+1:j*lw)).*wd)';
end;
srec = real(dum(lw-a+1:(lw-a)+l));
```

A.2 windows.m

```
function gd = dualsp(g,a)

% DUALSP.M, M.D.
% Calculates a reconstruction window
% for reconstruction from STFT of LONG signals,
% if the fft of the full window length is used.
% In this case red = length(g)/a, because the 'signal-length'
% and b factor out.
% USAGE: gd = dual(g,a);

l = length(g); dum = zeros(size(g')); g2 = [g.^2,g.^2]*1;

for i = 1:l/a
    dum = dum + g2((i-1)*a+1:(i-1)*a+l);
end

gd = g./dum';

%%%%%%%%%%%%%%%%%%%%%%%%%%%%%%%%%%%%%%%%%%%%%%%%%%%%%%%%%%%%%%%%%%%%%%%%

function gt = tightsp(g,a)

% TIGHTSP.M, M.D.
% Calculates a tight window for Gabor analysis of LONG signals,
% if the fft of the full window length is used.
% In this case red = length(g)/a, because the 'signal-length'
% and b factor out.
% This yields for G = gabop(g,a,n*1):
% G'*G = ID, for any multiple of l(window length)
% USAGE: gt = tightsp(g,a);

l = length(g); dum = zeros(size(g')); g2 = [g.^2,g.^2]*1;

for i = 1:l/a
    dum = dum + (g2((i-1)*a+1:(i-1)*a+l));
end

gt = g./sqrt(dum');
```

A.3 opeig.m

```

function G = opeig(G,delta);
% OPEIG.M M.D.
% ... comparing the numbers of significant eigenvalues of the Gramian
% matrix of the 'Operator' matrix A
% (comprised of n^2-dim, rank1 operators
% corresponding to a given Gabor family)
% INPUT: G (structure); delta (default: delta = .1)
% Requires: G.g or G.gt, G.la
% ADDS: G.ev ... sorted eigenvalues
%       G.nev... number of them > threshold delta
% If G.la.a,G.la.b, are vectors, this yields multipleoutout and plot
% Usage:   G = opeig(G,delta);

a = G.la.a;b=G.la.b; if nargin ==1, delta = .1;end

n = length(G.g);

if size([a,b]) == [1,2];
    if isfield(G,'gt');
        g = G.gt;
    else
        g = G.g;
    end;

    dd = abs(stft(g,g,a,b)).^2;
    fdd = fft2(dd);
    fdd = nl(sort(abs(fdd(:)))));
    plot(log(fdd(end:-1:1))),shg
    d = fdd(end:-1:1);
    ne = size(find(d>delta));
else
    kk=0;clf,hold
    ma=min(a);mb = min(b);m = n.^2/(ma*mb);nab=length(a)*length(b);
    d = zeros(nab,m);ne = zeros(1,nab);
    for ii=1:length(a);
        for jj= 1:length(b);
            kk= kk+1;
            if isfield(G,'gt');
                g = G.gt(kk,:);
            else
                g = G.g;
            end;
            g = g(:)';
            dd = abs(stft(g,g,a(ii),b(jj))).^2;
            fdd = fft2(dd);size(dd),pause
            fdd = nl(sort(abs(fdd(:)))));
            plot(log(fdd(end:-1:1))),shg
            d(kk,1:length(fdd)) = fdd(end:-1:1)';
            sfd=size(find(fdd>delta));
            ne(kk) = sfd(1,1);
        end
    end
end
G.ev = d; G.nev=ne;

```

A.4 ogabgrw.m

```
function [EIG,MO,MOW,w1] = ogabgrw(G,M);

% OGABGRW.M , HGFei, Dec. 1999
% adapted to new environment: October 2000 (M.D.)
% Input:  G, M Adds:  EIG.v      Requires: G.g, G.gt
%           EIG.w      G.la
%           M.xp (grid to mask) M.m  mask OR
%           EIG.coff      M.R1  radius1 of mask
%           MO.M          M.R2  radius2 of mask
%           MOW.M         M.w   shape of the weight:
%           EIG.sgp=[m1,n1] w=0--> product of Hanning windows
%                           w=1--> constant 1 (no weighting)
%                           w=2--> cone-shaped mask
%                           (function called: gabww.m)
% Output: EIG.v ... Matrix containing the eigenvectors
%         EIG.w ... eigenvalues
%         EIG.coff ... Gram Matrix of coefficients for eigenvectors
%         EIG.sgp=[m1,n1] ... sidelengths of masking rectangle on grid
%                           (m1*n1 = number of remaining building blocks)
% USAGE: [EIG,MO,MOW,w1] = ogabgrw(G,M);

G= addG(G);
% Adding a mask:
if (not(isfield(M,'m'))))
    M = ofltrecs(G,M);
else;
    M.xp = G.la.xpo .* M.m;
end; m1=max(size(find(M.xp(:,1)))); n1=max(size(find(M.xp(1,:))));
EIG.sgp=[m1,n1]; MO.M = gabbas(G.gt,M.xp);

w1 = M.m(find(abs(M.xp))); M.xp(find(abs(M.xp)))= w1;

w1 = w1/max(w1); % [h1,h2] = size(w1),pause
MOW.M = diag(w1)*MO.M;
GRW=MOW.M*MOW.M';
[EIG.coff,EIG.w]=eigsort(GRW);

% (GREIG'*GW) yields eigenvectors as
% linear combinations of components.
EIG.v = diag(oneover(sqrt(EIG.w)))*(EIG.coff'*MOW.M);
MOW.G=MOW.M; MOW.M=MOW.G'*MOW.G; MO.G=MO.M; MO.M=MO.G'*MO.G;
w1 =w1.^2; % Yields actual weight vector, as w1 is applied twice.
```



```

function [H2,wp1,AMPL] = gabww(AMPL,opt);

% GABWW.M , HGFei , Adapted by M.D.
%
% This file is meant to build a weight function over the mask-area
% such that there is no clustering of eigenvalues anymore. The
% practical effect of this is that the eigenvector system becomes
% numerically more stable.
% opt is an input variable specifying the shape of the weigth
% Default (or opt = 0): Product of Hanning windows,
% USAGE: % [AMPL,H2,wp1] = gabww(AMPL,opt);

[hig,wid] = size(AMPL); if nargin ==1 opt = 0; end

if size(opt)==[1,1]

    if opt ==0
        h1 = 0.5*(1 + fftshift(hanning(hig)));
        h2 = 0.5*(1+fftshift(hanning(wid)));
        h1 = (h1' + invol(h1))/2; h1 = real(h1);
        h2 = (h2' + invol(h2))/2; h2 = real(h2);
        H2 = h1(:) * h2(:).';
    elseif opt==1
        H2 = ones(size(AMPL));
    else
        st= 1/hig;
        d1=[0:st:.5];d2=[.5:-st:0];d = [d2,d1];
        h1 = (0.5+d)';
        st= 1/wid;
        d1=[0:st:.5];d2=[.5:-st:0];d = [d2,d1];
        h2 = (0.5+d)';
        h1 = (h1' + invol(h1))/2; h1 = real(h1);
        h2 = (h2' + invol(h2))/2; h2 = real(h2);
        h1=h1(2:length(h1)-1);h2=h2(2:length(h2)-1);
        H2 = h1(:) *h2(:).';
    end

else
    return;
end

wp1 = H2(find(abs(AMPL))); AMPL(find(abs(AMPL)))= wp1;

```

A.5 upp2low.m

```

function low=up2low(upp,g,a,b)

% UP2LOW.M M.D.
% function low=up2low(upp,g,a,b)
% calculates the lower symbol from the given upper symbol.
% USAGE: low=up2low(upp,g,a,b)

n=length(g);
l=zeros(n/b,n/a);l(:) =upp(:);
upp=l;
v=abs(stft(g,g,a,b)).^2; % 2-dimensional convolution kernel
low=ifft2(fft2(upp).*(fft2(v)));

```

A.6 gmult.m

```

function GM = gmult(M,gd,g,a,b);

% H=gmult(M,gd,g,a,b) computes the matrix kernel of an
% Gabor analysis-modification-synthesis system
%
% INPUT:
%   M ...is the multiplier either on the grid (length(g)/b times length(g)/a)
%       or of dimension length(g) times length(g), in the latter case
%       it will be automatically downsampled according to a, b
%   gd ... is the synthesis window (column vector)
%   g ... is the analysis window
%   a,b ... are the grid constants,
%           Default: 1,1 i.e. full grid
%
% W.Kozek 12.3.96 -- modified: M.D. 3/2001,
%%%%%%%%%%%%%%%%%%%%%%%%%%%%%%%%%%%%%%%%%%%%%%%%%%%%%%%%%%%%%%%%%%%%%%%%

% Flip of all rows except the first to achieve
% correct position of frequency modulations
M = flipv(M);

[hh,ww] = size(M); n = length(gd);

% Construct multiplier matrix on grid
if hh*ww < n*n;
    a = n/ww; b = n/hh;
else
    if nargin < 4; a=1;b=1;end
end;
if nargin ==2,g=gd;end;

M1 = zeros(n,n);
[h,w] = size(M);
M1(1:b:n,1:a:n) = M;

% The KN-symbol of the Gabor-multiplier is just the convolution
% of the multiplier-function given by M1 with the KN-symbol of
% the Projection onto g0. Here realized on the FT-side:

Pg = gd'*g; % Basic Projection operator
KPg = momat2kns(Pg); % KN-symbol of the projection operator
FKPg = fft2(KPg); % transform to FT--domain
FM = fft2(M1); % ...also of M1
KGM = ifft2( FM .* FKPg); % Multiplication+back to time-domain.,
% yields KN-symbol of the operator, so that:
GM = mokns2mat(KGM);

%%%%%%%%%%%%%%%%%%%%%%%%%%%%%%%%%%%%%%%%%%%%%%%%%%%%%%%%%%%%%%%%%%%%%%%%
function C = mokns2mat(SMF);

C = conj(side2mat(ifft(SMF)));

function KN = momat2kns(C);
KN = fft(sidedigm(conj(C)));

```

A.7 imp2mh.m

```
function S=imp2mh(G);

% H=imp2(G) computes the selfinverse map H(n,k) onto H(n,n-k)
% for quadratic matrices based on cyclic time--shifts
%%%%%%%%%%%%%%%%%%%%%%%%%%%%%%%%%%%%%%%%%%%%%%%%%%%%%%%%%%%%%%%%%%%%%%%%
% S=fftshift(fft(imp2(H))) leads to the
% (asymmetrical) spreading function
% where the origin is in the center and time lag is horizontal
% and frequency lag is vertical
%
% H=imp2(iff(fftshift(S))) leads to its inverse
%%%%%%%%%%%%%%%%%%%%%%%%%%%%%%%%%%%%%%%%%%%%%%%%%%%%%%%%%%%%%%%%%%%%%%%%
% Z=fft(rot90(imp2(H))) leads to the Kohn-Nirenberg
% symbol (Zadeh's time--varying transfer function) of H
%
% H=imp2(rot90(iff(Z),-1)); leads to its inverse
%%%%%%%%%%%%%%%%%%%%%%%%%%%%%%%%%%%%%%%%%%%%%%%%%%%%%%%%%%%%%%%%%%%%%%%%
% Z=fft(rot90(imp2(x*x')))) gives the Rihaczek distribution
% of the signal x
%
% A=fftshift(fft(imp2(x*x')))) gives the ambiguity function
%
% M.Hampejs 3.9.2000
%%%%%%%%%%%%%%%%%%%%%%%%%%%%%%%%%%%%%%%%%%%%%%%%%%%%%%%%%%%%%%%%%%%%%%%%
[dim,dim] = size(G); S=zeros(dim,dim); H=zeros(dim,2*dim);
H=[G,G]; for i=1:dim,
    S(i,:)=H(i,dim+i:-1:i+1);
end
```

A.8 fupro.m

```
function nor=fupro(EIG,nofeig,a,b);

% FUPRO.M M.D.
% For a given localisation operator of finite rank, which here is the
% projection onto the first 'nofeig' eigenvectors of
% a Gabor multiplier, the completeness of the resulting
% multi-window Gabor system is checked.
%
% INPUT: EIG - matrix containing the eigenvectors
%         nofeig - rank of projection operator
%         a,b - lattice constants
% The output is 'nor', for nor < 1, the family of projection
% operators yields a
% complete set of coefficients for reconstruction.
% USAGE: nor=fupro(EIG,nofeig,a,b);

size(EIG);n = ans(2);
DUM = zeros(b,a);

for i = 1:nofeig
    S = abs(stft(EIG(i,:),EIG(i,:),n/a,n/b));
    DUM = DUM+S;
end

DUM = DUM/nofeig^2;DUM(1,1)=0;

nor= norm(DUM(:),1);
```


Bibliography

- [1] ASSAYAG, G., FEICHTINGER, H. G., AND RODRIGUES, J. F., Eds. *Mathematics and Music*. Diderot Forum, Lisbon-Paris-Vienna. Springer, 2002.
- [2] BENEDEK, A., AND PANZONE, R. The space L^p , with mixed norm. *Duke Math. J.* 28 (1961), 301–324.
- [3] BENEDETTO, J., HEIL, C., AND WALNUT, D. Gabor systems and the Balian-Low theorem. In *Gabor analysis and algorithms*. Birkhäuser Boston, Boston, MA, 1998, pp. 85–122.
- [4] BENNETT, C., AND SHARPLEY, R. *Interpolation of Operators*, vol. 129 of *Pure and Applied Mathematics*. Academic Press, 1989.
- [5] BERGER, J., COIFMAN, R., AND GOLDBERG, M. Removing noise from music using local trigonometric bases and wavelet packets. *J. Audio Eng. Soc.* 42, 10 (1994), 808–818.
- [6] BÖLCSKEI, H., AND JANSSEN, J. Gabor frames, unimodularity, and window decay. *J. Fourier Anal. Appl.* 6, 3 (2000), 255–276.
- [7] BYRD, D., AND CRAWFORD, T. Problems of music information retrieval in the real world. *Information Processing and Management* 38, 2 (March 2002), 249–272.
- [8] CAMBOUROPOULOS, E. From MIDI to traditional musical notation. In *Proceedings of the AAAI Workshop on Artificial Intelligence and Music: Towards Formal Models for Composition, Performance and Analysis*.
- [9] CAVALIERE, S., AND PICCIALLI, A. *Granular Synthesis of musical signals*, vol. 2 of *SNMR*. Swets and Zeitlinger, Netherlands, 1997, ch. 5, pp. 155–186.
- [10] CEMGIL, A., DESAIN, P., AND KAPPEN, B. Rhythm quantization for transcription. *Computer Music Journal* 24:2 (Summer 2000), 60–76.
- [11] CHEN, S., DONOHO, D., AND SAUNDERS, M. Atomic decomposition by basis pursuit. *SIAM Review* 43, 1 (March 2001), 129–159.
- [12] CHRISTENSEN, O. Frames and pseudo-inverses. *J. Math. Anal. Appl.* 195 (1995), 401–414.

- [13] CHRISTENSEN, O. Perturbations of frames and applications to Gabor frames. 1st ed., vol. Research monograph ‘Gabor Analysis and Algorithms: Theory and Applications’. Birkhäuser, Boston, 1998, ch. 5, pp. 193–209.
- [14] CONWAY, J. *A Course in Functional Analysis*. Graduate Texts in Mathematics. Springer, New York, 1990.
- [15] DAUBECHIES, I. The wavelet transform, time-frequency localization and signal analysis. *IEEE Trans. Info.Theory* 36 (1990), 961–1005.
- [16] DIXON, S. Automatic extraction of tempo and beat from expressive performances. *Journal of New Music Research* 30, 1 (2001), 39–58.
- [17] DÖRFLER, M. Analyzing Music. Analytical tools and case studies. Master’s thesis, University of Vienna, Austria, 1996.
- [18] DÖRFLER, M. Time-frequency analysis for music signals: A mathematical approach. *Journal of New Music Research* 30, 1 (2001), 3–12.
- [19] DÖRFLER, M., FEICHTINGER, H., AND K.GRÖCHENIG. Compactness criteria in function spaces. *Colloq. Math.* (to appear).
- [20] DÖRFLER, M., AND FEICHTINGER, H. G. Quantitative description of expression in performance of music, using Gabor representations. In *Proceedings of the Diderot Forum on Mathematics and Music: Computational and Mathematical Methods in Music* (Vienna, 1999), H. G. Feichtinger and M. Dörfler, Eds., pp. 139–144.
- [21] FEICHTINGER, H. A compactness criterion for translation invariant Banach spaces of functions. *Anal. Math.* 8 (1982), 165–172.
- [22] FEICHTINGER, H. Compactness in translation invariant Banach spaces of distributions and compact multipliers. *J. Math. Anal. Appl.* 102, 2 (1984), 289–327.
- [23] FEICHTINGER, H. Wiener amalgams over Euclidean spaces and some of their applications. In *Function spaces, Proc. Conf., Edwardsville/IL (USA) 1990, Lect. Notes Pure Appl. Math* 136, 123–137. 1992.
- [24] FEICHTINGER, H. Gabor multipliers and spline-type spaces over lca groups. In *Wavelet Analysis: Twenty Years’ Developments*, D. X. Zhou, Ed. World Scientific Press, Singapore, 2002. to appear.
- [25] FEICHTINGER, H., CHRISTENSEN, O., AND STROHMER, T. Group theoretical approach to Gabor analysis. *Optical Engineering* 34, 6 (1995), 1697–1704.
- [26] FEICHTINGER, H., AND HAMPEJS, M. Best approximation of matrices by Gabor multipliers. *preprint* (2001).

- [27] FEICHTINGER, H., AND JANSSEN, A. Validity of WH-frame bound conditions depends on lattice parameters. *Appl. Comput. Harm. Anal.* 8, 1 (2000), 104–112.
- [28] FEICHTINGER, H., AND KAIBLINGER, N. Varying the time-frequency lattice of Gabor frames. *Preprint (submitted)* (2002).
- [29] FEICHTINGER, H., AND KOZEK, W. Operator quantization on lca groups. In *Gabor Analysis and Algorithms: Theory and Applications*, H. Feichtinger and T. Strohmer, Eds. Birkhäuser, Boston, 1998. Chap. 7.
- [30] FEICHTINGER, H., AND NOWAK, K. A first survey of Gabor multipliers. In *Advances in Gabor Analysis*, H. Feichtinger and T. Strohmer, Eds. Birkhäuser, Boston, 2002.
- [31] FEICHTINGER, H., AND WERTHER, T. Atomic systems for subspaces, 2001. preprint.
- [32] FEICHTINGER, H., AND ZIMMERMANN, G. A Banach space of test functions for Gabor analysis. In *Gabor Analysis and Algorithms: Theory and Applications*, H. Feichtinger and T. Strohmer, Eds. Birkhäuser, Boston, 1998, pp. 123–170. Chap. 3.
- [33] FEICHTINGER, H. G., AND GRÖCHENIG, K. Banach spaces related to integrable group representations and their atomic decompositions. I. *J. Funct. Anal.* 86, 2 (1989), 307–340.
- [34] FEICHTINGER, H. G., AND GRÖCHENIG, K. Banach spaces related to integrable group representations and their atomic decompositions. II. *Monatsh. Math.* 108, 2-3 (1989), 129–148.
- [35] FEICHTINGER, H. G., AND STROHMER, H. G., Eds. *Gabor Analysis and Algorithms: Theory and Applications*. Applied and Numerical Harmonic Analysis. Birkhäuser, Boston, 1998.
- [36] FITCH, J., AND SHABANA, W. A wavelet-based pitch detector for musical signals. In *Proceedings of DAFx99*, J. Tro and M. Larsson, Eds. Department of Telecommunications, Acoustics Group, Norwegian University of Science and Technology, December 1999.
- [37] GABOR, D. Theory of communication. *J. IEE (London)* 93, 26 (1946), 429–457.
- [38] GODSILL, S., AND RAYNER, J. *Digital Audio Restoration, A statistical Model based Approach*. Springer-Verlag, London, 1998.
- [39] GRÖCHENIG, K. Describing functions: Atomic decompositions versus frames. *Monatsh. Math.* 112, 1 (1991), 1–42.

- [40] GRÖCHENIG, K. *Foundations of Time-Frequency Analysis*. Applied and Numerical Harmonic Analysis. Birkhäuser, Boston, 2001.
- [41] GRÖCHENIG, K. Localization of frames, Banach frames and the invertibility of the frame operator. *Preprint* (2002).
- [42] HEIL, C. An introduction to Wiener amalgams. Technical Report, 1992.
- [43] HEIL, C., AND WALNUT, D. Continuous and discrete wavelet transforms. *SIAM Review* 31, 4 (1989), 628–666.
- [44] JANSSEN, A., AND STROHMER, T. Characterization and computation of canonical tight windows for Gabor frames. *J.Four.Anal.Appl.*, *submitted* (2000).
- [45] JEONG, J., AND WILLIAMS, W. *Time-Varying Filtering and Signal Synthesis, Time-Frequency Signal Analysis Methods and Applications*, ed. boualem boashash ed. Longman Cheshire, Wiley Halsted Press, 1992, ch. 17, pp. 389–405.
- [46] KOZEK, W. Adaption of Weyl-Heisenberg frames. In *Gabor Analysis and Algorithms: Theory and Applications*, H. Feichtinger and T. Strohmer, Eds. Birkhäuser, Boston, 1998. Chap. 10.
- [47] KOZEK, W., FEICHTINGER, H., PRINZ, P., AND STROHMER, T. On multidimensional nonseparable Gabor expansions. In *Proc. SPIE: Wavelet Applications in Signal and Image Processing IV* (1996), M. Unser, A. Aldroubi, and A. Laine, Eds. to appear.
- [48] LEVINE, M. *The Jazz Theory Book*. Sher Music Co., Petaluma, CA, 1995.
- [49] LI, S. A theory of generalized multiresolution structure and pseudoframes of translates. *J. Fourier Anal. Appl.* 7, 1 (2001), 23–40.
- [50] MALLAT, S. *A Wavelet Tour of Signal Processing*. Academic Press, San Diego, USA, 1998.
- [51] NG, W.-J. Noise reduction for audio signals using the Gabor expansion. M.Phil. thesis, University of Cambridge, 2000.
- [52] PAPADOPOULOS, A. Mathematics and music theory: From Pythagoras to Rameau. *The Mathematical Intellegencer* 24, 1 (2002), 65–73.
- [53] PEGO, R. Compactness in L^2 and the Fourier transform. *Proc. Amer. Math. Soc.* 95, 2 (1985), 252–254.
- [54] PIELEMEIER, W. J., AND WAKEFIELD, G. H. A high-resolution time-frequency representation for musical instrument signals. *Journal of the Acoustical Society of America* 99, 4 (1996), 2382–2396.

- [55] QIAN, S., AND CHEN, D. *Joint Time-Frequency Analysis: Method and Application*. Prentice Hall, Englewood Cliffs, NJ, 1996.
- [56] RAMEAU, J. *Complete Theoretical Writings*. American Institute of Musicology, 1967.
- [57] RAZ, S., AND FARKASH, S. Time variant filtering via the Gabor representation. In *Proceedings of the EUSIPCO-90, European Signal Processing Conference* (Barcelona, Spain, Sept. 1990), L. Torres, E. Masgrau, and M. Lagunas, Eds., pp. 509 – 512.
- [58] REITER, H. *Classical harmonic analysis and locally compact groups*. Clarendon Press, Oxford, 1968.
- [59] ROADS, C. *The Computer Music Tutorial*. Computer Science. MIT press, Cambridge, MA, 1996.
- [60] ROBERT, C. P., AND CASELLA, G. *Monte Carlo Statistical Methods*. Springer, 1999.
- [61] RUDIN, W. *Functional Analysis*. McGraw-Hill, New York, 1973.
- [62] TEOLIS, A. *Computational Signal Processing with Wavelets*. Birkhäuser, Boston-Basel-Berlin, 1998.
- [63] VETTERLI, M., AND KOVACEVIC, J. *Wavelets and Subband Coding*. Signal Processing. Prentice Hall, New Jersey, 1995.
- [64] WALMSLEY, P., GODSILL, S., AND RAYNER, P. Bayesian graphical models for polyphonic pitch tracking. In *Proceedings of the Diderot Forum on Mathematics and Music: Computational and Mathematical Methods in Music* (Vienna, 1999), H. G. Feichtinger and M. Dörfler, Eds., pp. 353–366.
- [65] WEIL, A. *L'integration dans les Groupes Topologiques*, 2 ed. Hermann, 1965.
- [66] WOLFE, P. J., DÖRFLER, M., AND GODSILL, S. J. Multi-Gabor dictionaries for audio time-frequency analysis. In *Proceedings of the IEEE Workshop on Applications of Signal Processing to Audio and Acoustics* (Mohonk, NY, 2001), pp. 43–46.
- [67] ZEEVI, Y. Y., ZIBULSKI, M., AND PORAT, M. Multi-window Gabor schemes in signal and image representations. In *Gabor Analysis and Algorithms: Theory and Applications*, H. G. Feichtinger and T. Strohmer, Eds., Applied and Numerical Harmonic Analysis. Birkhäuser, Boston, 1998, pp. 381–407.
- [68] ZHENG, Z., AND FEICHTINGER, H. Gabor eigenspace time-variant filter. In *Proc. 2000 IEEE Electro/Information Technology Conference* (Chicago, USA, 2000).

- [69] ZIBULSKI, M., AND ZEEVI, Y. Discrete multiwindow Gabor-type transforms.
IEEE Trans. Signal Processing 45, 6 (June 1997), 1428–1442.

Curriculum Vitae

Name: Monika Dörfler

Adress: Apostelgasse 24/10, 1030 Wien

Austria, Europe

Nationality: Austria

Born on 24th of December, 1972 in Vienna

1978-1982 Primary School in Krumpendorf/Kärnten

1982-1990 Highschool in Klagenfurt

1986-1990 Student at the Conservatory of Carinthia (piano, chamber music, music theory)

1990 "Matura" (main subjects: music, languages and mathematics)

1990-1996 Studies of Mathematics at the University of Vienna

1990-2001 Student of piano at the University of Music in Vienna (Classical and jazz piano)

1995, Summerterm: Exchange Student at the University of Michigan, Ann Arbor, USA

Masters Thesis: 'Analysing Music: Mathematical Tools and Case Studies'

1996 Masters Degree in Mathematics. University of Vienna

1996-1998 Scientific researcher at the Technical University of Vienna (non-linear systems theory)

1997 Teaching qualification for classical piano (University of Music, Vienna)

1998 Piano teacher at the Music school in Krems/Niederösterreich

1999 Summerterm: Erasmus Student at the Guildhall School of Music and Drama (London) in the Postgraduate Jazz Course

1992-now : Varied performance projects in classic and jazz

1999-present: researcher in a scientific project (Gabor Analysis and Music) at the University of Vienna (Supported by the National Bank fund and the Austrian Science fund FWF)

December 1999: Co-organising the Diderot Conference on Mathematics and Music in Vienna

1999 - 2001: Several short stays in Cambridge, UK, for joint scientific work with members of the Signal processing Laboratory, focussing on the processing of music signals

2001: CD *Nebensonnen* issued (Jazz-quartet performing original compositions and arrangements based on Schubert's Winterreise)

December 2001: Co-organising the Second International Gabor Workshop in Vienna